



FACULTY OF SCIENCE AND TECHNOLOGY

MASTER THESIS

Study programme / specialisation: Engineering structures and Materials / Building structures

The spring semester, 2022

Author: Paulos Haile Ghebremichael

Open / ~~Confidential~~

.....
(signature author)

Course coordinator: Associate professor Ashish Aeran

Supervisor(s): Associate professor Ashish Aeran

Thesis title: Material degradation in mooring chains for floating structures in deep waters

Credits (ECTS): 30

Keywords: mooring chains, corrosion, codes and standards, MIC, corrosion allowance, model, FEA, cathodic protection

Pages: 98

+ appendix: 9

Stavanger, 22.07.2022
date/year



The broken chain (Brutt lenke), Stavanger, Norway

It is located 600m from the place where I live.

Photo by: Paulos Haile Ghebremichael

01st July 2022

Abstract

There is a dire need for an efficient, trustworthy, and financially feasible positioning technique for offshore large floating structures. Of all the methods of positioning the offshore structures, the mooring chains play a significant role. There is a need for explicit knowledge of the properties of mooring systems so that the design, operation, and analysis of large floating structures, particularly in deep water, should be reliable. Experts from the oil and gas industry have experienced actual corrosion loss rates data for mooring systems that they get are different from those allowed for in traditional design guidance and have long been a recognized challenge. The corrosion allowances from the codes are sometimes very conservative leading to an over design (thicker); this could be the other way round, in some cases. Recently, as long as corrosion has been tolerated with an 'allowance', thicker and heavier chains have been the only way to extend the life of these mooring chains.

On the other hand, Corrosion rates can be unpredictable and vary greatly around the world due to the diverse marine environments. As a worst-case scenario, this results in significantly shortened chain lifespans and, at the very least, increased failure rates and integrity issues in the mooring systems.

The findings of this study will result in a practical equation function from previous studies that can be used to estimate corrosion loss in deep water based on parameters that have a significant impact on the corrosion, such as temperature, and dissolved inorganic nitrogen (nitrates, nitrites, and ammonia) usually measured together as DIN concentration levels. Data may be unavailable in some regions, or finding them may be difficult, and using the allowances during design from the standards without considering the parameters may lead to inappropriate allowances, and as a result failure may occur. Thereafter, estimating the rest life of inservice degraded mooring chains is another issue and how can this be done through FEM analysis. Finally, although Cathodic Protection has long been a part of corrosion prevention strategies for offshore steel structures, the mooring lines have never been successfully protected in deep waters. Finding a method of protection to extend the lifetime of these degraded chains is another challenge. Following extensive research, a new sacrificial anode cathodic protection system technology has been found in recent years. Considering this method has guaranteed efficiency and a cathodic protection calculation has been made using these anode types.

Acknowledgment

This thesis finalizes my Master of Science degree in Engineering structures and materials, specializing in building structures, and is the final work I do before completing my degree at the University of Stavanger in the spring of 2022. The thesis is based on extensive available research, inspection data, and projects, in which most of the time and workload were produced.

In this context, I would like to thank my supervisor, Associate professor Ashish Aeran, for providing me with this interesting task. I appreciate his support, guidance, and valuable contributions during our meetings. His knowledge and passion for this field of engineering have been an inspiration. Furthermore, I would like to thank IMENCO AS. for their advice and providing me with the necessary materials.

Finally, I must express my gratitude to my parents, my brother professor Estifanos Haile and especially to my wife, for providing me with unfailing support and continuous encouragement through my years of study. This accomplishment would not have been possible without them.

Table of contents

1. Introduction.....	1
1.1. Background and motivation for the present work.....	1
1.2. Problem statement.....	1
1.3. Objectives.....	2
1.4. Organization of the Thesis.....	2
2. Offshore structures and positioning systems.....	3
2.1. Offshore oil and gas structures.....	3
2.2. Dynamic positioning.....	4
2.3. Mooring system.....	5
2.3.1. Classification of mooring systems.....	5
2.3.2. Mooring components.....	11
3. Degradation of mooring chains.....	13
3.1. Corrosion.....	13
3.1.1. Pitting corrosion.....	15
3.1.2. Interlink wear.....	15
3.1.3. Abrasion.....	16
3.2. Mooring configuration and corrosion.....	16
3.3. Offshore corrosion zones.....	17
3.4. Service life of mooring chains.....	18
4. Comparison of codes (standards) and research findings.....	20
4.1. Mooring corrosion allowance from codes and standards.....	20
4.2. Microbiologically influenced corrosion (MIC).....	24
4.2.1. MIC on mooring systems.....	29
4.2.2. Diagnosis of MIC.....	31
4.2.3. Prevention of MIC.....	32
4.2.4. Consequences of MIC.....	32
4.3. SCORCH JIP.....	32
4.3.1. Overview of project.....	32
4.3.2. SCORCH JIP findings.....	35
4.4. Empirical estimation for corrosion loss.....	37

4.4.1.	Previous models.....	37
4.4.2.	Melcher' s model.....	37
5.	Effects of uniform corrosion on residual strength of degraded offshore mooring chain...	48
5.1.	Chain design.....	49
5.2.	Chain properties.....	49
5.3.	Capacity of chains.....	50
5.4.	Chain Strength Behavior and Ductile Failure.....	51
5.5.	Strength analysis of uniform corrosion on chains.....	52
6.	Cathodic protection (CP).....	57
6.1.	Galvanic effects.....	57
6.2.	CP systems and offshore corrosion zones.....	58
6.3.	Cathodic protection systems.....	59
6.4.	Cathodic protection system selection.....	59
6.5.	Cathodic protection of chains.....	61
6.6.	Sacrificial anode cathodic protection design criteria.....	62
6.6.1.	Design consideration and parameters.....	64
6.6.2.	CP calculation and design procedures.....	68
7.	Case study 1: Long-term corrosion estimation due to MIC using melcher's model	71
7.1.	Case data requirements for modeling.....	71
7.2.	Estimation of mooring chain corrosion with an elevated nutrient concentration	72
7.3.	Results and discussion	73
8.	Case study 2: Residual strength assessment of degraded offshore mooring chain.....	76
8.1.	Data input.....	76
8.1.1.	Chain geometry	76
8.1.2.	Material properties	78
8.1.3.	Interaction.....	78
8.1.4.	Loading and boundary conditions	79
8.1.5.	Element selection and mesh convergence	80
8.2.	Results and discussion	81
9.	Case study 3: Cathodic protection design.....	84
9.1.	Cathodic protection design	84

9.1.1.	Basic design data	85
9.1.2.	Structure design data	86
9.1.3.	Design current density - for seawater exposed bare metal surfaces	88
9.1.4.	Required current for CP	89
9.1.5.	Anode mass calculations	89
9.1.6.	Details of anode selected.....	89
9.1.7.	Number of anode requirement.....	91
9.1.8.	Anode current capacity (life).....	92
9.2.	Results and discussion	93
10.	Conclusions	94
	References.....	95
	Appendix.....	I
	Appendix A: Cathodic protection design spreadsheets	I
	Appendix B: Market recommendation of CP for mooring chains in deep water	IV

List of Figures

Figure 2-1: Types of offshore oil and gas structures.....	3
Figure 2-2: Dynamic Positioning System for an FPSO, with thrusters attached to the hull.[7]	5
Figure 2-3: (Left) Typical spread mooring system. (Right) Typical single-point mooring system[7].....	6
Figure 2-4: Illustration of FPSO and internal turret mooring system[8].	7
Figure 2-5: External turret system[8].	8
Figure 2-6: Catenary mooring system	9
Figure 2-7: A sketch of a typical catenary mooring line configuration of oil and gas platforms in the North Sea and the Norwegian Sea.....	9
Figure 2-8: Taut mooring system	10
Figure 2-9: Tention leg mooring system.....	11
Figure 2-10: Stud(left) and studless(right) chain links.....	12
Figure 3-1: Mooring Failures Root Cause on FPSO[16].....	13
Figure 3-2: Schematic of Anodes, Cathodes and Pitting[17]	14
Figure 3-3: Illustrates the four types of degradation modes and their impact on the mooring chain cross-section.	16
Figure 3-4: Degradation Encountered in a Chain Mooring System [18]	17
Figure 4-1: The North sea [21].	21
Figure 4-2: The location of the data source for the corrosion rate observation in the field [24].....	22
Figure 4-3: Illustration of build-up of bio film on a steel surface	25
Figure 4-4: Example of Typical Sulphate Reducing Bacteria	26
Figure 4-5: Preconditions for Development of MIC[16]	27
Figure 4-6: Progression of SRB involvement[24]	28
Figure 4-7: Chain Links from the Touchdown Zone, Uncleaned and Cleaned[16].....	31
Figure 4-8: Corrosion site testing by SCORCH JIP[15].....	33
Figure 4-9: Contributing locations to SCORCH JIP corrosion data.....	34
Figure 4-10: Multi-phase phenomenological corrosion-time model and adopted parameterization.	38
Figure 4-11: Melcher’s model, shows short-term(unshaded part) corrosionloss–exposure time model.[28]	40

Figure 4-12: Schematic non-linear (bi-modal) model for the progression of corrosion loss with time showing the influence of some of the major parameters, such as the amount of nutrients and other factors, on long-term corrosion. 43

Figure 4-13: The model in Figure 4-12 for long-term corrosion is simplified schematically as a long-term linear function parameterized by c_s and r_s . This simplification is true for $t > B$. Also demonstrated is that the initial corrosion rate r_o approximates Figure 4-12 for just a brief period of time(left figure).44

Figure 4-14: Parameter c_s (left) and r_s (right) (defined in Figure 4-13) as a function of average annual seawater temperature T and dissolved inorganic nitrogen (DIN)..... 45

Figure 4-15: Annual change in seawater temperature as depicted by a diagram illustrating the analytical parameters..... 46

Figure -5-1: Common link design [31] 49

Figure 5-2: Steel grades and their corresponding breaking loads [14]..... 51

Figure 5-3: Chain surface location names[18] 52

Figure 5-4: Normalized Break Load versus Single Bar Diameter Reduction for All Degradation Modes 53

Figure 5-5: Actual Ultimate Strength vs. Break Test Results: IACS CBS Curve and Predictions 54

Figure 5-6: Measurement Locations for Estimation of Average Diameter 55

Figure 5-7: Key aspects of chain model construction[18] 56

Figure 6-1: The galvanic series of metals in slow moving sea water[34] 58

Figure 6-2:ClumpAnodes(left) and Chain-Stud anodes(right)[37]..... 62

Figure 6-3: The flow of CP design [45] 63

Figure 7-1: North Sea max/min water temperature ($^{\circ}$ C)[38] 72

Figure 7-2: Estimated corrosion loss trends as a function of exposure period for 8 $^{\circ}$ C average seawater temperature and four levels of elevated average seawater bulk DIN concentration. The bi-modal model (Figure 4-12) is sketched to scale in the lower left corner for this water temperature. 75

Figure 8-1: Path sketch of 76mm diameter studless link 77

Figure 8-2: Section sketch of 76mm diameter studless link..... 77

Figure 8-3: Break load for 76mm diameter chain link from INTERMOOR catalogue 78

Figure 8-4: The red zone is the master surface, while the pink zones are the slave ones..... 79

Figure 8-5:3D FE Model of Chain Links in Abaqus 80

Figure 8-6: Meshed studless link in Abaqus 81

Figure 8-7: Strain Profile of 76mm Chain Links at MBL..... 81

Figure 8-8: Von Mises Stress Profile 76mm Chain Links at MBL 82

Figure 8-9: load-elongation curves	83
Figure 9-1: An illustration of a torus section	87
Figure 9-2: An illustration of Pacu® anode (left) and Piranha® anode Clamp (right)[40]	90
Figure 9-3: Pacu anode attached to the chain using Piranha clump[40]	91

List of Tables

Table 4-1: Corrosion Allowances from DNV OS-E301, Recommended corrosion allowance referred to the chain diameter for different locations [22].	21
Table 4-2: Summary of mooring chain corrosion rates from various design codes [23].	22
Table 4-3: Description of the phases of the model[16].	39
Table 4-4: Summary of phases of corrosion loss–time model[28].	39
Table 5-1: Dimensions and tolerance for studless common link[31].	49
Table 5-2: Mechanical properties of offshore mooring chain and accessories[32].	50
Table 5-3: Formulas for proof and break test loads[31].	51
Table 6-1: Comparison of Galvanic Anodes and Impressed Current Cathodic Protection Systems for Offshore Structures[35].	59
Table 6-2: Proposed Layout at seawater ambient temperatures, anode materials' electrochemical capacity and design closed circuit potential.[36].	65
Table 6-3: Initial and final recommended design current densities (A/m^2) for seawater-exposed bare metal surfaces as a function of depth and 'climatic zone' based on surface water temperature. [36].	66
Table 6-4: Mean recommended design current densities (A/m^2) for seawater-exposed bare metal surfaces as a function of depth and 'climatic zone' based on surface water temperature. [36].	66
Table 6-5: Recommended Anode Utilization Factors for CP[36].	67
Table 6-6: Recommended Anode Resistance Formulae for CP Design Calculations.	70
Table 7-1: Monthly max/min/mean North Sea water temperature($^{\circ}C$).	72
Table 7-2: Interception (c_s) and slope (r_s) values of an assumed area with an average temperature of 8 $^{\circ}C$ and at different DIN values(from Figure 4-14).	73
Table 7-3: Corrosion loss from the time of immersion to the end life of the mooring chain.	74

Abbreviations

DIN:	Dissolved inorganic nitrogen
FEM:	Finite element method
CP:	Cathodic protection
MIC:	Microbiologically Influenced Corrosion
FPSO:	Floating Production Storage and Offloading
MODU:	Mobile Operating Drilling Units
DP:	Dynamic positioning
SPM:	Single-point moorings
FPS:	Floating Production Systems
ROV:	Remotely operated underwater vehicle
DNV:	Den Norske Veritas
API:	The American Petroleum Institute
BV:	Bureau Veritas
ISO:	International Standards Organization
BS:	British Standard
SRP:	Sulfate-reducing prokaryotes
SPP:	Sulfide producing prokaryotes
APB:	Acid-producing bacteria (APB).
HDP:	Hydrocarbon-degrading prokaryotes
NRB:	Nitrate-reducing bacteria
NOB:	Nitrite-oxidizing bacteria
MOB:	Metal-oxidizing bacteria
MRB:	Metal-reducing bacteria
HIC:	Hydrogen induced cracking
SCORCH JIP:	Seawater Corrosion of Rope and Chain Collaborative Research Industry
MBL:	Minimum break load
IACS:	International Association of Classification Societies
CBS:	Catalogue Break Strength
FEA:	Finite element analysis
SACP:	Sacrificial anode cathodic protection
ICCP:	Impressed current cathodic protection

DC: Direct current

NACE: Nomenclature of Economic Activities

1. Introduction

1.1. Background and motivation for the present work

In order to meet modern-day resource needs and demands, many nations are exploring marine environments. Because of extreme conditions in such environments, effective explorations/exploitation of resources requires detailed long-term planning, development of engineering technologies and facilities, and the final implementation phase. Different types of bulky floating structures such as oil and gas platforms, undersea pipelines, artificial islands, and storage bases require active, reliable, and affordable positioning methods. Usually, these floating structures can be positioned by applying either a mooring system, or a dynamic positioning system, or a combination of both. When applying the mooring technique, the response of the mooring chains is of vital importance.

A broken mooring line could have devastating safety and financial consequences. Production on the moored structure is often shut down for a short period when a damaged or broken mooring line is to be replaced with a new one. Of course, the oil and gas sector is doing all in its power to minimize the odds of an accident. Offshore structural components have a better design and a longer service life if corrosion and related types of degradation are accounted at the outset and if engineered protection methods are implemented during their design or operation stages. This thesis is a continuation of the work made by some studies regarding the aforementioned problems and solutions.

1.2. Problem statement

Mooring system comprises of a mooring line, anchor, and connectors and is used to anchor floating structures (ships, platforms etc.) in deep waters. A mooring line connects an anchor on the seafloor to a floating structure and can be severely corroded by seawater. In many designs, a part of the mooring chain near the anchor is often buried and is therefore even more severely subjected to corrosion, called MIC – Microbial Induced Corrosion. As a result, these chains are either designed with corrosion allowances or are fitted with cathodic protection (CP) systems. However, the code given corrosion allowances (for uniform corrosion and for MIC in buried part of the chain) are sometimes very conservative, leading to a conservative design (thicker, longer chains) - this could be the other way round as well in some cases and need to be investigated as well. Also, the cathodic protection systems are hard to maintain due to the harsh sea environment and the fitted anodes become loose or get dislodged due to constant wave motions. Therefore, there is a need to use more

precise material loss parameters based on data from inspection agencies and literature. Furthermore, there is a need for better and long-lasting cathodic protection systems.

1.3. Objectives

The main objectives of this thesis are:

- to study various material degradation parameters involved in offshore mooring chains and compare the corrosion allowances from codes/guidelines with conducted research findings. This part will mainly deal with chains located in the North Sea exposed to Microbiologically Influenced Corrosion (MIC) and empirical estimation of their allowances.
- to demonstrate the effect of these parameters (corrosion) on mooring chain strength through a case study and how these parameters can be assessed using finite element software. The thesis will particularly focus on the prevalence of uniform corrosion and its associated stress concentration factors. And,
- to study various Cathodic Protection (CP) systems for mooring chains in deep water, their comparison, and kind of recommendations on what type of CP systems are useful for mooring systems in deep water. This part also includes CP design and calculations to understand the system better.

1.4. Organization of the Thesis

This thesis has been divided into 10 chapters. Chapter 2 covers fundamental concepts about mooring systems in deep water, i.e. maintaining constant position and configuration of moorings. Chapter 3 addresses main factors that affect the degradation of moorings. A literature review on the comparison of corrosion allowance of codes(Standards) and research findings is given in chapter 4. Chapter 5 discusses the effect of uniform corrosion on residual strength of mooring chains. Chapter 6 outlines cathodic protection and anode design for mooring chains. Chapter 7 presents a case study on the estimation of corrosion allowance during the design of a mooring chain in the North Sea exposed to a high MIC level. Chapter 8 outlines methods for estimating the strength of an existing on-site mooring chain, assuming a uniform corrosion type throughout their cross-sections. Analysis of chains exposed to large pits is out of the scope of this study. Finally, having these degraded chains, the design of cathodic protection is necessary to keep them in shape and extend their service life. Cathodic protection design and calculations for estimating anode mass in presented chapter 9. And chapter 10 gives the conclusion of the major findings of the thesis.

2. Offshore structures and positioning systems

This chapter outlines the application and composition of offshore structures and mooring systems in briefly.

2.1. Offshore oil and gas structures

Offshore resource exploration and exploitation structures are widely available worldwide, especially in the oil and gas industry. The facilities could be fixed or floating in order to have safe and fully functional, efficient marine operation activities[1]. Fixed systems are challenging and expensive to dock in deep water. A picture illustrating the main offshore structure types can be seen in

Figure 2-1. The first three and the last one are fixed to the seabed using either steel trusses or concrete. The rest six, denoted as 4,5,6,7,8 and 9, are floating structures anchored to the seabed using a mooring system.

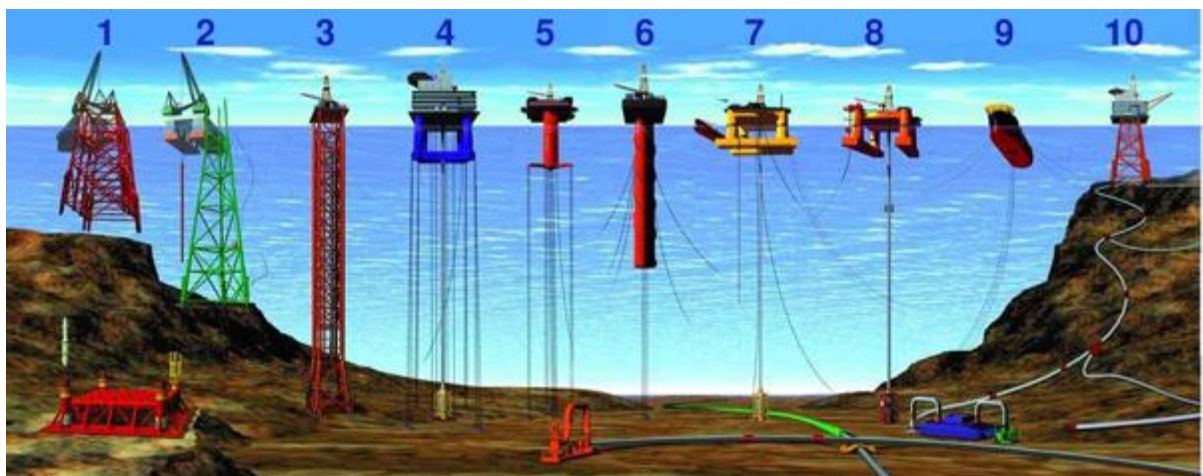


Figure 2-1: Types of offshore oil and gas structures

Error! Reference source not found. shows the types of offshore oil and gas structures: 1), 2) conventional fixed platforms, 3) compliant tower, 4), 5) vertically moored tension leg and mini-tension leg platform, 6) Spar, 7), 8) Semi-submersibles, 9) Floating production, storage, and offloading facility, and 10) sub-sea completion and tie-back to host facility [2].

Tension leg platforms (number 5 in Figure 2-1) have strong buoyancy that each of the structure's corners is always in tension permanently moored to the seabed using grouped vertical mooring lines called tethers or tendons. All floating structures except tension leg platforms have six degrees of

freedom in three-dimensional space; three displacements and three rotations called heave, surge, sway, yaw, roll and pitch. But tension leg platforms have three. This thesis focuses on the ones that exhibit permanent mooring systems, that being semi-submersible and floating production units because mooring chains are included in their system configuration in addition to the reason explained above.

Floating Production Storage and Offloading (FPSO) units are currently popular features in the offshore oil and gas industry to refine, process and store oil and gas temporarily that comes from production platforms or direct from subsea wells and transfer it to shuttle tankers periodically. They versatile both in deep and shallow waters, are far more economical than big oil platforms in small oil fields with short service lives and can be shifted from one offshore field to another conveniently and economically. They are used in both deep and shallow water, especially in areas where piping is costly. However, FPSOs are complex ship-shaped structures where mooring lines spread out from their front and back. of the structure and are used in shallow waters to restrain with seabed in areas sheltered from environmental loads. On the other hand, they are prone to hazards and failures during operations. In such cases, turrets are used to connect the mooring system to one single point, which allows the FPSO to rotate freely about the vertical axis to reduced total loading [1], [3], [4].

Semi-submersible platforms are more stable and are commonly used as drilling rigs, production or lifting cranes. They are multi-legged floating structures with large slab decks. The slab decks are interconnected to the pontoons below sea level which are horizontal buoyant parts of the structures. The pontoons in return are attached to mooring lines that are anchored down to the seabed. They can be used several times by moving them from one place to another. At the same time, they can be used in different water depths by ballasting or de-ballasting them to buoyancy tanks [3], [4].

Maintaining a stable position is crucial for floating structures in the sea. It allows them to operate continuously even when the weather is harsh. It would be difficult to drill and transport hydrocarbons from a reservoir without a stable position above a particular location on the seabed. Drifting of units can cause ruptures resulting in an environmental disaster, economic losses, and in the worst cases loss of human lives. Neglect of such problems where it is not possible using fixed structures, station keeping of offshore oil and gas structures is either using mooring system (anchors and mooring lines) or by using Dynamic positioning is the only solution[5].

2.2. Dynamic positioning

Dynamic positioning is usually deployed as an alternative to mooring systems. It is suited to vessels that arrive and depart a specific platform often. It is a computer-controlled GPS navigated to automatically maintain the position of Mobile Operating Drilling Units(MODU) vessels or flotels within a specified tolerance by controlling the utilization and direction of own onboard thrusters and propellers, which generate thrust vectors to counter the wind, wave, and current forces [6]. Dynamic positioning (DP) in combination with passive mooring systems are used to lower the load on the system.



Figure 2-2: Dynamic Positioning System for an FPSO, with thrusters attached to the hull.[7]

2.3. Mooring system

Mooring systems are an essential components of station-keeping systems designed to keep dynamically floating structures on a fixed geographical position with a specified tolerance. They were developed and traditionally used by the oil and gas industry for production units. Recently, they have been used on offshore renewable energy structures like wind turbines. Offshore structures are exposed to loads from vessels' static movements and environmental loads (waves, wind, and currents). The purpose of moorings lines is to withstand these forces that act directly on the mooring lines. Unlike DP, moorings establish a physical connection between the floating structure and the seabed. Rather than keeping the structure in a specific position, they are used to ensure the integrity and operability of the drilling and production facilities. They can be deployed in harsh environments and water depths of over 3000m [4], [7], [8].

2.3.1. Classification of mooring systems

Mooring systems can be classified based on their operational longevity, or their requirement to restrict the floater's heading/station keeping, or their profile and configuration.

1. Based on the duration of the offshore operation

Based on their operational time frame, moorings are classified into two broad categories. These are:

- a. *Temporary*: moorings that have a station-keeping life span range from few days to several months. They are suitable for drilling semis, drill ships, pipe laying vessels, crane vessels, flotels, logistics supply vessels, etc.
- b. *Permanent*: moorings that maintain station-keeping at a host location for several years to decades. They are suitable for a variety of long-term floating structures.

2. Based on the mooring system's requirement to restrict the floater's station keeping

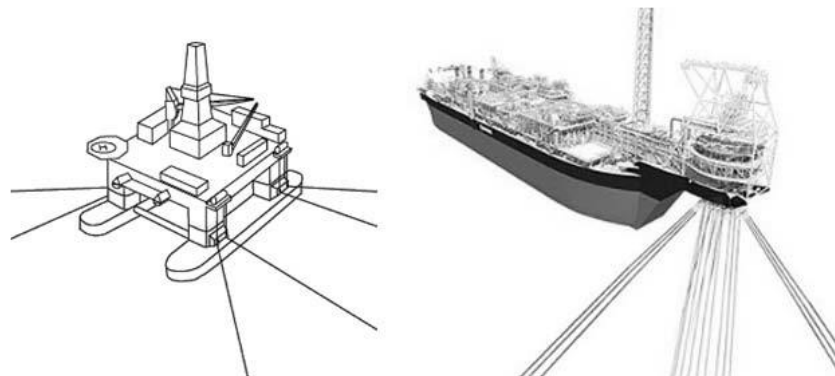


Figure 2-3: (Left) Typical spread mooring system. (Right) Typical single-point mooring system [7].

A. Spread mooring system

Spread moorings are used to restrict a floating structure's offset and heading. Multiple mooring lines extend around the structure to ensure the designated operation. The ideal heading is decided by the local environmental circumstances during installation of the spread mooring system configuration. A spread mooring system is simple and inexpensive, and does not require sophisticated rotating mechanical systems. The location and direction of the floating vessel are effectively limited after the anchors are deployed, and risers and umbilical systems may be built and operated. Most Mobile Offshore Drilling Units and certain floating production systems use spread mooring for station-keeping [7].

The mooring lines are linked at the bow and stern and spread outward on ship-shaped floating boats with spread moorings, which can limit the lateral offset and heading of the hull. A spread mooring system can theoretically be used in any geographic area as long as it is strong enough. However, if the ship-shaped floating structure is subjected to large lateral environmental loads, the mooring lines may not be able to withstand the excessive loading. As a result, while the spread mooring method is cost-effective and simplistic in design, it is only appropriate for big floating constructions in locations with consistent weather conditions, ideally mild environmental forces, such as offshores of West Africa[7].

B. Single-point moorings (SPM)

These systems feature one or more mooring lines linking the floater's centre of rotation to the bottom, allowing the floater to weathervane around this centre of rotation to decrease environmental stress. Single-point moorings for FPSOs are highly adaptable and may function in a variety of environments like the North Sea. They allow the structure to face the weather in the direction of least resistance, thus reducing the total load on the mooring system [9].

They are, however, technically difficult, and costly to construct. There are different types of SPMs, and are classified according to their distinct operational characteristics and placement of the turret: internal turret system and external turret system. A turret is a steel structure with decks supporting a stack of swivels. Its upper portion is directly attached to the FPSO topsides, its mid-part connected to the FPSO hull through bearings, and its lower part connected to the mooring lines. In response to wind, waves, and current action, the turret moored FPSO may spin around the inner bearing of the turret[8].

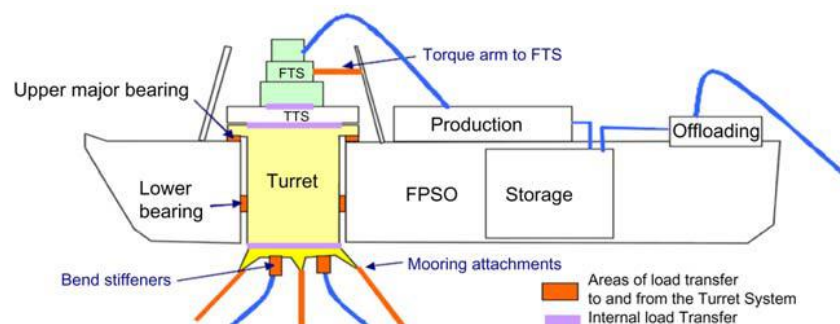


Figure 2-4: Illustration of FPSO and internal turret mooring system[8].

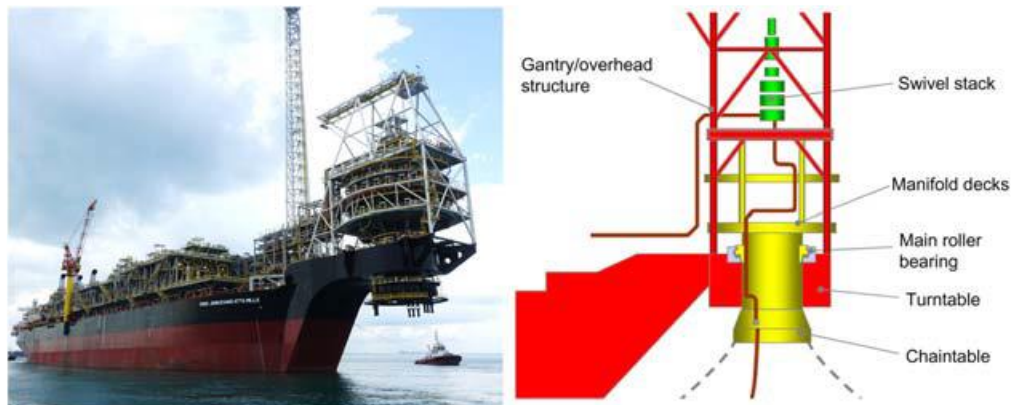


Figure 2-5: *External turret system*[8].

3. Based on the profiles and configurations:

Mooring systems can be of different configurations, depending on what is most suitable for a specific location. Factors that affect their configurations are the type of unit, water depth, seabed layout, soil, water contamination, etc. Accounting for all factors, it can be concluded that no mooring systems are configured similarly to each other under different field conditions [6].

A. Catenary mooring system

The catenary mooring system features a line profile with a portion of the mooring line in the static equilibrium position on the seabed. The mooring leg develops a catenary shape due to the self-weight of the mooring line with a considerable quantity of chains situated at the seabed. In addition, frictional forces at the bottom provide the necessary compliance to deal with the floater's static offset and dynamic movements. The catenary mooring method is the most commonly utilized, particularly at shallow to moderate depths. In water depths up to 1000 meters, a composite of chain and steel wire rope catenary mooring methods is successfully used on floating systems. The horizontal span of a catenary line is commonly 5-20 times the vertical dimension.

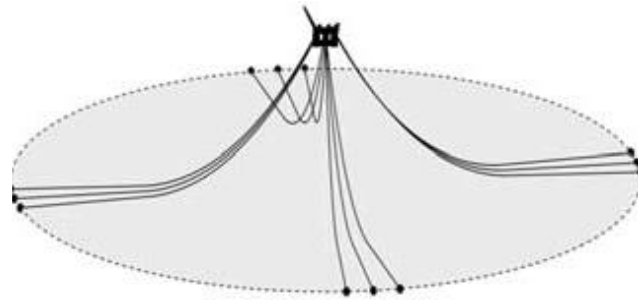


Figure 2-6: Catenary mooring system

Catenary mooring lines can be configured in a combination of heavy chains on the lower and upper part of the line, and wires and fibre ropes in the middle part of the line. It is common to separate steel chains using steel wire ropes [6], [10].

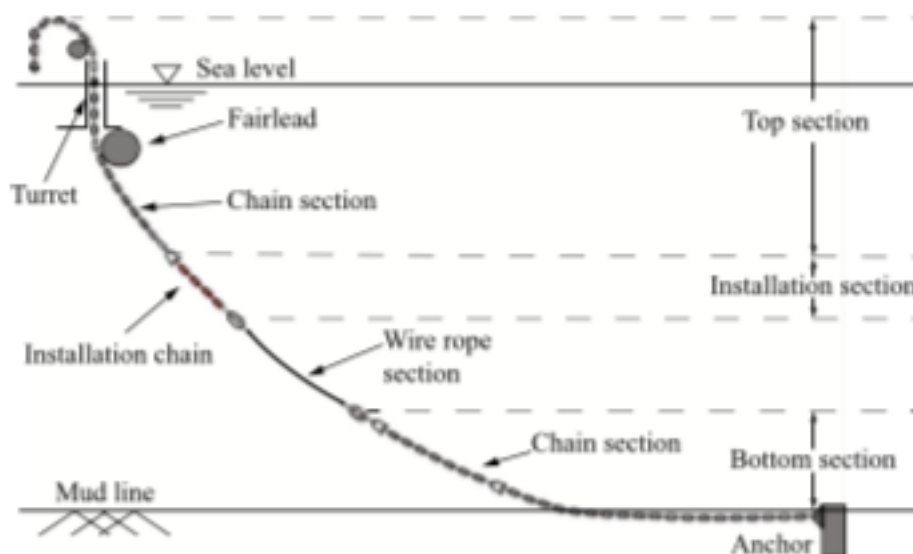


Figure 2-7: A sketch of a typical catenary mooring line configuration of oil and gas platforms in the North Sea and the Norwegian Sea

The idea behind the different material combinations (segments) is that lightweight rope reduces the dead load. Fibre rope should not be in contact with the seabed as the seabed may contain rocks that have sharp edges. These edges wear down or cut the rope resulting to a more rapid mooring line failure than anticipated [6]. The chain on the other hand increases the stiffness and material strength of the line; thus, a unit increases its flexibility where possible in areas with large movements [11]. Another advantage of using chain links is that they are resistant to degradation in response to wear and corrosion, especially near the surface (called the splash zone) and near the sea floor (called the trash zone) [10]. Only horizontal forces are transmitted to the anchor by catenary cables. Then, even

in the worst load condition, a piece of the bottom chain must always lay above the seabed to guarantee that no vertical force operates on the anchor.

B. Taut mooring system

In this configuration, no lines lie on the bottom in the static equilibrium position. Using the taut leg mooring method, mooring lines extend from the seabed anchor to the floater's fairlead, usually at an angle of 30-45 degrees. Compared to a catenary mooring system, the anchor footprint is lower and requires less line material. However, because the lines are tight, the line tensile stretch is primarily responsible for the compliance to floater offset and dynamic responsiveness. As a result, a tight leg system may be overly stiff in shallow water, increasing line tension unnecessarily. The mooring lines' elasticity must be high enough to absorb the structure's motion without creating overload. It is better suited to applications in deep or ultradeep water [12]. Semi-taut and inverted catenary mooring configurations integrate buoyancy into the mooring line combination to minimize the vertical stress of the mooring line in depths greater than 1000 meters.

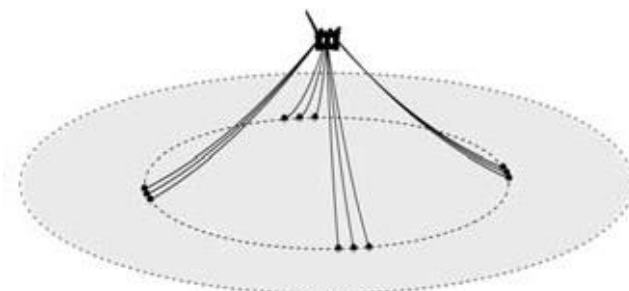


Figure 2-8: *Taut mooring system*

Semi-taut mooring systems have a short chain length attached to the anchor in its static starting configuration on the seabed. The mooring line extended to the anchor has to withstand vertical loads, if the platform is loaded by either wind or waves forces, attaining a particular surge offset. In such cases, driven piles, suction piles, plate anchors, or unique drag embedded anchors must be used to limit weights in both vertical and horizontal directions.

C. Tension leg mooring system

Tension leg moorings are utilized when a structure's buoyancy exceeds its dead load. The top end of the tension legs (tendons) is linked to the platform, and the lower end is tied to the seafloor. Tendons are vertical and must sustain significant tensile stresses. Large circular steel tubes and ropes are used to construct them.

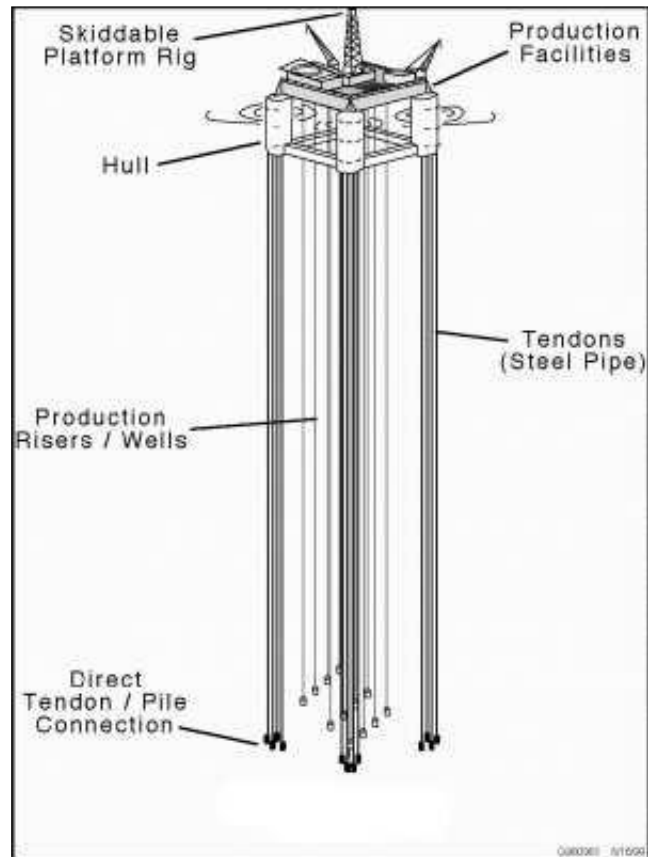


Figure 2-9: Tension leg mooring system

2.3.2. Mooring components

A typical mooring system has three different components, the mooring line, the connectors, and the anchor point. According to DNV-OS-E301 [13], a mooring system normally consists of:

- mooring chains,
- anchor,
- windlass or winch,
- fairlead,
- anchor chain cable and accessories,
- steel wire rope,
- fibre rope segments and termination hardware,
- chain stopper,
- towing equipment,
- Mooring Line Buoyancy Element (MLBE),

- thrusters,
- turret,
- soft yoke systems, and
- pull-in systems.

Steel components in mooring systems are not covered in this study, but with an emphasis on a chain. Due to its strength, chain is commonly used in vulnerable areas of the mooring line, such as the top under high tension and the touchdown or "thrash zone." [2]

Chains, which come in a variety of diameters and grades, are the most commonly used component in mooring lines. Offshore mooring chains are typically relatively large, with bar diameters ranging between 70 and 200 mm. Chains are classified into two types based on their appearance: studlink and studless chain.[14] An interbar stud, or brace, is placed between the bars to prevent flexure and improve fatigue endurance. Stud-less chains lack a bracing stud.

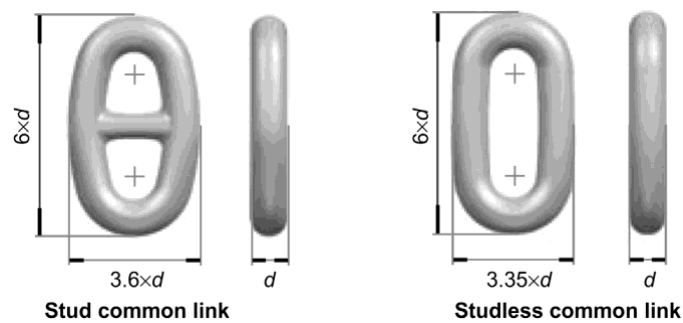


Figure 2-10: Stud(left) and studless(right) chain links.

3. Degradation of mooring chains

Floating Production Systems (FPSs) are designed to remain at a specific location. With time, their mooring systems eventually deteriorate, causing individual lines and the entire system to lose strength. In the case of mooring chains, this degradation is caused by corrosion, wear (abrasion and interlink), and fatigue. This study focuses on the loss of mooring chain sections due to corrosion rather than wear. The effect of wear is addressed when appropriate.

3.1. Corrosion

Infrastructures, such as offshore structures, ships, bridges, industrial facilities, coastal and harbor structures, and pipelines, are vulnerable to marine corrosion. According to a survey by DeepStar (project CTR11405-A), ~22% of mooring chain failures were caused by either corrosion or fatigue exacerbated by corrosion. The effect of corrosion was not clearly understood or accounted for during the mooring design phase [15].

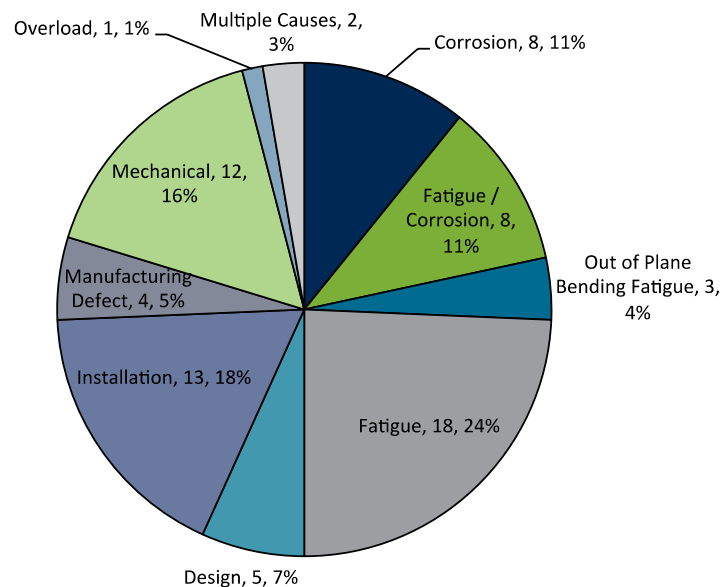


Figure 3-1: Mooring Failures Root Cause on FPSO [16]

Corrosion of a metal (such as steel) is an electrochemical process in which metallic atoms get oxidized, typically resulting in oxides or salts. Typical corrosion of steel occurs when iron atoms oxidize into cation (Fe^{2+}) that dissolve in the surrounding water. They typically react with other ions

and molecules to form oxides and salts on this surface. The anodic sites are represented by the locations on the metal surface where the metal ions are oxidized in which excess electrons flow out. There must be a corresponding cathodic reaction (reduction) at cathodic sites for the overall corrosion process, where extra electrons leave the metal to participate in the cathodic reaction. The cathodic process in oxygen-driven corrosion leads to OH⁻ ions, which include oxygen, water, and metal electrons. Ferrous oxide (Fe₂O₃) is formed when oxygen from OH⁻ ion reacts with the iron ion, i.e., $4\text{Fe} + 3\text{O}_2 = 2\text{Fe}_2\text{O}_3$ [17].

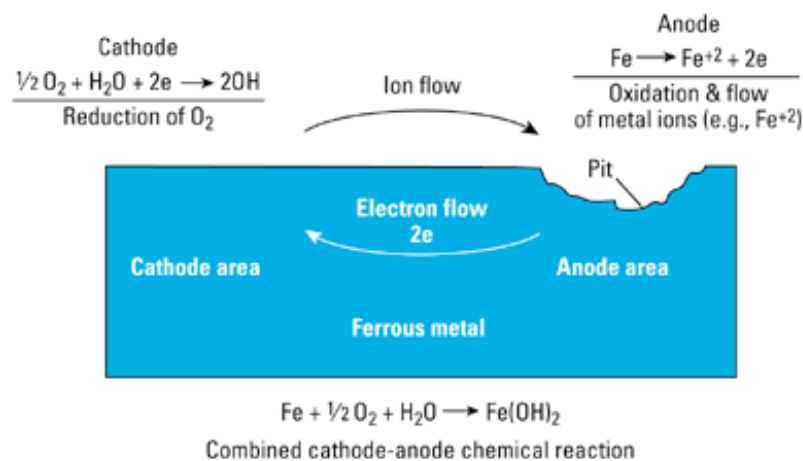


Figure 3-2: Schematic of Anodes, Cathodes and Pitting[17]

Commonly, a distinction is made between different types of corrosion that affect chain moorings, namely uniform and pitting corrosion. Uniform and/or pitting corrosion, along with mechanical loading that causes wear on mooring chains, are the most common causes of mooring system failures. The details of these types of corrosion and some other types of degradation modes are described below.

Corrosion will also cause a sequence of other failures, thus the actual design life will not be sufficient to cover the end of the operating service life.

Uniform corrosion

Uniform corrosion is the most dominant type of corrosion in mild and low alloy steel. Usually, general corrosion occurs when the entire exposed surface corrodes. The steel may lose integrity at a somewhat consistent pace. This implies that anodic and cathodic sites will shift in a seemingly random way. The development of oxides on the surface, which partially prevents the transit of ions and molecules necessary for the reactions, typically limits the pace of corrosion. This is also known

as passivation because it effectively changes the metal's galvanic potential in the "noble" direction [17].

3.1.1. Pitting corrosion

Pitting corrosion is the most common type of localized corrosion and occurs when anodic and cathodic sites remain in the same position over time. It shows up as deep cavities or holes in the metal surface where localized metal loss has occurred, with the rest of the surface remaining comparatively uncorroded.

There are several causes for this, including:

- Degradation of passivation (disruption of current corrosion layer by uniform corrosion) or other protective coatings on a local scale.
- Conditions in which localized "aggressive" habitats (low pH) are permitted to develop and persist. This might be due to deposits or other factors causing sluggish conditions.
- Variation in metal characteristics (inhomogeneities) impacting galvanic potential, for example, welds or the macrostructure of tempered steels. Mechanical or chemical damage, the presence of impurities in the metal, metallic grain boundaries, or surface roughness can all cause a lack of homogeneity. The rupture of the corrosion products' passive coating results into the formation of a concentration cell on the metal surface. That in turn, results to localized attacks.

Once pit corrosion has formed, the topography and chemistry may favour continued deterioration in the same place at a relatively rapid pace. Another reason pits have significant corrosion rates is because they have limited anodic zones compared to considerably bigger cathodic regions. As a result, "anodic pits" become sacrificial compared to the cathodic areas [17].

3.1.2. Interlink wear

It is a type of degradation seen on mooring chains due to the interaction between chain links. Chains are exposed to high environmental loads, and the outcomes of such actions result in interlink wear. Interlink wear is localized at the chain's weakest point, which is the chain's crown intrados. As interlink wear diminishes the chain crown's cross-sectional area, the chain's strength is instantly affected [18].

3.1.3. Abrasion

Chains can also be exposed to abrasion due to contact with the seabed. The chain sidebars are stronger than the crown early in the abrasion process safety. The total strength of the two sidebars eventually becomes less than that of the chain crown as abrasion occurs on one or both sidebars. Ultimately the failure location shifts from the chain crown to the chain sidebars [18].

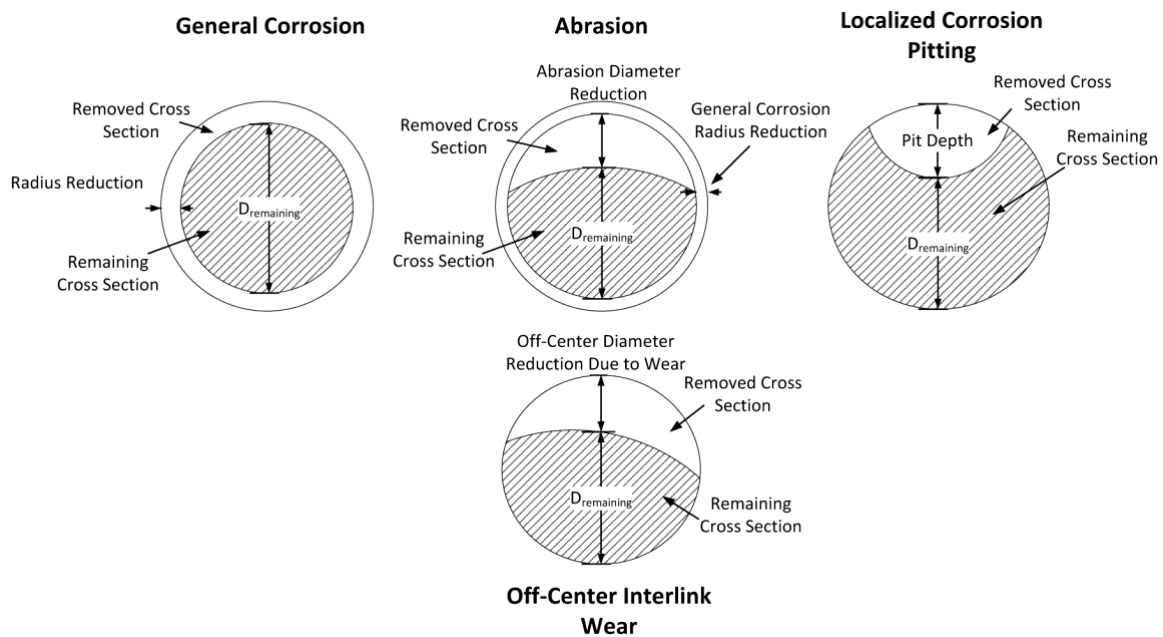


Figure 3-3: Illustrates the four types of degradation modes and their impact on the mooring chain cross-section.

Corrosion may be directly responsible for some mooring component structural failures. This corrosion has occurred in both uniform and non-uniform patterns. Non-uniform corrosion, in particular, when the material loss is localized and produces a reduction in capacity in important parts of the mooring component, has long been recognized as a primary driver of mooring system deterioration and a trigger for mooring replacement. Microbiologically Influenced Corrosion(MIC) is commonly blamed for such localized material loss and is briefly discussed in section 4.2 [16].

3.2. Mooring configuration and corrosion

A mooring system traverses the entire water column, with a significant portion of it often resting on or on the sea bed. Before diving into what MIC is, it is necessary to know the regions where the mooring line expands in sea water and how corrosion interconnects with it. As it's shown in Figure 3-4 (and in the previous chapter), under catenary configuration, a typical mooring configuration is

- a chain at the top that extends near the sea surface in the region called the splash zone. This section of the mooring system extends from just above sea level to depths where the influence of waves on water flow is minimal;
- a wire rope in the middle of the submerged zone, and
- another chain submerged and is extended to the seabed in the region called the thrash zone.

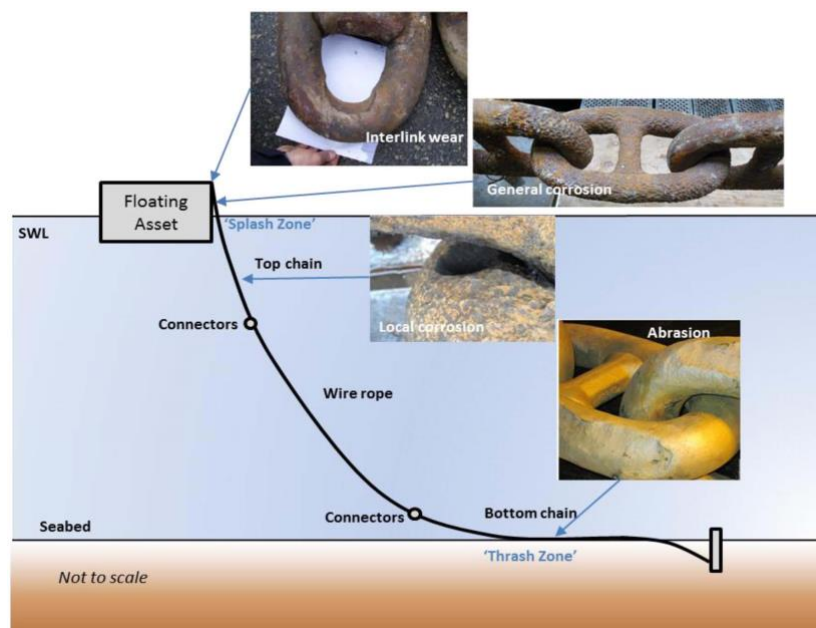


Figure 3-4: *Degradation Encountered in a Chain Mooring System [18]*

Typically, general corrosion occurs on the links in-air, in the splash zone, in the riser section and in deeply submerged chains. Interlink wear happens on links close to the fairlead and in the thrash zone. Local corrosion has been found on the links under the waterline and typically occurs under marine growth. Abrasion has been found on bottom chains in the thrash zone due to repeated contact with the seabed and a certain amount of dynamic motion. The degradation is often multi-modal, such as abrasion, local corrosion, or interlink wear combined with general corrosion [18]. In addition, the occurrence of microbiologically mediated corrosion along the mooring line, especially at the seabed, has a significant role, as discussed in the next chapter.

3.3. Offshore corrosion zones

Submerged zone of offshore structures can be divided into internal and external areas. Internal areas deal with the surfaces of tanks and flooded compartments in offshore structures. Mooring chains don't have internal areas. The external part of offshore structures is often separated into three

corrosion zones to ease corrosion control of structural steel: atmospheric zone, splash zone, and submerged zone.

Atmospheric zone: extends upward from the splash zone and is exposed to the elements, including the sun, wind, spray, and rain [19].

Splash zone: gets wet by Waves, wind-blown water spray, and tidal movements. The splash zone in the Gulf of Mexico, USA, is usually around 2 m thick. This zone is about 9 m thick in Cook Inlet, Alaska. During winter storms, the North Sea splash zone can reach up to 10 m. Coatings and cathodic protection (CP) are two methods for controlling corrosion in the splash zone [19]. Key characteristics of the splash zone:

- small segment is alternately aerially exposed and submerged in water during wave action.
- has an abundant oxygen supply.
- has significant marine expansion.
- water has a high speed due to wave action and FPSO activity during high sea states.
- seasonal fluctuations in wave activity and temperature occur in many geographical locations [17].

Submerged zone: is the area below the splash zone, which includes any construction below the mudline [19].

3.4. Service life of mooring chains

Mooring lines should be inspected on a regular basis to identify flaws and potential causes of line failure. If there is a problem with the mooring lines, they must be found as soon as possible in order to take action before the unit falls. There are two sorts of inspection: in-air and in-water. When FPSOs go from one area to another, air inspections are possible. In-air inspections are simpler than in-water inspections, although it may be more difficult to determine whether part of the chain have been in the thrash zone or the splash zone. Divers, autonomous robotic systems, or ROV-deployed systems are used for underwater inspections. Because mooring lines are very dynamic and possibly hazardous for unprotected divers, diver inspections are not recommended. The water depth is another element that restricts divers. Despite the development of autonomous robotic systems, they are sometimes too large and bulky for realistic offshore operations. Due to their size, it is tough to check the thrash zone and get near the fairleads. The ROV-deployed inspection system is the most established system

for underwater inspection. "Optical caliper" chain measurement equipment can be installed on an ROV to measure the size of a chain [19].

In the case of a mooring chain design for a new offshore platform, there are two options for ameliorating mooring line degradation during its design life. It can be protected using an appropriate corrosion allowance or the right cathodic protection system. In the case of a mooring line that is severely damaged, there are two options. The most obvious solution is to replace the damaged or broken mooring line with a new one, but this is a costly option. Another easy solution is to halt production and relocate the unit to a new location with a better mooring system. This is true for mobile units like mobile offshore drilling units (MODUs) or floating production and storage units (FPSUs) [19]. During replacement, mooring lines can either be designed with additional corrosion allowance or are equipped with a proper cathodic protection system (CP). The other option is to make them last longer, without replacing the mooring lines they are already attached to, by applying cathodic protection.

Typically, the owner specifies a CP system's design life, considering the probability that the protection object's design life will be extended. In addition, the design life must account for any period of time while the CP system is operational prior to the execution of the protection object. Maintenance and repair of CP systems for permanent offshore structures is frequently prohibitively expensive and infeasible. Consequently, employing at least the same anode design life as the protective object is customary. Under certain circumstances, a deliberate retrofitting of sacrificial anodes may be an economically feasible alternative to the original installation of very large anodes. Then, measures for retrofitting should be built into this option when it is first designed and built [20].

After inspection, it is necessary to make an analysis of the degraded chain to decide whether the chain needs to be replaced or protected, and this can be done using a finite element analysis (FEA).

Each one of these procedures, including corrosion allowances, finite element analysis for degraded mooring chains, and cathodic protection, are discussed in the following chapters, but inspection is out of the scope of this thesis.

4. Comparison of codes (standards) and research findings

The goals of this chapter are, first, to offer designers and operators useful information about expected mooring chain corrosion rates early in the design process. When considering the chain allowance for a mooring system design, it is recommended that this chapter be read alongside the Classification Society Rules and DNV guidance. And secondly, to provide typical and anomalous indicative corrosion rates that may help operators and integrity managers in their decision making process.

4.1. Mooring corrosion allowance from codes and standards

The loss of metallic area due to corrosion must be included in the design of long-term mooring systems employing steel mooring components like wire rope and chain. An allowance is often included in the chain size such that the degraded chain has adequate strength to resist the loadings imposed by the end of its projected design life. The American Petroleum Institute (API) (2005), Bureau Veritas (BV), Det Norske Veritas (DNV) (2013), and the International Standards Organization (ISO) (2013) suggested chain corrosion tolerances or allowances ranging from 0.1 to 1.0 mm per year, depending on the position of the chain link along the line and location in the world. Only DNV recommends differing corrosion tolerances in tropical waters and these guidelines were created in the context of mooring lines used in cold water settings. For comparison, corrosion rates from British Standard (BS) 6349-1 derived for steel components not susceptible to the combined corrosion-wear action of the mooring chain are presented. Galvanic corrosion or repetitive elimination of corrosion products are the two types of concentrated corrosion circumstances mentioned in the British Standard. All these regulations are mostly based on North Sea cold-water guidelines and codes.

Comprehensive investigations on the corrosion of steel mooring components reveal that, particularly in tropical environments, corrosion of both mooring chain and steel wire rope might be greater than in design guidance. Furthermore, current corrosion guidance provides little insight into the negative and positive impacts of environmental and operational variables on-chain and wire rope corrosion [15][20].



Figure 4-1: The North sea [21].

Table 4-1: Corrosion Allowances from DNV OS-E301, Recommended corrosion allowance referred to the chain diameter for different locations [22].

Part of mooring line	Corrosion allowance referred to the chain diameter			
	Regular inspection ¹⁾ (mm/year)	Regular inspection ²⁾ (mm/year)	Requirements for the Norwegian continental shelf	Requirements for tropical waters
Splash zone ⁴⁾	0.4	0.2	0.8 ³⁾	1.0
Catenary ⁵⁾	0.3	0.2	0.2	0.3
Bottom ⁶⁾	0.4	0.3	0.2 ⁷⁾	0.4

1) Recommended minimum corrosion allowance when the regular inspection is carried out by ROV according to DNVGL-RU-OU-0300 or according to operators' inspection program approved by the National Authorities if necessary.

2) Recommended minimum corrosion allowance when the regular inspection is carried out according to DNVGL- RU-OU-0300 or according to operators' inspection program approved by the National Authorities if necessary.

3) The increased high corrosion allowance in the splash zone is required by NORSOK M-001 and is required for compliance with PSA, see DNVGL-SI-0166.

4) Splash Zone is defined as 5 m above the still water level and 4 m below the still water level.

5) Suspended length of the mooring line below the splash zone and always above the touch down point.

6) The corrosion allowance given in the table is given as guidance., A significantly larger corrosion allowance should be considered if bacterial corrosion is suspected.

7) Investigation of the soil condition shall be carried out in order to document that bacterial corrosion is not taking place.

Table 4-2: Summary of mooring chain corrosion rates from various design codes [23].

Codes/Standards		Chain Wear Allowance (mm/year On Chain Diameter)		
		Splash Zone	Mid-Catenary Zone	Touch-Down Zone
ABS		Rates as per API RP 2SK		
API RP 2SK		0.2-0.4	0.1-0.2	0.2-0.4
ISO 19907-1		0.2-0.8	0.1-0.2	0.2-0.8
BS 6349-1	Corrosion Rate Temperate Waters	0.16-0.34	0.08-0.26 ²	0.08-0.26
BS 6349-1	Corrosion Rate Cold Waters ¹	0.11-0.23	0.05-0.17 ²	0.05-0.17
BS 6349-1	Concentrated Corrosion Rate (Cold Waters) ¹	0.33-0.53	-	0.33-0.53
BV NI 493		Rates as per ISO 19907-1 or API RP 2SK		
Lloyds Register		0.3	0.2	0.4

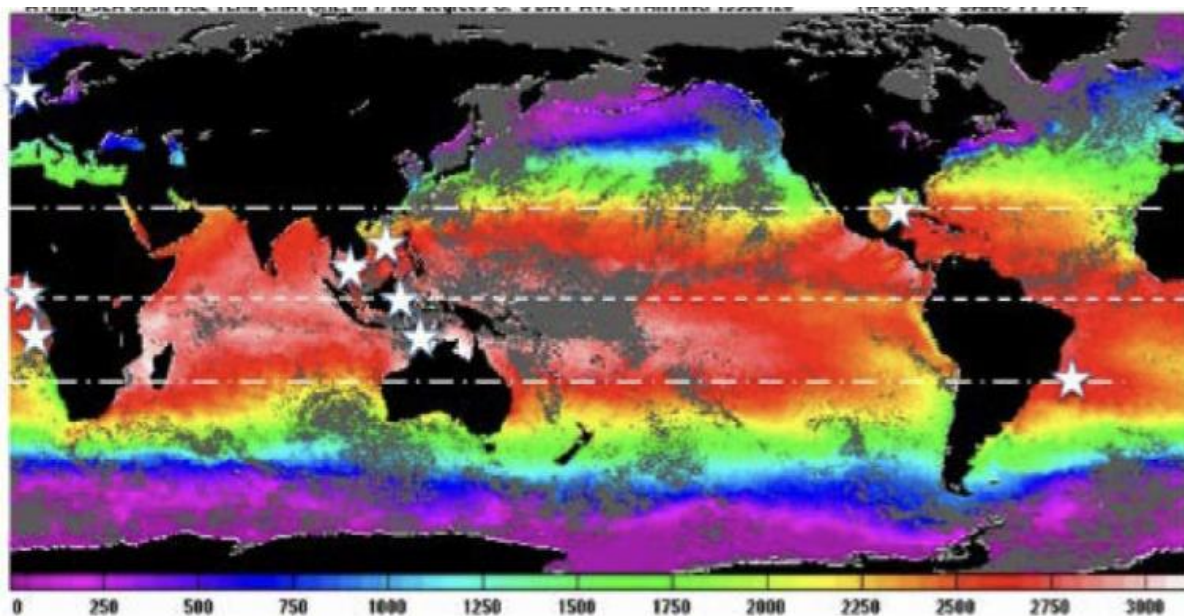


Figure 4-2: The location of the data source for the corrosion rate observation in the field [24].

This study is focused on the North-sea. and all results and analyses are made for this area. The North Sea covers a vast area as it's been indicated in Figure 4-1. The motivation of this thesis is inspired by a number of recognized problems in the industry located in the North Sea that hampered designers' and operators' capacity to accurately anticipate the corrosion of mooring components and their expected design life. Some of these problems were due to:

- the scarcity of codified information on the impact of site location and conditions (especially water temperature and MIC – Microbial Induced Corrosion) on the corrosion rates of steel mooring chains.
- the use of corrosion allowances in mooring chain design, deliberately obscured the relative relevance of this phenomena in various situations such as the use of corrosion allowances in different environmental conditions and locations. The corrosion rates might become higher than predicted rates of mooring chain corrosion made during design taken from the allowances.

The corrosion rate of certain specific sites is determined by different ranges in distinct design codes. There have been incidents of intense (high) corrosion and significantly less corrosion than these estimates. However, the origin of these statistics and other mooring codes are not well documented. Because the range that governs the structure's design is relatively broad, designers may opt for the lowest corrosion rate value to minimize upfront cost. On the other hand, a conservative designer may opt for the highest corrosion rate to improve safety assurance. Due to the high investment costs, the mooring system design is frequently based on the lowest predicted corrosion rate. The repair cost of a mooring system failure due to an underestimation of the corrosion rate factor is very high. When the risk of death and environmental damage posed by this mooring system's failure are accounted for, the cost is much higher. In the offshore business, mooring integrity is a major concern. In the past, several mooring system failures due to chain corrosion had resulted in the mooring system's actual design life being shorter than the operating service life. Most of the incidents occurred in tropical waters and rarely in other regions. These incidents are linked to microbiologically mediated corrosion (see section 4.2). To date, many design regulations for structures in tropical waters and other parts of the world have been based on those used in the North Sea, despite the fact that the environments are vastly different [18].

As listed on DNV 301 in descriptions 6 and 7 of

Table **4-1** , a significantly larger corrosion allowance should be considered if bacterial corrosion is suspected. An investigation of soil (seabed material?) conditions must be carried out to understand the bacterial influence on corrosion [22]. A comprehensive study on the effect of MIC was conducted by SCORCH JIP. Their findings are practical in relation to conditions set from the DNV standards.

4.2. Microbiologically influenced corrosion (MIC)

It is widely accepted that corrosion, particularly marine corrosion, is a complex process governed by a number of variables, including temperature, water velocity, pH, dissolved oxygen, nitrate concentration, water depth, hydrostatic pressure, bacterial activity, pollutants, erosion, and surface roughness [25]. Of all these variables, MICs play major role in compromising mooring chains.

Microbiologically influenced corrosion is a corrosion type influenced or induced by the presence of microorganisms on the surface of the material in question. Microorganisms accelerate the corrosion rate or modify the mechanism of corrosion. The high rates of localized pitting corrosion reported on moorings deployed in some offshore areas positively correlate with MIC. Bacteria, algae, and fungi are examples of microorganisms. Through their actions, the organisms do not create corrosion processes but rather amplify or accelerate established ones and increase the corrosion rate or shift the mechanism. Their metabolic byproducts may drive corrosion-related processes, or their consumption or absorption of molecules may alter the neighbouring environment in such a way that reaction rates vary[17].

There have been instances of MIC on mooring system components that were severe in terms of reported corrosion rates or had resulted in failures. Irrespective of MIC or other causes, the industry's major concerns are unexpected breakdowns and/or anomalous corrosion. Understanding the mechanisms and hazards may help enhance procedures and decision-making in the area of integrity management [17].

The high rates of localized pitting corrosion reported on moorings are closely linked with MIC. Hence, it is important to understand the mechanisms by which they are linked with corrosion. It has been hypothesized that non-uniform corrosion, shown as asymmetric material loss of chain links in contact with the seafloor, is predominantly caused by the MIC process. According to several research, long-term pitting is substantially impacted by the activities of microorganisms, resulting in microbiologically induced corrosion (MIC).

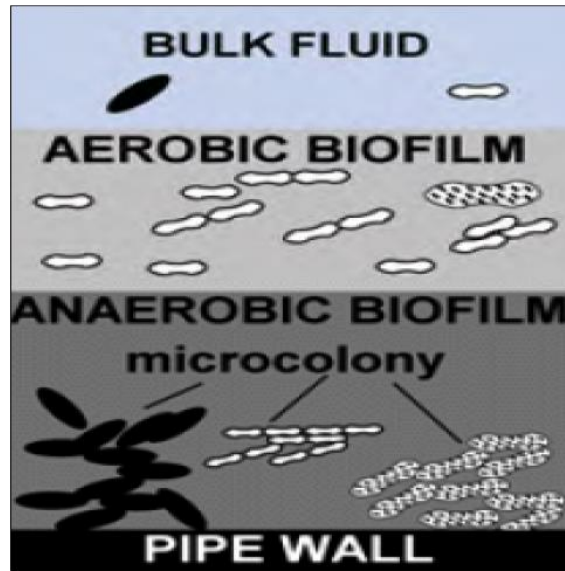


Figure 4-3: *Illustration of build-up of bio film on a steel surface*

Microorganisms settle and grow as components of biofilms (Figure 4-3), which form on all subsea surfaces, including steel exposed to water. Typical microorganism groups associated with MIC include:

- sulfate-reducing prokaryotes (SRP), also referred to in older literature as sulfate-reducing bacteria (SRB),
- sulfide-producing prokaryotes (SPP),
- methanogens,
- acid-producing bacteria (APB),
- hydrocarbon-degrading prokaryotes (HDP),
- acetogenic organisms,
- nitrate-reducing bacteria (NRB),
- nitrite-oxidizing bacteria (NOB),
- metal-oxidizing bacteria (MOB) and metal-reducing bacteria (MRB), and
- fermentative hydrogen sulfide-producing bacteria. [16]

There is a wide diversity of bacteria in the water environment, and there are likely more bacteria that have yet to be found and described than those that have. Figure 4-4 is an enlarged image of typical Sulphate Reducing Bacteria.

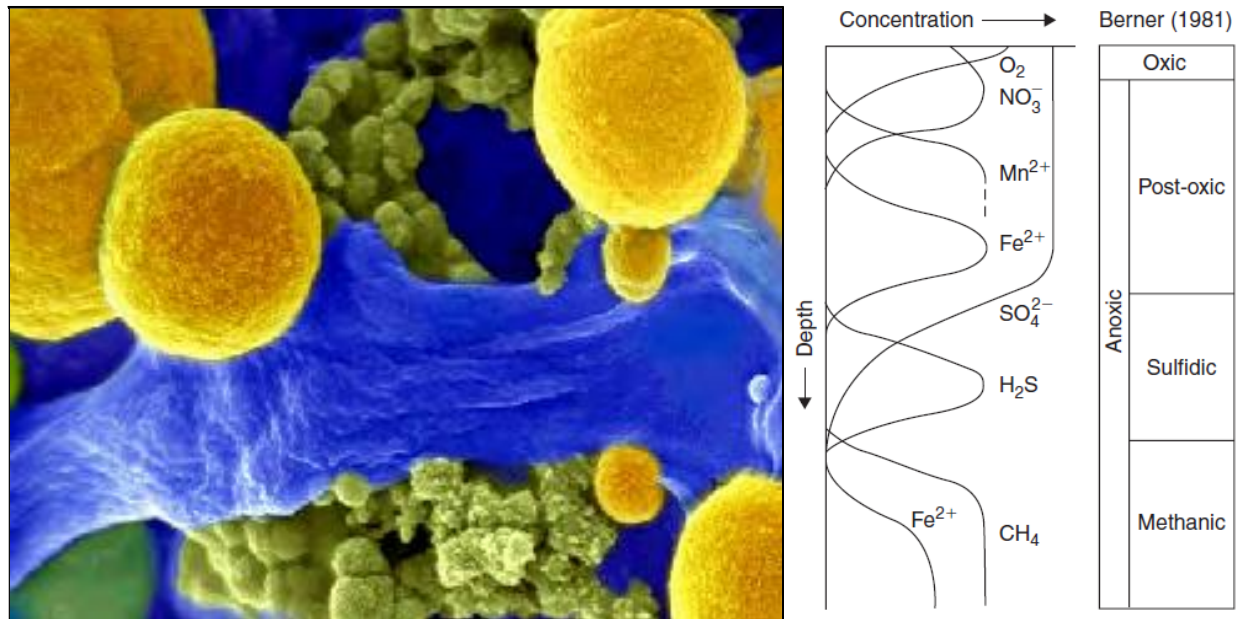


Figure 4-4: Example of Typical Sulphate Reducing Bacteria

Micro-organisms are dependent on water, nutrients, and electron acceptors for existence. Typically, seawater includes carbon, nitrogen, phosphorus, and sulfur in forms that facilitate microbial metabolism [24]. Bacteria require nutrients for energy and growth. Carbon, nitrogen, phosphor, and sulphur are the primary nutrients. These nutrients must be present in the proper amounts for a certain variety of bacteria. Shortage of nutrition restricts the bacterium's activity [17].

All charges of MIC in connection with mooring systems are based on SRB. It's widely regarded as the primary hazard under the conditions in which mooring chains function. Bacteria require electron acceptors for respiration, commonly oxygen. In anaerobic (oxygen-depleted) environments, bacteria utilize nitrate (NO_3^-) as an electron acceptor to produce nitrogen (N_2). The next electron acceptor is sulphate (SO_4^-), that is reduced to H_2S . Once the sulfate is removed, the reducing environment becomes methanogenic in which CO_2 and organic matter are electron acceptors to produce methane (CH_4). Some bacteria are strictly aerobic or strictly anaerobic, while others can live both with and without oxygen. Some bacteria only use a small amount of oxygen [16]. The metabolic byproducts, organic acids, reduced metal ions, hydrogen sulphide, methan, and other chemicals alters the microenvironment and surface chemistry, thereby influencing corrosion-related reactions [17].

Bacteria require nutrients for energy and development in order to function. Carbon, Nitrogen, Phosphor, and Sulphur are normally required for this. These components must be present in the proper amounts for a certain variety of bacteria, since a shortage of nutrition will restrict the bacterium's activity. [17] Existing as bacteria, fungus, and micro-algae, micro-organisms are

dependent on water, nutrients, and electron acceptors for existence. Typically, seawater includes carbon, nitrogen, phosphorus, and sulfur in forms that facilitate microbial metabolism.[24]

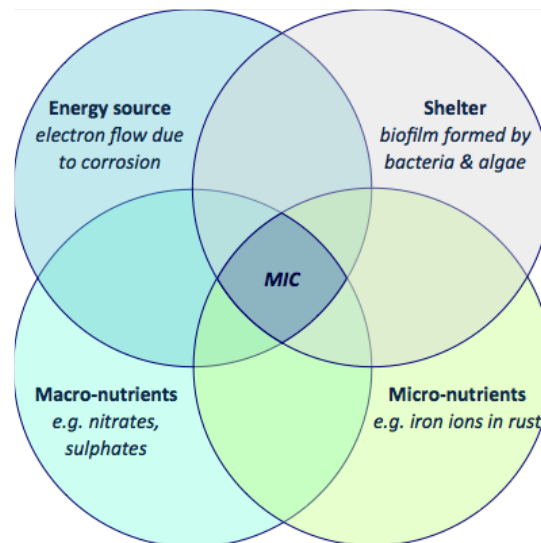


Figure 4-5: Preconditions for Development of MIC[16]

Bio-films are often a heterogeneous mixture of bacteria, slime substances known as extracellular polymeric compounds and organic macromolecules. It is made of clusters of bacteria cells, as well as voids and channels. Adhesion to a steel surface is depends on various parameters, including surface characteristics, film composition, and chemistry. Bio-films are frequently irregular, which can result in the formation of concentration cells for certain substances and impact the development of anodic and cathodic areas, which can lead to corrosion. Lateral differences in bio-film formation can result in low oxygen concentrations in some parts, resulting in anodic sites with cathodic sites in areas where oxygen is more prevalent [17].

Bacteria proliferate rapidly, and when metal is submerged in saltwater, a biofilm similar to that seen in Figure 4-6 forms within the first few hours. A biofilm is a coating of bacteria that attaches to the metal's surface and may subsequently develop into biodeposits. Bacteria in biofilms can facilitate the survival and proliferation of other bacterial species by fostering favourable conditions [24]. When a bio film builds up in thickness (but still thin in comparison to macro fouling), typically, oxygen consumption is high on the surface. This results lowering of oxygen concentration as a function of depth into the film, possibly resulting in anaerobic conditions close to the steel surface. Thus the bio film can generate environments where anaerobic bacteria can become active, provided they are present along with the right electron acceptor they require for metabolism [17]. For example, bacteria

at the biofilm-water interface receive nutrients and oxygen from the saltwater, which they can convert into simple polymers, fatty acids, and other waste products. These byproducts can serve as a source of nutrition for bacteria located deeper into the biofilm profile. As they concurrently consume oxygen at the water interface, they provide an anaerobic environment near to the metal surface, which can support the survival of anaerobic bacteria [24].

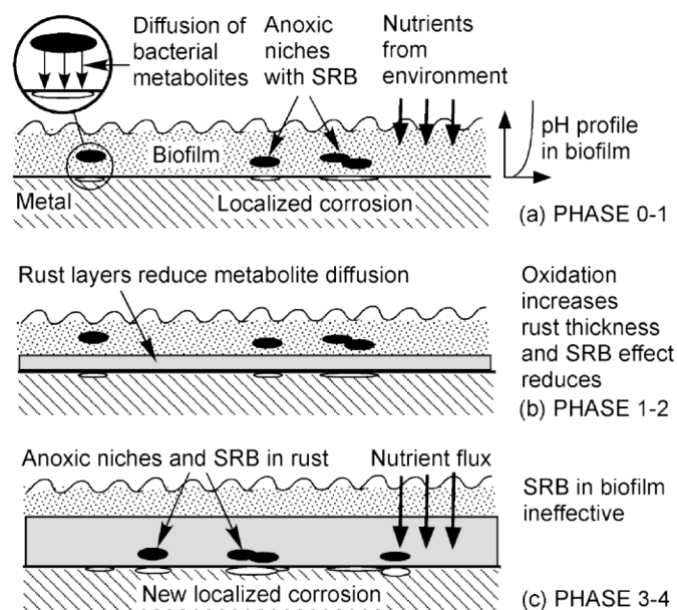


Figure 4-6: Progression of SRB involvement [24]

In short, the mechanisms of MIC include:

- production of chemicals that create a corrosive environment,
- creation of concentration cells on the metal surface,
- attack of surface films,
- acceleration of anodic or cathodic reactions, and
- alteration of the chemical environment [24].

A chemical gradients runs throughout the bulk thickness of a bio-film is essential for the activity of various bacteria. Bacterial activity in a biofilm might be high in certain regions and low in others, depending on the local environment. Some bacteria's metabolic products, as well as dead bacteria, can feed on other bacteria [17].

One critical question is the significance of the different types of bacteria and their role in the conditions under which mooring lines work. Some bacteria leave no evidence that can be directly linked to their activities and can only by their species identification. Some bacteria, SRBs in particular, can leave quantifiable traces of their activity. Their byproduct, hydrogen sulphide, interacts with iron to form iron sulphide (FeS). Iron sulfide has very low solubility in water and deposits a measurable layer [17].

A single variety of microbe can impact corrosion through many processes at the same time [17]. It is important to note that not all bacteria survive independently. Their cohabitation and interaction with other bacteria are critical to the likelihood of MIC. These organisms can coexist naturally in the biofilms that form on surfaces almost immediately after exposure. They can form synergistic communities (consortia) that can influence electrochemical processes through cooperative metabolism that is not observed in the individual species [24].

It should also be emphasized that biofilms and microorganisms can help to reduce or prevent corrosion. Biofilms can impede the transfer of oxygen to the steel surface, lowering the cathodic reaction rate. There have also been reports of certain bacteria that, by their activity, change reactions in such a manner that corrosion processes are slowed. The use of iron-reducing bacteria or magnetic bacteria to regulate or mitigate MIC the potential induced by other bacteria [17].

4.2.1. MIC on mooring systems

As previously stated, a mooring system will traverse the whole water column, with a significant portion of it often resting on the seabed. In general, sea water contains a diversity of microorganisms and has a dissolved oxygen content of 8 ppm or less. Because air is mixed in as a gas phase, the oxygen content of near the sea surface is higher. Anaerobic bacteria, such as SRB, may exist, but they are not be active until they reach places favorable for their metabolism [17]. The effect of MIC in different zones of seawater are described as follows:

A. Upper part

Depending on prevailing conditions in the splash zone (see section 3.3), biofilms can form on steel surfaces in conjunction with macrofouling. The biofilm varies significantly in terms of composition and density throughout the surfaces. The macrofouling may encourage the formation of protected niches within the biofilm, allowing for a range of bacterial activity. The macroscopic marine development can also provide nutrients to the bacteria in the biofilm. In general, the settings are favourable for the development of MIC, in terms of corrosion "cells" with varying aerobic and

anaerobic conditions. High dissolved oxygen concentration in the splash zone cause corrosion. Seasonal or periodic shift of strong tidal waves can eliminate both macro fouling and bio-film, resulting in aerated conditions previously anaerobic regions while the biofilm is intact. Some of the most severe corrosion due to SRB can occur when the circumstances fluctuate between anaerobic and aerobic settings. As a result, the importance of removing macrofouling and biofilm should not be overlooked [17]. Unlike in the north sea, these situations usually happen in tropical regions due to higher water temperature and other factors like nutrient levels. The majority of documented occurrences are from cold climates, with the most severe corrosion occurring in warmer zones.

B. Bottom part

Seafloor environments vary significantly. Mud, sand, gravel, organic matter, and other materials are present in variable quantities and thicknesses. Micro organisms require nutrients to function, and their activity on the seafloor depends on the availability of organic material such as dead plants and marine organisms. It varies with location and water depth. Usually bacteria use organic matter of dead marine organism from the water column. If the sea floor has thick layers of mud and sand, one can expect bacterial activity on the surface layer. Aerobic bacteria at the top and anaerobic bacteria immediately below if the aerobic bacteria have depleted oxygen. The likelihood of bacterial activity below the top layer is very small if no organic material is deposited into the soft bottom layer. Pollution from drill cuttings and other disposals can combine hydrocarbons with sediments (deposits of high nutrient material) on the sea floor, producing the ideal habitat for high bacterial activity that increases the risk for MIC. High quantities of organic material can also originate from other sources, such as adjacent rivers, naturally and anthropogenic pollution. Chains in the touch down zone may rest at the bottom of the seafloor or may be suspended in the water above the seafloor. As a result, conditions along the chain might range from anoxic to oxic, resulting in higher corrosion rates. If there are reasons to believe that there are risks of bottom chain corrosion, mud and bottom sediments should be analyzed for pollution in different layers (typically top layer, 3-5 cm into mud, 15-25 cm, and 50-100 cm depth) to measure and quantify organic nutrients, bacterial activity, sulphides, metals, and other indicators [17].

In order to check the presence of MIC it is necessary to take samples from Corrosion products from chain links associated with the presence of SRP, mud and water(elevated level of nitrogenous material which can increase the amount of corrosion and pitting in seawater environments).



Figure 4-7: *Chain Links from the Touchdown Zone, Uncleaned and Cleaned*[16]

Visual signs on chain links, such as black crusts of corrosion product and a shiny steel surface visible beneath (after high-pressure water jet cleaning), are described as consistent with SRP. The mechanism for the accelerated material loss is subsequently identified as MIC where the chain link was in contact with the seabed [16]. To lower inaccuracies in the identification of corrosion visually, numerous phases of corrosion and their effect on servicing damaged chain are incorporated in Melcher's model (Figure 4-11 and section 4.4.2).

4.2.2. Diagnosis of MIC

Diagnosis of MIC in the field can be difficult, relying mostly on visual examination and microbiological reactivity assays. Both methods have limitations in terms of accuracy and reliability. As a result, various types of corrosion and wear can be wrongly identified as MIC, potentially influencing later mooring system integrity maintenance [16].

The first step in evaluating impact of MIC is to investigate all other probable causes of corrosion. If this fails to produce a credible explanation, the possibility of MIC should be investigated [17]. Four main steps are recommended in order to investigate MIC:

- i. Identify the microorganisms involved.
- ii. Determine the morphology of the corrosion pit.
- iii. Characterize the chemical environment and corrosion product.
- iv. Recreate the environment in a laboratory setting to demonstrate the postulated process.

4.2.3. Prevention of MIC

- Avoid contamination from oil drilling, production operation, and other nutrient depositions to prevent MIC.
- Cathodic protection using anodes or impressed current can be used; however, overprotection potential should be avoided as it might cause hydrogen embrittlement and hydrogen-induced fracture (HIC). For more, refer to chapter 6.
- Avoiding anaerobic conditions can help reduce SRB effect. But this may be difficult to attain if anaerobic conditions develop beneath biofilms. Periodic cleaning can exacerbate the problem. It has been observed that fluctuations in oxic and anoxic conditions are the most crucial element in SRB corrosion.

4.2.4. Consequences of MIC

- Higher metal loss rates drive chain link thickness below the minimum break load.
- Sharp pits might serve as the starting point for fatigue cracks.
- Hydrogen created by SRB activity might cause embrittlement and HIC, but no clear evidence for chain failures has been documented.

4.3. SCORCH JIP

4.3.1. Overview of project

One of the best research made on corrosion of mooring chains was the SCORCH JIP. SCORCH JIP (Seawater Corrosion of Rope and Chain Collaborative Research Industry) is a multi-stakeholder joint project that looks at how chains and mooring ropes corrode in tropical waters in different parts of the world. The SCORCH JIP's goal was to explore and describe the corrosion of steel chain and wire rope moorings on a variety of Floating Production Units (FPUs) and Floating Production Storage and Offtake vessels (FPSOs) operating in a warm sea (particularly in tropical water). Prior to the SCORCH JIP, there was little evidence of greater corrosion rates for chain moorings in tropical waters, and most of it was anecdotal. The SCORCH JIP entailed an enormous, detailed input of corrosion measurements from oil and gas corporations and contractors all around the world. In warmer seas, operators have observed faster corrosion rates in wire rope and chain for years. The corrosion resistance(allowance) of these components is mostly specified by mooring design rules based on experience from the cooler waters of the North Sea.

Through over 750 sample and full-scale experiments spanning 3.5 years at sites around Australia, the SCORCH JIP looked into the effects of sea temperature, water velocity, depth, oxygenation, steel grade, and chain and wire rope construction. Microbiologically Influenced Corrosion (MIC) and the combined effect of corrosion and wear on mooring chains were also investigated in the lab. This study was conducted on three locations along the coast of Australia. The chain samples were reviewed every six months during a two-year exposure period (Figure 4-8).



Figure 4-8: Corrosion site testing by SCORCH JIP[15]

In addition, the SCORCH JIP database compiled detailed corrosion measurements and inspections from in-service and retired mooring chains of 18 FPSOs in warm waters of Southeast Asia, West Africa, the Gulf of Mexico, Brazil, North Sea, and Australia's North West Shelf. To provide an up-to-date and complete database of corrosion endurance, these results were added to a compilation of measures from technical literature (see Figure 4-9). The database included measurements of uniform and pitting corrosion in different zones of the mooring chains. [20]

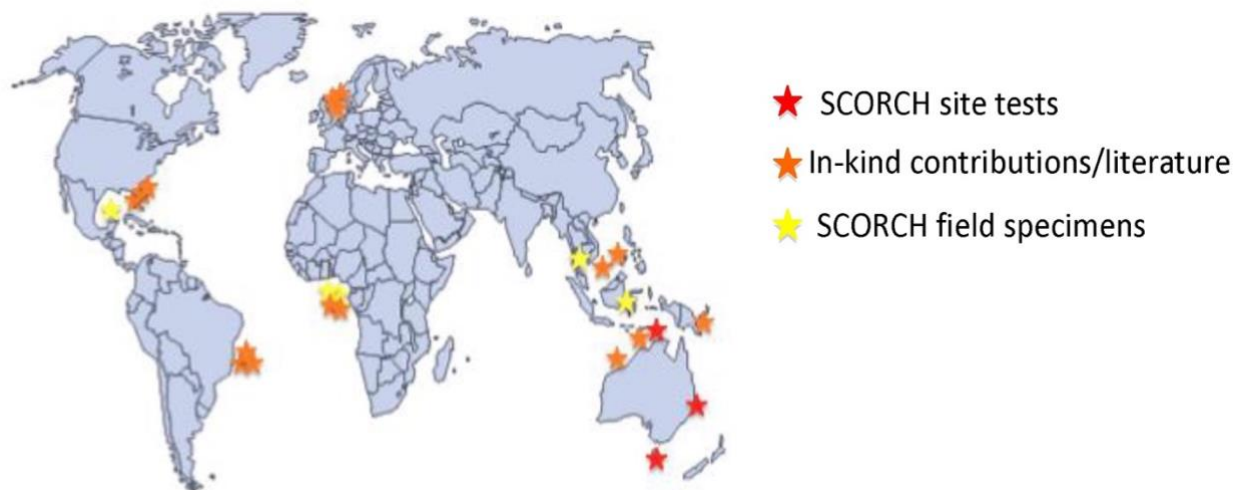


Figure 4-9: *Contributing locations to SCORCH JIP corrosion data*

The SCORCH JIP has yielded a number of results that have long-term significance for the industry, including extensive analyses of corrosion parameters such as MIC, chain pitting, chain wear, wire rope blocking compound effectiveness, and the influence of environmental and operational factors. The SCORCH JIP has tabulated corrosion forecasts for various temperatures, mooring line placements, and nutrient levels that might favour MIC. The forecasts are based on large number of field test data from operational FPU's, and they're backed up by thorough operational instructions and recommendations for extending the life of the moorings [20].

According to SCORCH JIP, in order to analyze the corrosion rates, the effect of a variety of variables on corrosion should be considered, including:

- water temperature;
- MIC, especially with respect to dissolved nutrients such as Dissolved Nitrogen (DIN);
- current velocity;
- chain grade; and
- chain link location along the mooring line.

The study determined that pitting was caused mostly by MIC, probably related to SRB. The nutrient content in the water was shown to be directly related to pitting corrosion. Nitrate levels were extremely high, far higher than in typical coastal saltwater. This was considered to be the outcome of significant agricultural fertilizer runoff, which provided huge doses of nitrate and other nutrients known to increase bacterial activity. Chain link MIC deterioration has been observed to be considerable at specific areas within the submerged near-surface zone and may be the controlling

mechanism for chain life. While it was not the goal of the SCORCH JIP to completely examine the causative processes and implications of MIC, the project did identify the possibility of severe corrosion as a result of MIC, which needs additional investigation. Lee and Melchers provided a full account of the SCORCH findings as they pertain to MIC, as well as subsequent studies that advanced our knowledge of these phenomena [15].

4.3.2. SCORCH JIP findings

The SCORCH JIP brought up a variety of operational factors, such as improved design guidelines and operational considerations to maximize the life of chain links in functioning mooring systems. The following is a summary of key points:

- When developing inspection programs for mooring lines, extra attention should be paid to the sites with the highest probability of rapid chain deterioration. When there is a greater nutrient concentration in saltwater with a high temperature, it is also reasonable to anticipate high uniform corrosion above sea water level and high pitting corrosion in the upper water column below sea water level.
- Periodically assessing the seawater temperature and nutrient contents, as well as any discharges from the floating facility, is necessary to determine the floating facility's possible vulnerability to pitting corrosion.
- The uniform corrosion rates around a chain link will vary according to the surfaces' exposure. Away from the interlink contact zone, the body of the link will undergo uniform corrosion across the whole diameter of the bar, which will eventually settle to the long-term anaerobic corrosion rate. If there is little interlink motion in the interlink contact zone, the oxide biofilms will remain intact and there will be negligible corrosion on the contacting surfaces. Significant regularly occurring interlink movements will tend to dissolve the oxide biofilm layers, resulting in fast early phase corrosion on the interlink contact surface.
- Seawater temperature, dissolved oxygen, water particle velocity, splash zone action, tidal zone wetting and drying, and nutrient contents were found to strongly regulate uniform corrosion of steel chain links (in particular, dissolved nitrogen). At various points along the mooring line, from the fairlead through the splash zone, upper catenary, lower catenary, thrash zone, and ground line, uniform corrosion rates vary.
- Particularly if there is a considerable pitting corrosion loss in the upper water column, lengthy corrosion resistance service lives will not be achievable. In the design of new mooring systems for tropical environments with high nutrient concentrations, the top length of the

mooring chain should be set to facilitate replacement on a periodic basis. During inspections of historical mooring systems, special attention should be paid to the quality of the chain, and if substantial pitting is observed, preemptive replacement should be planned for.

- One of the deliverables of the SCORCH JIP is a steel chain corrosion model (based on Melchers' five-phase empirical model) for different environmental exposure circumstances and load duty effects inside the mooring line configuration. This model was calibrated using steel coupon data from engineering literature, field exposure experiments of mooring chain coupons, retrievals of mooring chains evaluated during the SCORCH JIP, and operator-provided measurements from in-service mooring chains. The SCORCH JIP also proposed models for the development of MIC pits over time.
- It has been determined that Melchers' five-phase empirical model is suitable to the characterization of uniform corrosion of steel mooring chains. In simple words, the early phases of corrosion are dominated by aerobic corrosion, whereas the long-term corrosion rate is determined by the growth and maintenance of anaerobic corrosion. Early-stage corrosion progresses at a quick pace until the formation of oxide and biofilms. After that, the long-term corrosion rates are drastically reduced. If the oxide and biofilm layers are eliminated by mechanical action or washing, the increased short-term aerobic corrosion rate will be reinstated.
- Current industrial practice for mooring inspections comprises brushing or high-pressure spraying on the outside surface of the chain. The results of SCORCH JIP show that such techniques are expected to significantly lower corrosion endurance by removing the oxide and biofilm layers, hence reactivating a greater aerobic corrosion rate. Consideration should be given to cleaning techniques that do not have such negative results.[20]

According to SCORCH JIP research, service lives estimated using the SCORCH JIP chain corrosion model in cold-water conditions (annual average water temperature approximately 10 °C) and low nutrient concentrations (0.2 mgN/L DIN) are generally consistent with existing design guidance for mooring chains in these conditions[20]. This means, considering these conditions, the allowance from the DNV standards can be used for an area in the North Sea without any problem. If values of these parameters are large, concurrently, a significantly larger corrosion allowance should be considered. In order to come up with these additional allowances, the empirical estimation for corrosion loss by Melcher (year) seems practical. The SCORCH JIP resulted in the creation of analytical/semi-empirical models for forecasting corrosion of steel mooring chains and steel wire rope in a variety of realistic field circumstances, including high nutrient levels that induce MIC.

The Melchers model was built for uniform corrosion, however, it may also be used for non-uniform corrosion processes with caution (see section 4.4) [16].

In response to reports of extreme chain degradation, Scorch JIP developed a second JIP, Chain FEARS, to explore the loss of strength of severely deteriorated chains (chapter 5).

4.4. Empirical estimation for corrosion loss

4.4.1. Previous models

There have been two basic groups of previous attempts to build corrosion-time models for steel in seawater immersion: purely empirical models that can only be used in scenarios when the same conditions exist. Southwell's model is the most well-known of the first. Anaerobic conditions limit long-term corrosion, which develops swiftly in tropical seas. Using a linear combination of temperature and water oxygen concentration, Reinhart and Jenkins established a corrosion rate models. It was calibrated using only one year's worth of data. To that effect, they are not applicable outside the range of data they were calibrated against (one year). Corrosion data shows that the parameters characterizing the models are extremely sensitive to even slight changes in data. In addition, there is a lot of room for error in these models due to a lack of understanding of the impact of environmental processes on corrosion. Predictive outputs are limited to models that are based only on empirical data. Evans and Tomashev theorized ion transport through the corrosion product (rust) layer controls the corrosion process. It is comparable to Chernov and Ponomarenko's approach, except that oxygen diffusion regulates the oxidation process in their case. For seawater temperature, velocity, and salinity, they provided semiempirical factors. Two assumptions underlie all models: 1) Corrosion process is permanently governed by the diffusion-controlled phase, 2) which diffusion control begins immediately after immersion. Neither of these assumptions can be correct in general for several reasons. On the basis of previously established theoretical and empirical corrosion mechanics, a model with many phases (kinetic, diffusion, transition, and anaerobic) was put out. Melcher's models are more advanced version of the earlier model [26].

4.4.2. Melcher's model

4.4.2.1 Non-linear bi-modal corrosion trend

Structures exposed to seawater must be assessed for material loss continuously. As a result, strength loss is evaluated by describing the general corrosion that is anticipated to occur under near-surface immersion circumstances. For mild and low-alloy steel, general corrosion is the most significant kind of corrosion. Structural steel applications, such as mooring chains, commonly use these types of steel.

Pitting and other kinds of localized corrosion may be essential in these situations because they help with containment and local strength concerns. Only chains constructed of low-alloy steel are included in this discussion [26].

Diverse studies indicate that steel corrosion loss under maritime exposure settings is not a linear function of time. In addition to being a function of water temperature, it may also be affected by MIC. This is recognized as an effect of the nutrients in saltwater, namely dissolved inorganic nitrogen (DIN). As it has been described in previous sections (Section 4.2), the species often involved with corrosion of steel in saltwater are the anaerobic sulphate-reducing bacteria (SRB). Their metabolic byproduct, H_2S , has been regarded the root cause of MIC. In theory, a link between the long-term marine immersion corrosion loss of steel, the DIN content in the bulk seawater, the average water temperature, and the exposure duration may be empirically derived using just field measurements. However, a more practical method would be to additionally incorporate information gathered from previous research regarding the projected evolution of corrosion with exposure time [27].

A description of recently developed probabilistic, phenomenological models for generic corrosion loss is next given attention. An example of a basic application for MIC corrosion is provided in the case study chapter to demonstrate the ideas.

Melcher developed a multi-phase phenomenological corrosion loss–time model (Figure 4-10) based on data and other comparable influencing parameters for sites across the world. The model is divided into two major categories: aerobic corrosion and anaerobic corrosion. There are many phases within each division, as outlined in Table 4-3 and Table 4-4 [28].

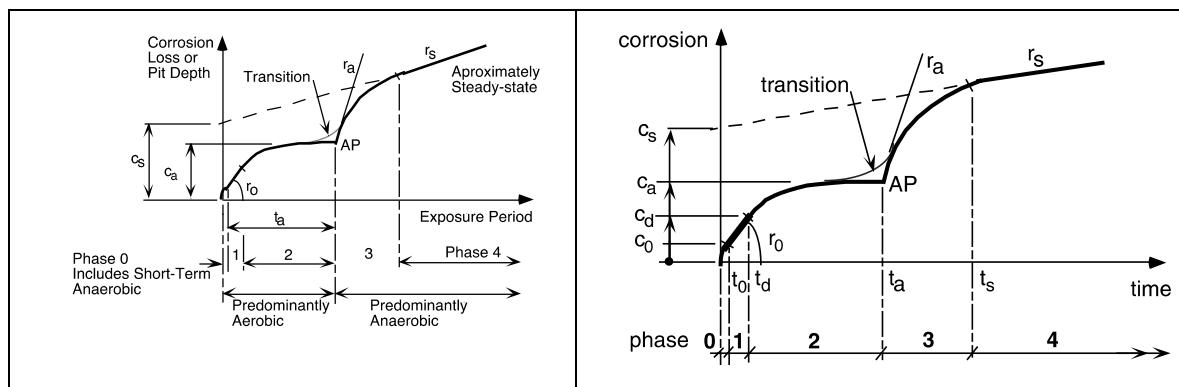


Figure 4-10: Multi-phase phenomenological corrosion-time model and adopted parameterization.

Table 4-3: Description of the phases of the model[16]

Phase	Corrosion Process
0	On immersion, the steel surface is colonized by biofilm, bacteria, and marine organisms and subject to a complex mix of localized influences. Bacterial metabolites may influence early corrosion if nutrient supply is elevated.
1	Oxidation process is controlled by the flux rate of oxygen at the metal surface from the surrounding seawater ('oxygen concentration' control). Rust layers are still very thin. The resulting corrosion loss may be modelled closely as a linear function.
2	Build-up of corrosion products (rust) increasingly retards the rate of oxygen supply to the corroding surface ('oxygen diffusion' control). Increasing thickness of the rust layer reduces the capability for oxygen to reach the corroding surface, thereby allowing localized anaerobic conditions to develop at AP.
3	Anoxic conditions permit changes of corrosion mechanisms at the corrosion interface, including the occurrence of microbiological activity, principally caused by the sulfate-reducing prokaryotes (SRP). Their effect on the rate of corrosion depends on the rate of bacterial metabolism. This depends on the rate of supply of nutrients, including those stored in the rust layers.
4	This is a semi-steady state phase that may involve the metabolism of SRP as well as other processes, including the slow loss of the rust layer through erosion and wear. It may be modelled as an almost linear phase in time.

Table 4-4: Summary of phases of corrosion loss–time model[28]

	Phase	Description of rate controlling process
Aerobic	0	Very short-term activation polarization with the influence of water velocity and other short-term influences
	1	Oxygen diffusion through surrounding water (concentration control)
	2	Oxygen diffusion through corrosion products
Anaerobic	3	Approximately steady-state anaerobic activity
	4	Anaerobic activity fostered by aerobic-based energy sources

It has been determined that Melchers' five-phase empirical model is suitable to characterise uniform corrosion of steel mooring chains. In other words, the initial phases of corrosion are predominantly aerobic, but the pace of corrosion over the long term is determined by the formation and maintenance of anaerobic corrosion. The initial phase of corrosion progresses rapidly until oxides and biofilms become well-established. After that, the long-term corrosion rates are drastically reduced. If the oxide and biofilm layers are removed by mechanical action or washing, the increased short-term rate of aerobic corrosion will be restored [15].

Melchers' approach is used to model the corrosion that happens in the mooring chain. By splitting corrosion into two stages, the short-term phase and the long-term phase, this model can be used to

investigate uniform corrosion. These two phases can be used to make useful corrosion trends for metals that are submerged in seawater [29].

The unshaded half in Figure 4-11 depicts the short-term general corrosion loss function, in which the corrosion layer (c_d) grows as the corrosion rate (r_o) increases over time (t_d). Temperature has a significant impact on the corrosion that happens in phases 0-1 [29].

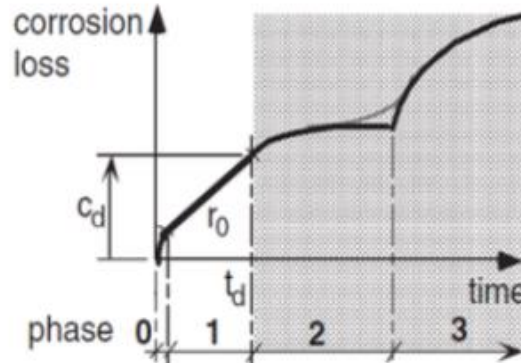


Figure 4-11: Melcher's model, shows short-term (unshaded part) corrosion loss-exposure time model. [28]

Melchers' model proposed two ways of corrosion loss estimation methods. 1) For the 5-phase model, water current velocity data are required in addition to water temperature and DIN/MIC. 2) The involved parameters were then inputted into a function to find corrosion loss estimates. This earlier non-linear model function is:

$$r(T, D, V) = r_o \cdot f(T) \cdot f(D) \cdot f(V) \quad (4.1)$$

Where

$f(T)$ is function for seawater temperature

$f(D)$ is function for DIN level

$f(V)$ is function for water current velocity

r_o is initial corrosion rate (mm/year/side)

r is corrosion rate affected by parameters above (mm/year/side)

An empirical estimate for corrosion loss is obtained after creating functions from the average temperature, velocity, and DIN level data. The involved parameters (water temperature, microbially influenced corrosion with respect to DIN, and current velocity) are plugged into a function to find the total corrosion loss estimates using the Melchers empirical model. As a sample of this method refer to , the reader can refer to the journal written by Hasan Ikhvani et al. (2021). The aforementioned study applied Melchers' model and incorporated a function that accounts for 'the chain's location along the line'.

For long-term immersed steels, like mooring chains, Melchers developed a corrosion loss model. This thesis addresses this later developed method as it can predict the long-term corrosion loss based on average water temperature and DIN.

4.4.2.2 Linearized corrosion rate estimation for long-term immersion steels

Steel corrosion in open saltwater is mostly impacted by water temperature. It is also be affected by microbiological activity, provided that optimal levels of essential nutrients are maintained in the water. The combined effect is explored in the case of considerable fluctuations in seawater temperature and dissolved nutrient content. There is a theoretical study of these effects functioning in conjunction, with or without time-dependent variations. The primary purpose of this part is to develop long-term immersion corrosion of mooring chain corrosion model that may be utilized efficiently in environments with considerable seasonal variations in water temperature and nutrient availability. This section addresses the estimation of fundamental corrosion loss – an exposure time model and its linearization under immersion settings with the combined effect of increased seawater temperature and DIN (dissolved nutrients) concentrations. Specifically, a quantitative link is established between immersion corrosion loss and the average DIN concentration in the saltwater around mooring chains.

Melchers' predictive model of corrosion for long-term immersion of steel may be effectively used in conditions with increased nutrient availability and water temperature. The model can estimate the additional corrosion loss due to MIC, which are indicated as points 6 and 7 of

Table **4-1** for the DNV allowances. A brief discussion of the methods and calculations is given in chapter 7.

As stated in section 4.2 and Figure **4-5**, it is recognized that microbial activity is contingent upon the availability of adequate microbiological habitats, energy supplies, and nutrients. In steel-saltwater corrosion scenarios, it is more realistic, albeit somewhat empirical, to attempt to construct connections between corrosion loss and nutrient availability, given that the other parameters for the

occurrence of MIC are typically met. This strategy has proven effective for both immersion and accelerated low water corrosion. In both instances, yearly averages of seawater temperature and concentration of the essential nutrient (mainly DIN), were deemed adequate [30].

Melchers' model relies on data from many different field exposure studies to calculate the influence of DIN concentration on long-term saltwater immersion corrosion of structural steels. As part of the previously described bi-modal corrosion loss model, a linear correlation model is employed to predict the long-term portion. A typical ocean temperature can be accommodated. The model can forecast long-term corrosion losses in nutrient-polluted waters with known average temperatures [27].

Major offshore structures can benefit from protective coatings, cathodic protection systems, or both, if they are properly maintained. A sacrificial corrosion allowance is often used to safeguard infrastructure like mooring chains, which are not well adapted to such procedures. When it comes to offshore constructions, corrosion allowances are usually expressed in terms of a corrosion rate expressed in millimeters per year (mm/y), meaning that corrosion loss is a linear function of time. Corrosion loss for steel under maritime exposure settings is not a simple linear function of time, according to a wide range of data. Corrosion that is caused by microorganisms can also have an impact, as can water temperature[27].

Steel's long-term corrosion loss in marine immersion can theoretically be correlated to a combination of factors, including DIN content in seawater and the average seawater temperature. A more sensible strategy, on the other hand, is to use the knowledge gathered from past research regarding the projected course of corrosion with exposure time. We will now go through the fundamental corrosion loss – exposure time model and linearized simplification in detail in this section[27].

As it has been discussed in section 4.4.2 part A, a nonlinear model for the progression of uniform or general corrosion through a number of successive stages was presented and calibrated using available long-term data that accounted for the substantial impact of seawater temperature. The theoretical foundation and corresponding mathematical expressions for the model's principal components have been described. The model has been modified and expanded to account for dissolved oxygen content, seawater velocity, and the impact of steel composition, and its applicability to tidal and marine coastal atmospheric exposures has been demonstrated.

Figure 4-12 depicts a schematic overview of the corrosion rates for long-term immersion. The solid line depicts the bi-modal corrosion trend under abiotic circumstances, whereas the dashed line demonstrates the influence of MIC on the longer-term corrosion loss.[27]

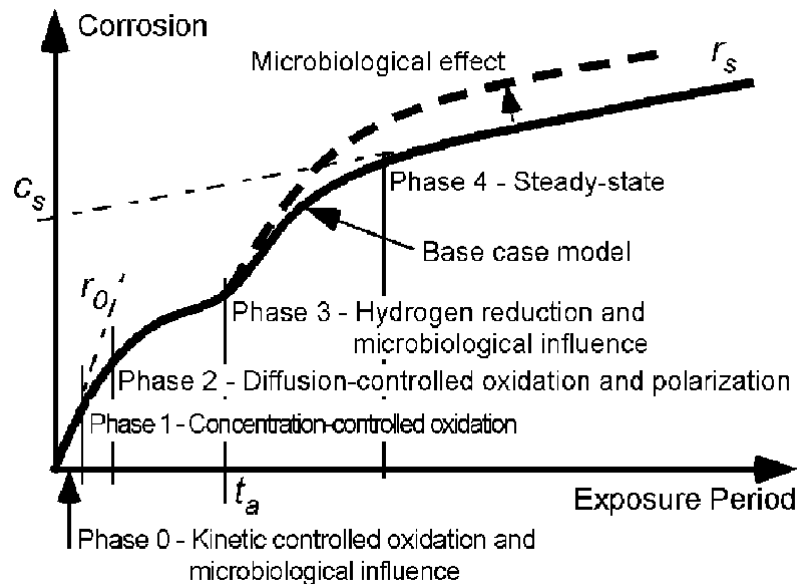


Figure 4-12: Schematic non-linear (bi-modal) model for the progression of corrosion loss with time showing the influence of some of the major parameters, such as the amount of nutrients and other factors, on long-term corrosion.

It is well-known that MIC may contribute to corrosion from the outset of exposure, as established by both laboratory and field experiments; however, for the purposes of this inquiry, only the effect on longer-term corrosion (phases 3 and 4) is of interest.

Based on literature data, it is expected that the model shown in Figure 4-12 may be reduced to the linear functional relationship seen in Figure 4-13 for long-term exposures. It is composed mostly of the linear function B–C showing the long-term trend of corrosion (phase 4 in Figure 4-12) back extended to intercept at $t = 0$ (point A). A refinement is to describe the rate of early corrosion loss as a linear function from $t = 0$ to $t = t_a$.

The linear function A–B–C does not pass through the origin, unlike the traditional average 'corrosion rate', it may be parameterized by c_s and r_s , which respectively represent the intercept and slope of the linear function on the corrosion loss axis. Both c_s and r_s are functions of mean seawater temperature, at least for unpolluted, aerated coastal seawaters with typical low water velocity and wave activity. The omission of phases 0–3 in the simplified model is acceptable for exposure periods above about $2 * t_a$ (Figure 4-12), where t_a is defined as a function of the temperature of the ocean.

In tropical seas, t_a is often less than one year, but in temperate waters such as the North Sea, it is around three years. Thus, c_s and r_s can be estimated as functions of both the average seawater temperature and the concentration of DIN in the bulk saltwater near to the steel.

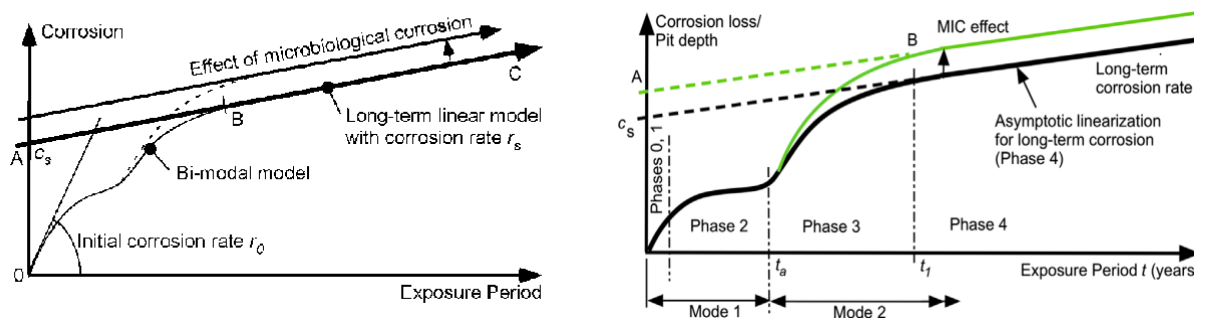


Figure 4-13: The model in Figure 4-12 for long-term corrosion is simplified schematically as a long-term linear function parameterized by c_s and r_s . This simplification is true for $t > B$. Also demonstrated is that the initial corrosion rate r_0 approximates Figure 4-12 for just a brief period of time (left figure).

Data analysis from field show positive correlation trends between c_s and r_s with their uncertainty estimates defined by ± 1 standard deviation. Uncertainty estimates for r_s of DIN level 0.4 mg N/L, 0.2 mg N/L and c_s of 0.4 mg N/L are shown in Figure 4-14. For exposures lasting more than six years, the effects of water temperature and DIN can be described using the linearized corrosion loss model depicted in Figure 4-13. It illustrates the bimodal model for the early phases of corrosion development and the linear asymptotic long-term corrosion trend given by the parameters c_s and r_s . For moderate annual fluctuations in seawater temperature and moderate annual variations in DIN, a substantial amount of data was used to calibrate these two parameters. Figure 4-14 illustrates the functional connections discovered earlier, extrapolated to slightly higher DIN values and also to lower average water temperatures [30].

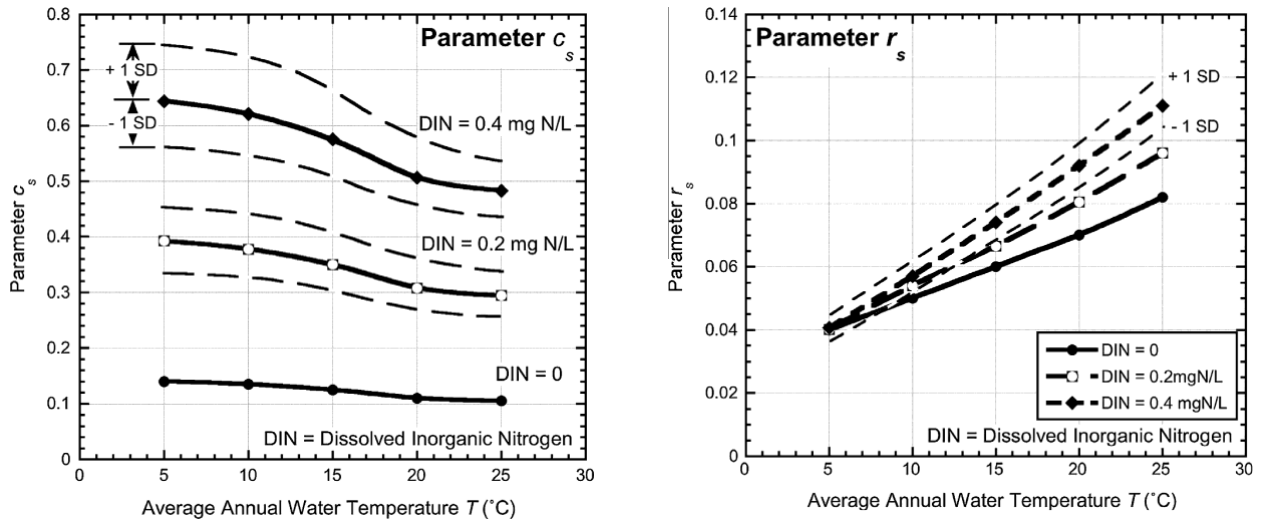


Figure 4-14: Parameter c_s (left) and r_s (right) (defined in Figure 4-13) as a function of average annual seawater temperature T and dissolved inorganic nitrogen (DIN).

In the North Sea, the highest water temperatures correspond to the lowest DIN concentrations, presumably as a result of the nutrient influx from major (fresh water) rivers. In general, the concentration maxima of DIN are influenced by human activities (fertilizer runoff and waste fluids that exacerbate eutrophication) and natural processes, such as biological processes and seasonal cycles of water flow. These remarks and observations suggest that a more refined approach is required to estimate the overall effect on corrosion, including that caused by MIC, when either or both the variations in water temperature and DIN concentration are high. Note that water temperature and DIN concentration are not highly correlated over time.

For longer-term exposures, corrosion loss of steel under seawater immersion circumstances may be modeled as a bilinear function of time as:

$$c(T, N, T_e) = c_s \cdot (T, N) + t_e \cdot r_s(T, N) \quad (4.2)$$

$c(T, N, t_1)$ is the corrosion loss at average seawater temperature T ($^{\circ}\text{C}$), average DIN concentration N (mgN/L) in the immediate vicinity of the corroding steel at time t_e (years)

$c_s(T, N)$ and $r_s(T, N)$ are model parameters (Figure 4-13), both functions of T and N , and typically the time t_1 exceeds 6 years.

Average water temperature and nutrient concentration is applicable only for areas with low variation in seawater temperature (around ± 5 $^{\circ}\text{C}$) and relatively small annual variations in DIN. Hence, the

calculation of corrosion loss for the long-term exposures is appropriate using average seawater temperature and DIN. The method is not applicable in locations with high variations in seawater temperature.

When MIC is predicted to be significantly greater than abiotic corrosion, it is necessary to determine an equivalent annual mean seawater temperature based on the portion of the year in which bacterial activity is sufficiently high for MIC to be non-negligible. This is due to the fact that the duration of metabolism necessary for MIC to occur is dependent on seawater temperature. Low seawater temperatures reduce bacterial activity nearly regardless of nutrient concentration.

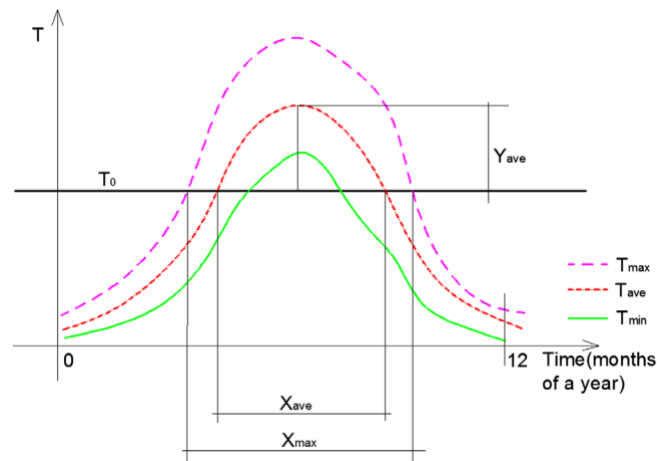


Figure 4-15: Annual change in seawater temperature as depicted by a diagram illustrating the analytical parameters

Let the temperature below which microbiological activity is extremely low be designated as T_0 . Assume bacterial metabolic rate is proportional to the seawater temperature above T_0 . By representing the analogous seawater temperature during this time as T_{cal} , using monthly recorded water temperature measurements (see Figure 4-15), the linear model can be written as:

$$T_{cal} = T_0 + Y_{avg} \cdot X_{avg} \quad (4.3)$$

Where Y_{ave} denotes the highest of the average temperature higher than T_0 over the time interval X_{ave} . Figure 4-15 depicts both parameters. Since the increase and fall in water temperature preceding and following the maximum typically occur fast (Figure 4-15), X_{ave} will typically coincide with the period when the seawater temperature is at or near its highest.

During the X_{max} interval, the value of N of interest is the average DIN for the corresponding (warmest) months. This value is denoted as N_{nom} and interpreted as follows:

$$N_{nom} = \frac{N_{max} + N_{mean}}{2} \quad (4.4)$$

The average temperature and nutrient concentration were used in all involved calculations in this thesis.

5. Effects of uniform corrosion on residual strength of degraded offshore mooring chain

To account for anticipated material loss due to in-service corrosion, the diameter of chain segments is increased during the design phase. A design code, as shown on

Table **4-1** and Table **4-2** typically gives a suggestion or requirement relating to an allowable yearly corrosion rate. This rate is multiplied by the mooring system's target design life to calculate the overall material loss allowance for the mooring chains.

Recent industry experiences have demonstrated that the material losses on chains caused by corrosion may exceed the design allowance in certain locations of the world. Material losses will reduce the strength of the chain. If the material loss exceeds the design allowance, the mooring systems may be unable to reach their design life (usually 20 to 25 years). This chapter aims to provide general guidelines on how degradation affects a mooring chain's minimum break load. A discussion of the down rating of aged offshore mooring chains guidelines, which outlines the factors to be considered in order to derive a minimum break load for an operational mooring chain, is included. Severely corroded in-service mooring chains should be inspected to evaluate their remaining expected life using a quantitative approach. Modern structural dependability theory, based on established mathematical ideas, is the most widely used method for determining a structure's remaining safe service life. This is usually implemented using finite element models.

In reality, different modes of degradation should be considered for the analysis of degraded chains, including general corrosion, localized corrosion with large single and dual pits, interlink wear, chain abrasion due to contact with the seabed and fatigue endurance of degraded chains. During design, neglect of degradation modes might result in deterioration rates higher than expected. The four types of degradation modes and their impact on the mooring chain cross section are shown on Figure **3-3** and Figure **3-4**. This thesis addresses uniform corrosion only because of data limitation and because the other degradation modes require either laser scanning or calliper measurement to obtain the degraded geometry of chains. As it has been discussed on section 2.3.2, mooring chains are classified in two, studlink and studless chain but this thesis will mainly concern with studless mooring chains. The design, properties, capacity, and ductile properties of studless chains will be discussed on the following sections before jumping to the assessment of degraded chains in chapter 8.

5.1. Chain design

Permanent anchoring methods have historically utilized studless or open link chains. Removing the stud decreases the weight per unit of strength and increases the fatigue life of the chain, but it also makes it difficult to manipulate the chain links [31].

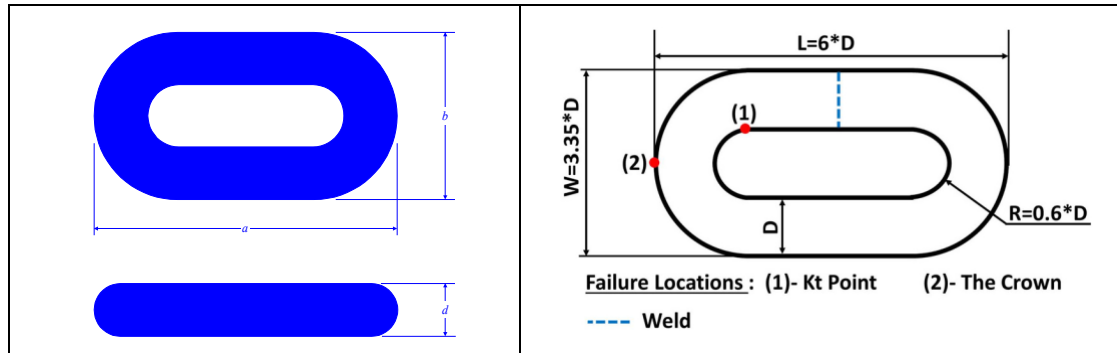


Figure -5-1: Common link design [31]

Table 5-1: Dimensions and tolerance for studless common link[31]

Designation	Description	Nominal Dimension of the Link	Minus Tolerance	Plus Tolerance
a	Link Length	6d	0.15d	0,15d
b	Link Width	3.35d	0.09d	0.09d
R	Inner Radius	0.6d	0	----

Chain size is specified as the nominal diameter of the link and denoted by letter *d* or *D*.

5.2. Chain properties

Depending on the mechanical parameters such as nominal tensile strength and toughness of the steels used for manufacture, chains are subdivided into five grades: R3, R3S, R4, R4S and R5. Table 5-2 shows the various classes minimum strength and impact energy values [31]. The steel used in mooring system components is low alloy steel. Low alloy steel is defined as steel with added 1 to 5% by weight of alloying elements.

Table 5-2: Mechanical properties of offshore mooring chain and accessories [32]

Steelgrade	Yield stress N/mm ²	Tensile strength N/mm ²	Elongation %	Reduction of area %	Charpy V-notch		
					Temperature °C	Average energy J	Single energy J
R3	410	690	17	50	0 -20	60 40	45 30
R3S	490	770	15	50	0 -20	65 45	49 34
R4	580	860	12	50	-20	50	38
R4S	700	960	12	50	-20	56	42
R5	760	1000	12	50	-20	58	44

5.3. Capacity of chains

Unlike typical anchor chains, mooring chains used on oil drilling platforms and other offshore constructions, such as offshore wind turbines, are unique. They are primarily intended to prevent platform movement caused by ocean current or wind. Unlike normal anchor chains, these chains are exposed to a harsh environment for a longer amount of time, thus, they must possess high strength, toughness, and fatigue and corrosion resistance as well. Chains must withstand the specified proof and break test loads based on steel grade and nominal cross-section diameter and can be calculated using the formulas in Table 5-3. The formulas used to calculate the capacity of chains are fully empirical and are based on the experimentally determined strength. The DNV-OS-E302 standard stipulates the minimum breaking load and minimum proof load for chains. Typically, the proof load is 70 to 80 % of the minimum breaking load.

In accordance with industry standards, the definition of chain break load is not the load at which the chain cross section fractures but the maximum load borne by the chain [2].

Table 5-3: Formulas for proof and break test loads[31]

Test Load, in kN	Grade R3	Grade R3S	Grade R4	Grade R4S	Grade R5
Proof	0.0156Z or 0.0148Z	0.0174Z	0.0192d2Z	0.0213Z	0.0223Z
Break	0.0223Z	0.0249Z	0.0274Z	0.0304Z	0.0320Z

Where $Z = d^2(44-0.08d)$

Note: The required proof load for steel grade R3 provided by DNV-OS-E302 differs from the proof load provided by IACS, which are 0.0156Z and 0.0148Z respectively.

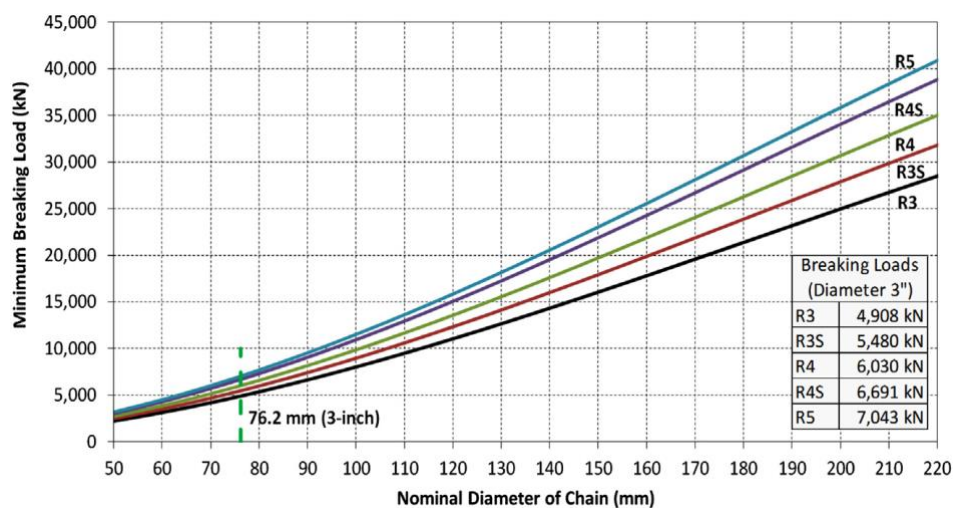


Figure 5-2: Steel grades and their corresponding breaking loads [14].

Minimum breaking loads (MBLs) are plotted against chain diameter in Figure 5-2 for studless chain. Out of all the steel grades, R5 has the strongest strength among them. The ratings were developed by Det Norske Veritas (DNV) [14].

5.4. Chain Strength Behavior and Ductile Failure

The mechanisms of the degradation modes affect different surfaces on the chain link structure (section 3.2 and Figure 3-4). The different locations on a chain are illustrated in Figure 5-3. It is critical to recognize the following for a phenomenological knowledge of chain ductility:

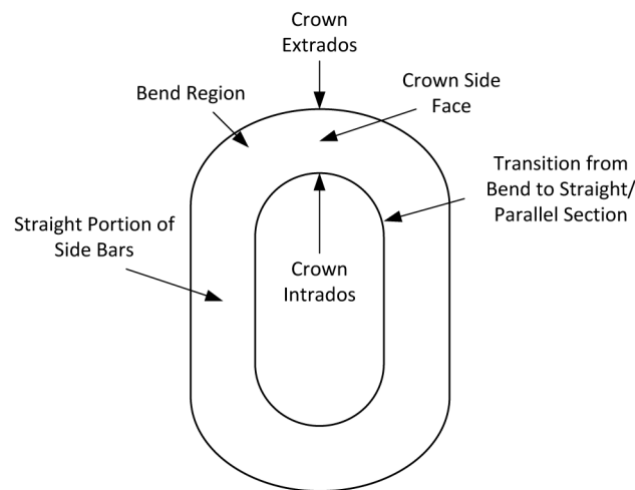


Figure 5-3: Chain surface location names [18]

The crown intrados is the "weakest" area. The crown side faces and/or crown extrados are the second weakest points. The intrados or extrados of the shoulder or bend region are the third weakest point. The side bars, from the bend region to the centre (parallel portion), are the fourth weakest point. The straight section of the side bars has the least crucial areas [18]. Identifying the order of strength of the different parts is critical to determining the location of failure during the analysis of degraded chains.

5.5. Strength analysis of uniform corrosion on chains

A verified approach made by some research Fears JIP for evaluating the strength of degraded mooring chains based on finite element simulation is presented for estimating the current chain strength and predicting the impact of continuous degradation. Figure 5-4 depicts the assessment curves generated using the approach. These assessment curves are plotted against percent decrease in diameter and percent reduction in cross-sectional area. Diameter reduction is frequently utilized, although cross-sectional area loss is the primary driver of strength loss. It was demonstrated that the IACS formula is adequate for assessing general corrosion. For each deterioration mechanism, the normalized chain breaking load is displayed against the percentage drop in single bar diameter. This dimension is commonly measured during mooring inspections. Interlink wear, on the other hand, causes the fastest drop in chain strength with the greatest reduction in single bar area. The IACS formula for prediction of chain breaking load assumes a consistent decline in chain diameter for computing the break load for a reduced chain size when evaluating strength loss due to degradation. The other curves for local abrasion, local corrosion pitting, and interlink wear take into account the location and cross-sectional area reduction features (location, loss amount, and shape) caused by each degradation mechanism.

All models were generated using finite element method and validated using full-scale chain break tests conducted on recovered degraded chains [18].

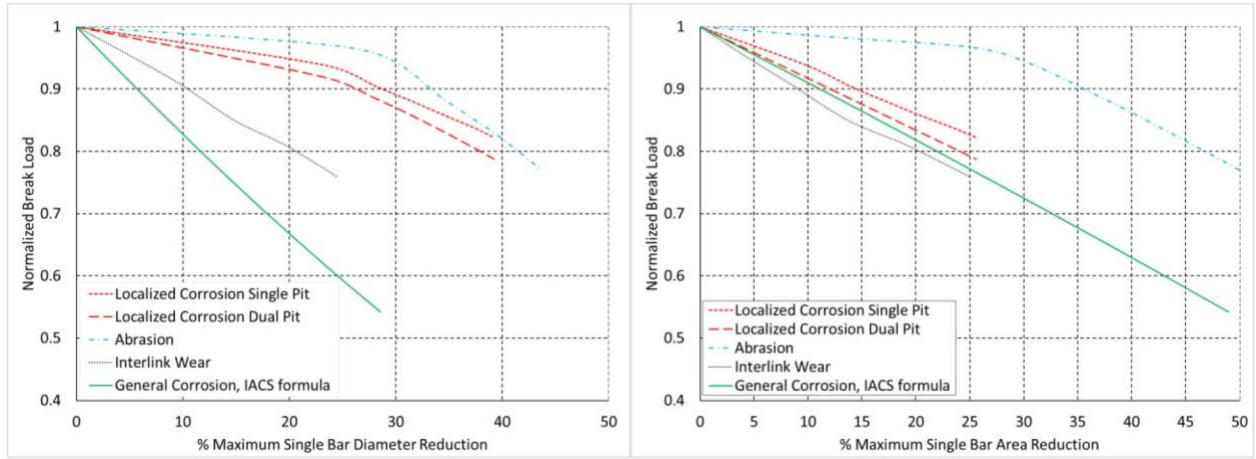


Figure 5-4: Normalized Break Load versus Single Bar Diameter Reduction for All Degradation Modes

The IACS formula can be used to construct the general corrosion assessment curve. Figure 5-5 depicts the IACS minimum breaking load as a function of percent area reduction in comparison to two chain break tests, as well as breaking load predictions using the IACS equation (eq 5.1) and actual material parameters.

$$CSB = G_d \cdot Z, \quad Z = D_{current}^2 (44 - 0.8 D_{current}) \quad (5.1)$$

Using the chain's diameter and a material factor, G_d , that varies linearly with the minimum ultimate strength of each chain grade, the IACS has developed a method to determine the Catalogue Break Strength (CBS). This linear dependence allows extrapolation of a specific number for G_d for a given chain of a given ultimate strength. The average diameter of the corroded chain was utilized in conjunction with the chain's particular G_d to derive the breaking strength via the IACS formula. The IACS formula provides a reliable estimate of corroded chain strength, and it is expected given that the diameter of the chain bars is being steadily and uniformly reduced due to corrosion [18].

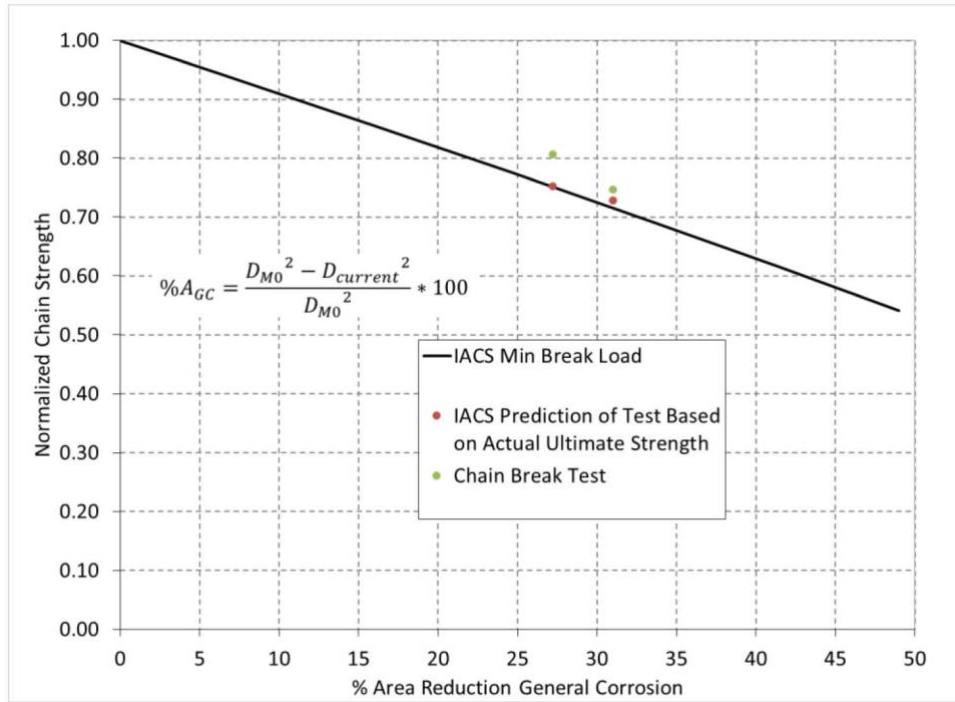


Figure 5-5: Actual Ultimate Strength vs. Break Test Results: IACS CBS Curve and Predictions

The percent area loss due to general corrosion (percent AGC) is found by:

$$\%A_{GC} = \frac{(D_{MO}^2 - D_{current}^2) * 100}{D_{MO}^2} \quad (5.2)$$

Where

D_{MO} and $D_{current}$ represent original and degraded chain diameter respectively.

The loss of chain link strength caused by uniform corrosion did not correspond with the loss of metallic area caused by any general or pitting processes. The distribution of corrosion in relation to the high-stress areas in the chain-link is clearly relevant in predicting residual strength. In order to provide a more suitable approach for assessing the residual strength of corroded chains, a high fidelity FEA modelling of loss of metallic area owing to corrosion must be provided [15]. Building a robust model capable of estimating residual chain strength requires obtaining degraded chain geometry and selecting FEA modelling parameters. Degraded moorings can be measured manually above water or underwater using photogrammetric techniques. Understanding the underlying physics of uniform corrosion when specifying and implementing chain measurements is crucial for the best results. The

average diameter of a typically corroded chain can be calculated by measuring the bar diameter in each bend using two perpendicular sites. **Figure 5-6** depicts studless chain measurement sites. So far, this has yielded accurate estimations of the average typically corroded chain bar diameter. However, it is the analyst's obligation to determine whether this approach is appropriate for estimating the average diameter. If general corrosion appears to be more prevalent in one region of the chain than another, a decision must be taken as to whether utilizing the average diameter and the IACS method is suitable or whether FEA modelling should be used [2].

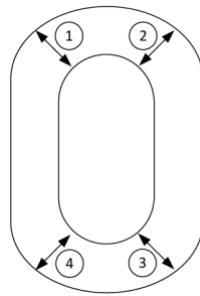


Figure 5-6: *Measurement Locations for Estimation of Average Diameter*

The focus of this study is on uniform corrosion (which is indicated by the green line on **Figure 5-4**). The results are used as a reference of validation for the comparison of the results from FEA in the case study of chapter 8. The results can be used to assess the remaining life based on strength. It provides details pertinent to the construction of a finite element analysis (FEA) model of a mooring chain for strength assessment and to predict the impact of ongoing degradation. Guidance is provided for how to model degraded mooring chains using FEA. The modelling discussion in chapter 8 includes obtaining the chain geometry, boundary conditions, element type and mesh convergence, interaction and friction coefficients, and material properties. The load-displacement response predicted by the FE model is used to determine the load-bearing capability of the deteriorated chain.

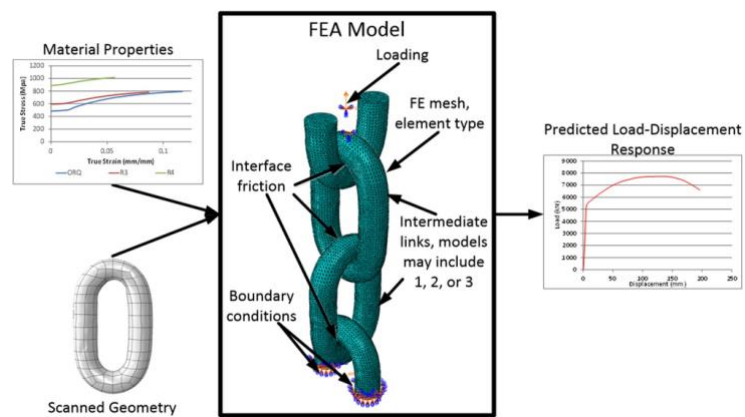


Figure 5-7: Key aspects of chain model construction[18]

In case of uniform corrosion, failure are identical to a new chain with the remaining corroded bar diameter for chain degraded by general corrosion, resulting in a consistent amount of cross-sectional area loss around the chain.

The ratio of capacity loss to area loss due to uniform corrosion is estimated to be 1.05:1 on average. This relationship agrees with the findings of a recent FEA research and is more demanding than presuming a capacity reduction based on the Code formulation for strength by merely assuming a bar diameter reduction [33].

6. Cathodic protection (CP)

Floating Production, Storage, and Offloading (FPSO) structures present some unique CP challenges. Prior to CP application, several questions need to be addressed first. Like: are there alternative methods to impressed currents? What are the options for mooring systems in deep water? How long can the systems last without maintenance? These and other questions are answered in this part.

It is possible for FPSOs to be either new-build vessels or retrofits. However, when deciding on a cathodic protection strategy, it is not about how it looks, but rather how well it works and how long it will last.

Corrosion allowances are common for corrosion protection of permanently moored structures. Other than this, replacement of mooring systems is another common solution against corrosion phenomenon, but it is not advisable to implement as it is so expensive, has its own associated risks, and results in the stoppage of the production units. In the past, some structures have shown severe corrosion after a considerably short period of time but out of the above described were no other measures to protect them.

6.1. Galvanic effects

Cathodic protection aims to prevent corrosion of metallic surfaces in contact with electrolytes such as seawater. The fundamental prerequisite for a corrosion reaction to occur is that it results in a decreased "energy state." The various electrode reactions involved in corrosion processes are distinguished by their electrical potential in reference to a given standard potential and hence to one another. For corrosion to occur, an anode reaction must have a lower potential than the equivalent cathode reaction. For the anode reaction, various metals have different electrical potentials. When in electrical contact with a specified metal item, a less "noble" metal can therefore be utilized as a sacrificial anode. All of the covered material's surfaces are electrically forced to become cathodic, preventing any anodic reaction. The same principles that apply to driving material to become completely cathodic may be used to avoid cathodic corrosion by imposing an appropriate electrical potential (and related electrical current) relative to a standard potential [17]. In conjunction with protective coatings, cathodic protection is a standard approach for protecting immersed steel surfaces against corrosion.

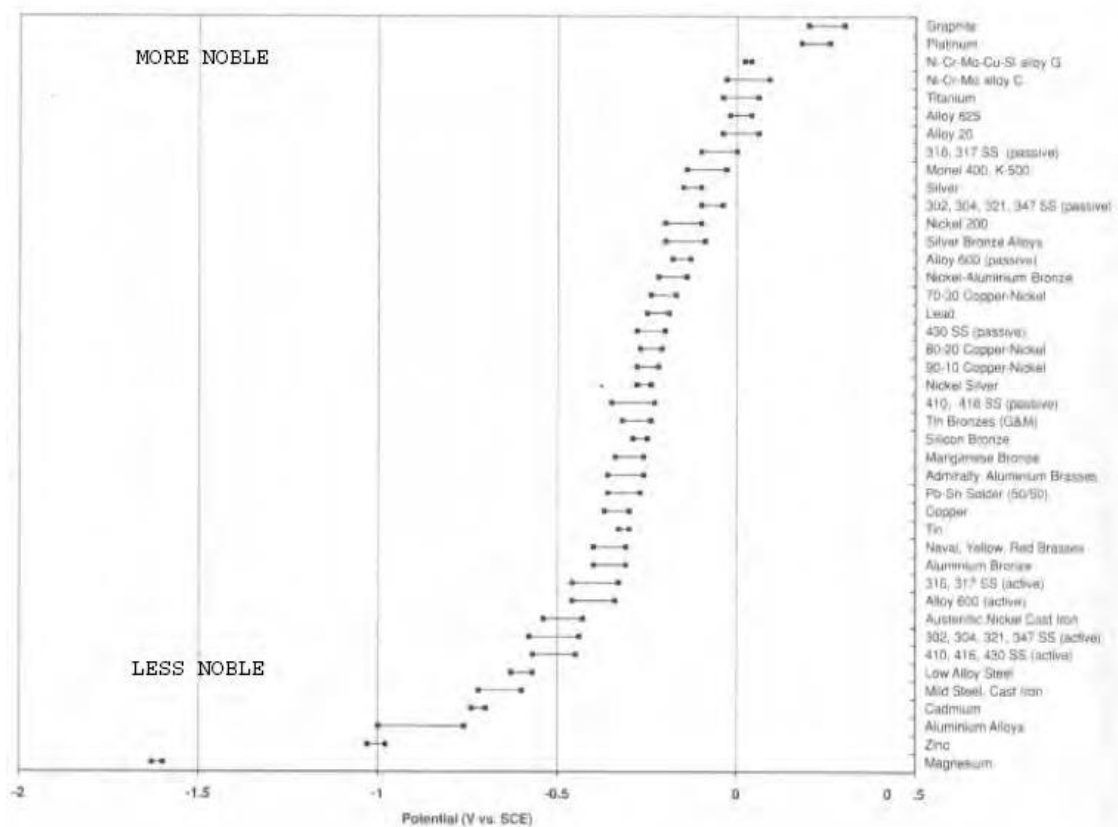


Figure 6-1: The galvanic series of metals in slow moving sea water[34]

6.2. CP systems and offshore corrosion zones

Corrosion protection of offshore structures in the three corrosion zones can be controlled:

Atmospheric zone: In this zone, corrosion is usually controlled by using a protective coating layer.

Splash zone: In a splash zone that is intermittently immersed, cathodic protection can be utilized as a supplement to protective coatings. Only when the immersion duration is long enough for the steel to become polarized is cathodic protection effective. The areas of the splash that are not frequently immersed are not protected by cathodic protection.

Submerged zone: Cathodic protection in combination with coatings can be used to prevent corrosion in this zone [19].

6.3. Cathodic protection systems

A floating structure may be protected from corrosion using either a sacrificial anode cathodic protection (SACP) or an impressed current cathodic protection (ICCP) system, or both. Common sacrificial anode metals include aluminium, zinc, and magnesium. These metals are alloyed to increase their strength and dissolvability. Impressed-current systems employ inert anodes (very low dissolution) and an external DC power supply to impress a current from an external anode onto a cathodically insulated metallic surface. Cathodic protection systems must be designed to transmit sufficient current to the structure to be protected for the duration of the structure's design life, so that the selected cathodic protection requirements may be met efficiently for all sections of the structure to be protected. Cathodic protection system design should incorporate cathodic protection system life extension where suitable by providing adequate rehabilitation techniques and appurtenances that can be used to allow anode system and impressed current system retrofits [35].

6.4. Cathodic protection system selection

During the conceptual phase, it should be determined whether a SACP system, an ICCP system, or both will be utilized. In order to assist in the selection of cathodic protection systems, Table 6-1 compares sacrificial and impressed current anode systems.

Table 6-1: Comparison of Galvanic Anodes and Impressed Current Cathodic Protection Systems for Offshore Structures [35]

Comparison Item	Sacrificial Anode Systems	Impressed Current Systems
Design and installation and maintenance costs	Simple in design and installation, generally no maintenance and supervision required, but costly labour of installation labour and anode replacement when consumed. Wrong connection is not possible.	Needs careful design and installation. Regular maintenance and monitoring are needed. Initial equipment cost is higher, but life-cycle cost is lower. Wrong connection is possible.
Consequence of anode damage	Where a system comprises a large number of anodes, the loss of a few anodes has little overall effect on the system.	Loss of anodes can be very critical to the effectiveness of a system.
Environment effect on cathodic protection efficiency	Only practical for low resistivity of electrolyte, such as seawater and mud. Protection potential and current are not controllable.	Less restriction from electrolyte resistivity. Protection potential and current can be automatically controlled by ICCP controller.
Detriment to coating and steel	Coating system is selected for resisting cathodic disbonding. Low potential anode material is needed for high	Due to high anode current, the structure can be over polarized and detrimental to coatings and high

	strength steels.	strength steel if not controlled.
Power source	No electric power supply is needed. Can be used where electrical power is not available.	Continuous DC power supply is required.
Water flow and weight increases	Bulk of anode material may restrict water flow and increase weight / turbulence / noise / drag on the hull. Galvanic anodes may interfere with subsea operations and increase drag forces by flowing seawater.	Lighter and fewer in number. Anodes may be designed to have minimum effect on water flow. Low hull profile reduces noise and drag.
Interaction	Less likely to affect any neighbouring structures.	Effects on other structures near the anodes need to be assessed.

The use of galvanic anodes is permissible under the following conditions:

- When only a little amount of electricity is required, a low-amperage circuit should be employed.
- When electrolytes with a lower resistance are present, such as seawater and mud, the conductivity typically drops.
- Local cathodic protection of a specific section of a structure is less challenging to implement.
- When greater current is required at problem areas, such as isolated sites from overall impressed current cathodic protection systems or electrically protected areas due to non-uniform current distribution from remotely located impressed current systems.

Experience indicates that the sacrificial anode cathodic protection (SACP) system is the most effective method for protecting underwater hulls with a service life of at least 15 years. Several factors contribute to this like, Capability to confidently design for a 15+ year lifespan, no maintenance requirement, extremely reliable, no internal modifications to the hull and no hull penetrations, very small likelihood of electric current interference, and conformity with existing subsea cathodic protection systems. As a result, the total cost of ownership for hulls deployed in deep water is reduced [35].

Under the following situations, impressed current cathodic protection devices are utilized for offshore structures:

- When weight and flow resistance are a concern and significant current demands exist, it is necessary to use a flexible cable.
- Operations in waters with fluctuating resistivity.

6.5. Cathodic protection of chains

For low-alloy steels, cathodic protection should be considered as a corrosion control technique rather than to provide immunity [36]. To avoid corrosion damage to the moorings, corrosion protection of all components of the mooring lines should be incorporated during the design phase. For long-term chain service, a corrosion allowance is provided. In the splash zone, a larger corrosion allowance should be used because of the chain handling, the wear could be significant. Additional anode weight for the cathodic protection systems on the hull to which the mooring lines are attached may be required for the cathodic protection current draining through mooring lines which are easily exposed to the harsh environment. For mooring lines and anchors, bacterial corrosion in the bottom components exposed to seabed sediments must be examined, taking cathodic protection, coating, or corrosion allowance into mind. Experience has demonstrated that cathodic protection for the hull structure is also effective for chains that extend around 30 to 60 meters from the structure. The length is determined by the chain's attachment to the structure, chain size, and line tension. Galvanic coatings or protective coatings are also used to protect chains against corrosion and reduce fatigue.[35]

Generally, in offshore structures, impressed current system uses a much higher driving voltage than a galvanic system does. It covers a much larger area than a galvanic system does. In the case of chains, the risk of over-protection (too high polarity value) needs to be addressed. One condition for using it over a large area is that there is a "resistance-free" (or close) connection in the metallic part of the structure. For chains, it's found that there is a noticeable resistance (normally low but not possible to actively control) between every link. It becomes this resistance that controls the length of chain one can protect. To protect a full chain length, one would need many ICCP anode locations, and it doesn't deem this to be a practical solution. Therefore, the SACC is more practical with chains.

As it's been described in Table 6-1, impressed current systems can offer several advantages over the sacrificial anode. When formulating a long-term C.P. strategy, other factors should be considered. This could make sacrificial anode systems more preferable to chains in deep water.

In recent years, cathodic protection of mooring lines was notoriously difficult to shield using cathodic protection system and is normally not provided due to:

- The discontinuous nature of chain links.
- Installation constraints.
- Chains are connected to mooring components (wire ropes, chain connectors, fairleads, pitfalls, and chains) and their CP system, they draw power from those systems. The extent of the current drain should be calculated, and additional anode weight is required to accommodate this drain.

According to US Navy (UFC 4-150-09), all chains in a mooring system must be cathodically protected between the mudline and the buoy. Attaching anodes in a way that protects each link is how protection is achieved. Chain-stud anodes and clump anodes are the two types anodes. Clump anodes are less effective for several reasons (1) When the chain is not under tension, the continuity between the links may be compromised. and (2) To ensure conductivity, the chain link and continuity wire contact area must be cleaned to bare metal. (3) In places where the chain leg moves because of loading or tidal effects, there is no guarantee that a continuous connection between the connecting wire rope and the chain leg will be maintained. When it comes to anode chain studs, each link is in direct contact with an anode regardless of whether or not the system is in tension, which provides maximum protection [37]. Deepwater mooring chains cannot be installed, maintained, or replaced using these CP methods because divers are required for each step of the installation, maintenance, and replacement process.



Figure 6-2: Clump Anodes(left) and Chain-Stud anodes(right)[37]

6.6. Sacrificial anode cathodic protection design criteria

A galvanic (or sacrificial) anode is a metal with greater negative potential than the structure metal being protected. Galvanic anodes corrode faster than the shielded structure, hence protecting the structure.

Typically, zinc or aluminium-based alloys are used to make marine galvanic anodes. Because of their high potential and the high conductivity of seawater, magnesium-based alloy anodes are only suitable for freshwater applications. The purpose of a galvanic anode system is to deliver enough current to safeguard a portion of the structure for the duration of the system's intended lifespan.

A maritime galvanic anode cathodic protection system has three fundamental elements: anodes, a connecting system that includes welding, bolting, cabling, and fasteners, and securing structure.

A minimum design specification for galvanic anode systems should include the following:

- Acceptance requirements for the finished system Specifications and drawings of anode alloys, sizes, and attachment
- Specific calculations using current density and anode resistance
- Specification in detail for inserts, attachment, and anode/structure continuity
- Detailed installation, testing, commissioning, and operation specifications

The cathodic protection design flow can be summarized as shown in Figure 6-3.

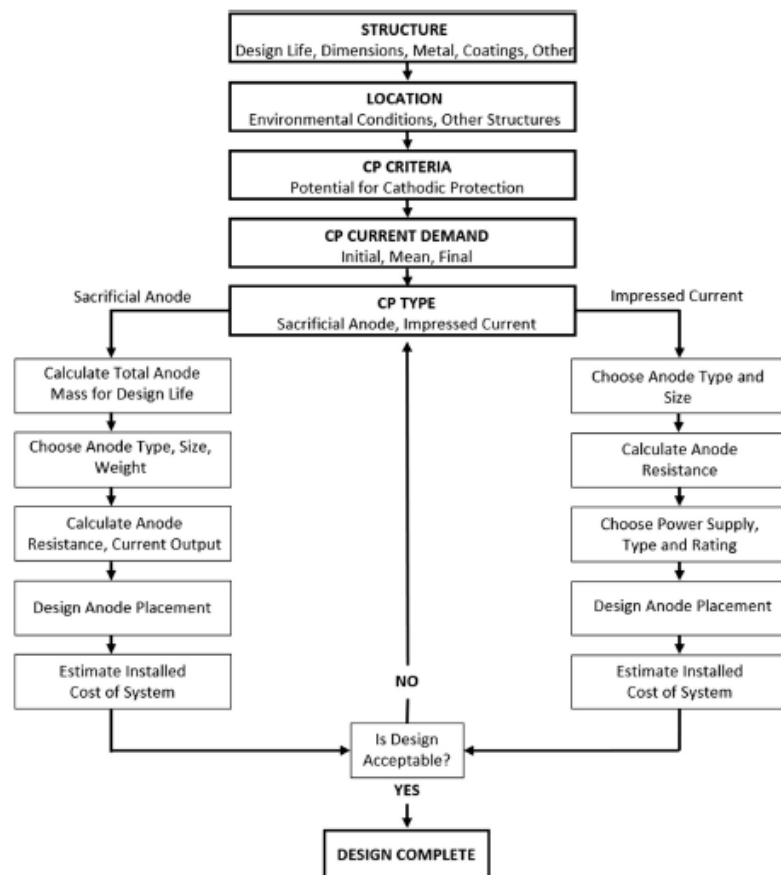


Figure 6-3: The flow of CP design [45]

6.6.1. Design consideration and parameters

Design life

Usually, the owner specifies the design life of a cathodic protection system of mooring chains of an offshore floating construction. Either the full design life or the dry-docking interval(s) must be considered. Additionally, the design life must account for any cathodic protection active period prior to the buildings' commissioning.

Offshore cathodic protection system maintenance and retrofitting are frequently prohibitively costly and impractical. As a result, it is common to utilize anodes with at least the same design life as the covered structure in order to minimize maintenance and retrofitting requirements. In certain circumstances, however, the deliberate retrofitting of sacrificial anodes may be a more cost-effective alternative to the initial installation of very large anodes [36][35].

Environment

The design of cathodic protection systems for the mooring chains of offshore floating structures must consider the anticipated service conditions at the location where they will be installed or relocated, including water salinity, dissolved oxygen, sea current, temperature, and ice conditions. The protective potential described below is dependent on temperature, dissolved oxygen concentration, salinity, water velocity, and water conductivity; therefore, the seawater parameters must be determined.

Potential criteria

The established criterion for the protection of carbon steels and low-alloy steels in aerated saltwater is a protection potential, E^0_c , of -0.80 V or greater, as measured with regard to the Ag/AgCl/seawater reference electrode. In mild steel with active sulfate-reducing bacteria (usually in anaerobic settings), the protection potential is -0.90 V (instead of -0.80 V) relative to Ag/AgCl/seawater reference electrodes. The Nernst equation can be used to determine the possibility for corrosion control in different situations.

It is essential to note that when negative potentials increase, there may be a detrimental influence on fatigue properties and a possibility of hydrogen embrittlement in vulnerable steels. For carbon steels and austenitic stainless steels, the polarization potential should not be greater than -1.10 V (Ag/AgCl (Seawater)).

Surface area calculation

Surface areas to receive cathodic protection should be computed separately for surfaces with and without a coating system for each cathodic protection zone. Surface areas influenced by other characteristics (for example, high and very cold surface temperatures) require special consideration in terms of their impact on cathodic protection current requirement. It is allowed to simplify surface area calculations for complex geometries as long as the simplification is conservative.

Galvanic anode materials

Aluminium or zinc galvanic anodes are commonly used in offshore applications. The generic kind of anode material (i.e., aluminium or zinc base) is normally chosen and defined by the Owner in the conceptual CP design report and/or in the design premises for detailed CP design.

Anodes made of aluminium are typically favoured due to their higher electrochemical capacity, ϵ (Ah/kg). However, zinc-based anodes are more dependable (in terms of electrochemical performance) for use in marine sediments or internal compartments with significant bacterial activity, both of which reflect anaerobic situations [36].

Design electrochemical capacity, ϵ , (Ah / kg) and design closed circuit anode potential, E^0_a , (V) are two of the CP design parameters that affect the performance of the anode material. Ohm's law and Faraday's theorem. They are used to determine the design anode current output and the required net anode mass from the given electrochemical capacity and design closed circuit anode potential [36].

Table 6-2: Proposed Layout at seawater ambient temperatures, anode materials' electrochemical capacity and design closed circuit potential.[36]

Anode Material Type	Environment	Electrochemical Capacity (Ah/kg)	Closed Circuit Potential (V)
Al-based	seawater	2,000	-1.05
	sediments	1,500	-0.95
Zn-based	seawater	780	-1.00
	sediments	700	-0.95

Anode geometry and fastening devices

Typical designs for sacrificial anodes include slender, flat-plate, long, flush-mounted, standoff, and bracelet types. In this thesis a new innovative clumped type of anodes is used to design the cathodic protection of mooring chains in deep water and will be discussed in detail in chapter 9 with a case study.

Current density

Current density requirements for the mooring chains of floating offshore constructions are heavily influenced by the structure's operating environment.

Table 6-3 and

Table 6-4 provide the recommended design current densities, i_c (A/m²) for polarizing seawater-exposed bare metal surfaces as a function of depth and 'climatic zone' based on surface water temperature.

Table 6-3: Initial and final recommended design current densities (A/m²) for seawater-exposed bare metal surfaces as a function of depth and 'climatic zone' based on surface water temperature. [36]

Depth (m)	'Tropical' (> 20 °C)		'Sub-Tropical' (12- 20 °C)		'Temperate' (7-11 °C)		'Arctic' (< 7 °C)	
	initial	final	initial	final	initial	final	initial	final
0-30	0.150	0.100	0.170	0.110	0.200	0.130	0.250	0.170
>30-100	0.120	0.080	0.140	0.090	0.170	0.110	0.200	0.130
>100-300	0.140	0.090	0.160	0.110	0.190	0.140	0.220	0.170
>300	0.180	0.130	0.200	0.150	0.220	0.170	0.220	0.170

Table 6-4: Mean recommended design current densities (A/m²) for seawater-exposed bare metal surfaces as a function of depth and 'climatic zone' based on surface water temperature. [36]

Depth (m)	'Tropical' (> 20 °C)	'Sub-Tropical' (12- 20 °C)	'Temperate' (7-12 °C)	'Arctic' (<7°C)
0-30	0.070	0.080	0.100	0.120
>30-100	0.060	0.070	0.080	0.100
>100-300	0.070	0.080	0.090	0.110
>300	0.090	0.100	0.110	0.110

Typically, the mean current density is approximately half of the initial current density (i.e., $i_{cm} = 1/2$ of i_{ci}). Final current density is approximately two-thirds of the initial current density (i.e., $i_{cf} = 2/3$ of i_{ci}).

The minimum number of anodes for adequate shielding should ordinarily meet three criteria. An adequate number of anodes is required to accomplish three distinct tasks: (a) polarizing the structure at the outset (initial current density); (b) providing adequate current to maintain protection throughout the structure's design life (mean current density); and (c) providing adequate current to terminate protection at the end of the design life (final current density) [35].

Coating breakdown factors for cp design

The application of an insulating coating influences the current reduction. When f_c equals zero, the coating is completely electrically insulating, reducing the cathodic current density to zero. $f_c = 1$ indicates that the coating does not have any current-reducing capabilities. Generally, mooring chains are designed without coatings, and this can lead to an f_c value of 1 [36].

Seawater and sediment resistivity

The resistivity of seawater is dependent on its salinity and temperature. In temperate regions with an annual average surface water temperature of 7 to 12°C, resistivities of 0.30 ohm.m and 1.30 ohm.m are recommended as conservative estimates for the computation of anode resistance in seawater and marine sediments, respectively, regardless of depth. Lower values must be supported by actual data that account for seasonal temperature fluctuations.[36]

Anode utilization factor

The anode utilization factor, u , is the fraction of anode material of a specific-design anode that may be used for calculating the net anode mass necessary to maintain protection during the design life of a CP system. When an anode reaches its utilization factor, the polarizing capacity (as indicated by the anode current output) becomes unpredictable due to lack of anode material support or quick rise in anode resistance caused by other factors.

The utilization factor is dependent on the anode's design, namely its size and core position. Unless otherwise agreed, the anode utilization factors shown in Table 6-5 must be applied to design calculations [36]

Table 6-5: Recommended Anode Utilization Factors for CP[36]

Anode Type	Anode Utilization Factor
Long slender stand-off $L \geq 4r$	0.90
Short slender stand-off $L < 4r$	0.85
Long flush mounted $L \geq 4$ width and $L \geq 4$ thickness	0.85

6.6.2. CP calculation and design procedures

Current demand

Each metallic part of the construction has its own current, I_c (A), to provide adequate polarizing capacity and maintain cathodic protection during design life, that is calculated by multiplying its surface area A_c (m^2), by the necessary design current density, i_c (A/ m^2), and the coating breakdown factor, f_c , if applicable:

$$I_c = A_c \cdot i_c \cdot f_c \quad (6.1)$$

This equation can be used to determine the initial, mean, and final demand for current. "Current density" (i_c) refers to the amount of current used for cathodic protection divided by the total area of a certain area. The "coating breakdown factor", f_c , affects current demand.

For a completely coated structure, the requirement for initial current (I_{ci}) is negligible. This feature is optional and can be left out of the cathodic protection layout. Both the mean current demand (I_{cm}) and the final current demand (I_{cf}) should be accounted for in the cathodic protection current demand calculations. The final current demand (I_{cf}) calculation is unnecessary if anode retrofitting to a mooring chain is envisaged.

Anode mass calculations

Cathodic protection net anode mass, M_a (kg), must be determined from I_{cm} (A) for each unit of the protection item during the design life, t_f (yrs). Where 8760 refers to hours per year.

$$M_a = \frac{I_{cm} \cdot t_f \cdot 8760}{u \cdot \epsilon} \quad (6.2)$$

Calculation of number of anodes

From the anode type selected, the number of anodes, (N), anode dimensions and anode net mass, m_a (kg), shall be defined to meet the requirements for initial/final current output, I_{ci} / I_{cf} (A) and anode current capacity C_a (Ah).

The Ohm's law is used to determine the amount of current output I_a (A), from each anode that is needed to supply the current demand, I_c (A).

$$I_a = \frac{E_c^0 - E_a^0}{R_a} \quad (6.3)$$

$$I_c = N \cdot I_a \quad (6.4)$$

The individual anode current capacity,

$$C_a = m_a \cdot \epsilon \cdot u \quad (6.5)$$

where m_a (kg) is the net mass per anode and the total current capacity for a CP unit with N anodes $= N \cdot C_a$ (A·h).

Finally, the following specifications require calculations to be performed as proof that they have been met:

$$C_{a \text{ tot}} = N \cdot C_a \geq I_{cm} \cdot t_f \cdot 8760 \quad (6.6)$$

$$I_{a \text{ tot } i} = N \cdot N_{ai} \geq I_{ci}$$

$$I_{a \text{ tot } f} = N \cdot N_{af} \geq I_{cf}$$

Anode resistance

The electrolyte's resistivity and the anode's size and shape determine the electrical resistance of the anode in contact with the electrolyte. The anode resistance, R_a (ohm), will be determined using the formula appropriate to the actual anode shape unless otherwise specified. It is necessary to calculate for the initial anode's size and estimate final anode dimensions once it has been used up to its full capacity (utilization factor).

Table 6-6: Recommended Anode Resistance Formulae for CP Design Calculations.

Anode Type	Resistance Formula
Long slender stand-off ^{1) 2)} $L \geq 4r$	$R_a = \frac{\rho}{2 \cdot \pi \cdot L} \left(\ln \frac{4 \cdot L}{r} - 1 \right)$
Short slender stand-off ^{1) 2)} $L < 4r$	$R_a = \frac{\rho}{2 \cdot \pi \cdot L} \left[\ln \left\{ \frac{2L}{r} \left(1 + \sqrt{1 + \left(\frac{r}{2L} \right)^2} \right) \right\} + \frac{r}{2L} - \sqrt{1 + \left(\frac{r}{2L} \right)^2} \right]$
Long flush mounted ²⁾ $L \geq 4 \cdot \text{width}$ and $L \geq 4 \cdot \text{thickness}$	$R_a = \frac{\rho}{2 \cdot S}$
Short flush-mounted, bracelet and other types	$R_a = \frac{0.315 \cdot \rho}{\sqrt{A}}$
1) The equation is valid for anodes with minimum distance 0.30 m from protection object. For anode-to-object distance less than 0.30 m but minimum 0.15 m the same equation may be applied with a correction factor of 1.3 2) For non-cylindrical anodes: $r = c / 2 \pi$ where c (m) is the anode cross sectional periphery	

When the anode has been consumed to its utilization factor, u , at the end of the design life, t_f (years), the remaining net anode mass.

$$m_{af} = m_{ai} \cdot (1 - u) \quad (6.7)$$

The dimensions predicted after the anode has been utilized to its utilization factor are used to calculate the final anode resistance, R_{af} (ohm)

7. Case study 1: Long-term corrosion estimation due to MIC using melcher's model

Knowing how long a mooring chain will last and how reliable it will be is easier when you have a better grasp of corrosion processes and rates. It can also help with maintenance scheduling, design (corrosion-resistant materials, acceptable corrosion rates, protective coatings, sacrificial anodes, etc.), and the usage of monitoring systems and instruments.

This section addresses the estimation of corrosion loss under immersion situations with increased DIN concentrations. It deals with how to create a theoretical framework for analyzing and modeling corrosion rates. This model can be used anywhere in the world during the design and installation of mooring chains due to its scientific proof and results in practice. Despite the fact that the North Sea and tropical seas have quite distinct environmental conditions, many design standards for constructions in other parts of the world are still based on the North Sea. This study was carried out to obtain empirical estimates of the characteristics that have a significant impact on the corrosion that happens in the North Sea waters and to examine the influence parameters of the North Sea water environments when there is an elevated nutrient concentration and will discuss chains exposed to MIC in deep-water of the North Sea. The findings of the model by Robert E. Melchers result in a practical equation function that can be used to estimate corrosion loss based on dissolved Nitrogen (DIN) and temperature considering all other parameters constant since the allowances from the codes and standards are designed for the cold water of the North Sea. Finally, the resulting estimation findings will be added to the existing corrosion allowance from the DNV standards.

7.1. Case data requirements for modeling

To develop a quantified relationship between immersion corrosion loss and the average DIN in the seawater local to a mooring chain of interest, it is necessary to have the required data of dissolved inorganic nitrogen and temperature of the area of interest. In areas where there is not significant change in microbial growth with increased temperature, an average temperature and nutrient level can be used to make an estimation of the long-term corrosion loss due to MIC. On the other hand, in areas where there is increase in nutrient concentration with gradual increase in temperature, it is necessary to have a monthly data of the average temperature and DIN level for that specific area. The graph below illustrates the range of monthly North Sea water temperatures taken from numerous years of sea surface temperature records.

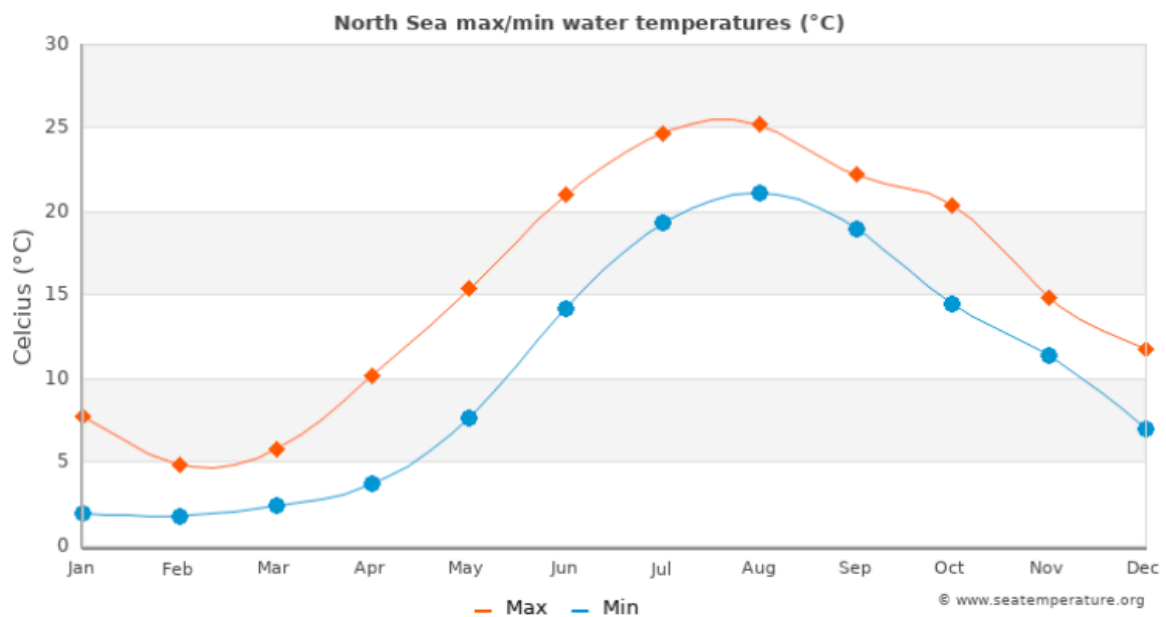


Figure 7-1: North Sea max/min water temperature (°c)[38]

Table 7-1: Monthly max/min/mean North Sea water temperature(°c)

Month	J	F	M	A	M	J	J	A	S	O	N	D
Min °C	2	1,8	2,4	3,7	7,7	14,2	19,3	21,1	19	14,5	11,4	7
Max °C	7,8	4,9	5,8	10,2	15,4	21	24,7	25,2	22,2	20,4	14,9	11,8
Mean	4,9	3,35	4,1	6,95	11,55	17,6	22	23,15	20,6	17,45	13,15	9,4

From the above figure and Table 7-1, the average surface water temperature of the North Sea is 12.85 °c. All these being said, it does not mean that the average temperature all over the North Sea is the same and it varies with increase in depth. The decrease in temperature, with increase in depth also varies from one area to another.

Depending on location, DIN in the North Sea ranges from 0 to 0.1 mg N/L in summer and up to 0.5 mg N/L along the coast in winter. So, in this case study different DIN levels will be applied due to the fact that it is hard to find raw DIN data and for the sake of simplicity to understand the model.

7.2. Estimation of mooring chain corrosion with an elevated nutrient concentration

As a reminder, it has been discussed previously (Section 4.3.2) and according to Melchers findings from the SCORCH JIP, it is not necessary to make additional allowance in the North Sea if the DIN level is less than 0.2 mgN/L and the temperature is less than 10°C. This means that there are no suspects of microbial growth in the area and the raw corrosion allowances from DNV 301 can be

used as they are. In case of areas in the North Sea with elevated nutrient concentration (greater than 0.2 mgN/L), Melchers model for long-term immersion of steels in seawater with elevated nutrient concentration can be applied to estimate the corrosion loss due to microbial effects.

The average surface water temperature of the North Sea is 12.85 °C and according to some research studies water temperature decreases gradually with depth. Let's assume water temperature at certain depth in the ocean floor is 8 °C. So, to calculate the long-term corrosion on mooring chains due to microbial activity, different ranges of DIN levels were assumed and their resulting interception and slope values are as follows:

Table 7-2: Interception (c_s) and slope (r_s) values of an assumed area with an average temperature of 8 °C and at different DIN values (from Figure 4-14)

Average temperature 8 °C		
DIN	c_s	r_s
0	0,14	0,045
0,2	0,38	0,047
0,4	0,625	0,049
0,6	0,925	0,051
0,8	1,175	0,053

7.3. Results and discussion

Let's assume the design life (t_c) of the mooring chains is 25 years. From these values on the table above, the results for the corrosion loss from the time of immersion to 25 years are calculated using the following equation 4.2 and the results are shown on Table 7-3.

Table 7-3: Corrosion loss from the time of immersion to the end life of the mooring chain

Year	DIN=0	DIN=0,2	DIN=0,4	DIN=0,6	DIN=0,8
0	0,14	0,38	0,625	0,925	1,175
1	0,185	0,427	0,674	0,976	1,228
2	0,23	0,474	0,723	1,027	1,281
3	0,275	0,521	0,772	1,078	1,334
4	0,32	0,568	0,821	1,129	1,387
5	0,365	0,615	0,87	1,18	1,44
6	0,41	0,662	0,919	1,231	1,493
7	0,455	0,709	0,968	1,282	1,546
8	0,5	0,756	1,017	1,333	1,599
9	0,545	0,803	1,066	1,384	1,652
10	0,59	0,85	1,115	1,435	1,705
11	0,635	0,897	1,164	1,486	1,758
12	0,68	0,944	1,213	1,537	1,811
13	0,725	0,991	1,262	1,588	1,864
14	0,77	1,038	1,311	1,639	1,917
15	0,815	1,085	1,36	1,69	1,97
16	0,86	1,132	1,409	1,741	2,023
17	0,905	1,179	1,458	1,792	2,076
18	0,95	1,226	1,507	1,843	2,129
19	0,995	1,273	1,556	1,894	2,182
20	1,04	1,32	1,605	1,945	2,235
21	1,085	1,367	1,654	1,996	2,288
22	1,13	1,414	1,703	2,047	2,341
23	1,175	1,461	1,752	2,098	2,394
24	1,22	1,508	1,801	2,149	2,447
25	1,265	1,555	1,85	2,2	2,5

Corrosion loss trend

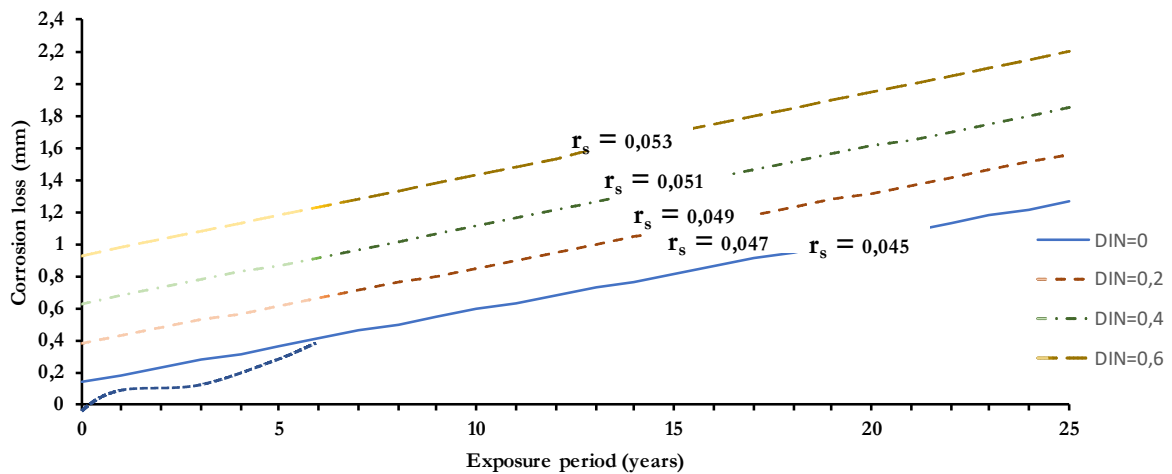


Figure 7-2: Estimated corrosion loss trends as a function of exposure period for 8 °C average seawater temperature and four levels of elevated average seawater bulk DIN concentration. The bi-modal model (Figure 4-12) is sketched to scale in the lower left corner for this water temperature.

Error! Reference source not found. depicts the significant increase in longer-term corrosion caused by DIN for $T = 8\text{ }^{\circ}\text{C}$. As anticipated from the preceding discussion, **Error! Reference source not found.** demonstrates that, relative to Figure 4-13, the parameter c_s has the greatest impact on the corrosion loss trend, generating an upward shift, while the actual slope of the corrosion trend, given by r_s , varies very slightly. The immediate implication of this result is that the influence of nutrient contamination on corrosion should be visible within a few years after first exposure. This may be seen by comparing the basic linear model to the full bi-modal model, illustrated schematically at lower left and scaled for time and 8 °C seawater. It indicates that the corrosion tendency at this temperature develops after approximately six years of exposure. This indicates that the full effect of increased nutritional levels should be detectable within this time frame.

8. Case study 2: Residual strength assessment of degraded offshore mooring chain

This section presents a framework for strength assessment of a degraded mooring chains, based upon finite element simulations of degraded chain. The mooring chains might be degraded either with uniform corrosion, pit corrosion, interlink wear, or chain abrasion due to contact with the seabed but this study mainly deals only with uniform corrosion. Strength analysis of pit, interlink and abrasion is not included in this thesis as they require laser scanning to obtain the actual and detailed geometry of degraded chain from the field, and this is beyond the capacity of this study since such details cannot easily be found. Case study detailing the development of strength assessment curves for general corrosion is presented. The annual corrosion rate is often recommended by a design code or an operator-specific practice. The overall material loss allowance for the mooring chains is calculated by multiplying this rate by the target design life of the mooring system. However, it is probable that not all degradation modes have been accounted for in the design and/or that the degradation rates are greater than anticipated. In these cases, it is of the utmost importance to understand the mooring system's integrity so that we can calculate the time frames required to manage the mooring system's life cycle properly. This chapter describes a method for calculating the strength capacity of deteriorated mooring chains which relies upon finite element simulation to estimate current chain strength using the static (implicit) solver within Abaqus general purpose FEA tool (v6.14-1) and to predict the impact of ongoing degradation. Material properties and component geometry must be represented appropriately in the model. In addition, appropriate incorporation of parameters describing boundary conditions, friction, and element type is required and all will be discussed one by one on the next sections.

8.1. Data input

8.1.1. Chain geometry

The geometry of the modeled chain links must correspond to the design on section 5.1 dimensions and the nominal dimension of the chain is given as a function of the diameter. The cross-sectional diameter was adjusted to 76 mm and the type of link is unstudded. The finite element model has comprises one full link in the middle and 2 half links at both ends. At one end, the model is held fixed, and at the other, a force load is put on it. With couplings, loads and boundary conditions can be sent to the ends of the model. For the sake of the FE calculation's efficiency, a compact model with one-eighth of a full link would be more preferable and sufficient for creating a calculating model

and for saving computational time but for the sake of knowledge and seeking for a challenge a model with three components is chosen because when more connections are made between the various parts of the model, more elements and contact surfaces are generated. In particular, employing chain geometries on contact surfaces might be problematic for convergence. Using Abaqus FEA, a 3D model of the chain links was constructed. As depicted in Figure 8-1., the pieces were modeled as 3D deformable solids based on a path sketch.

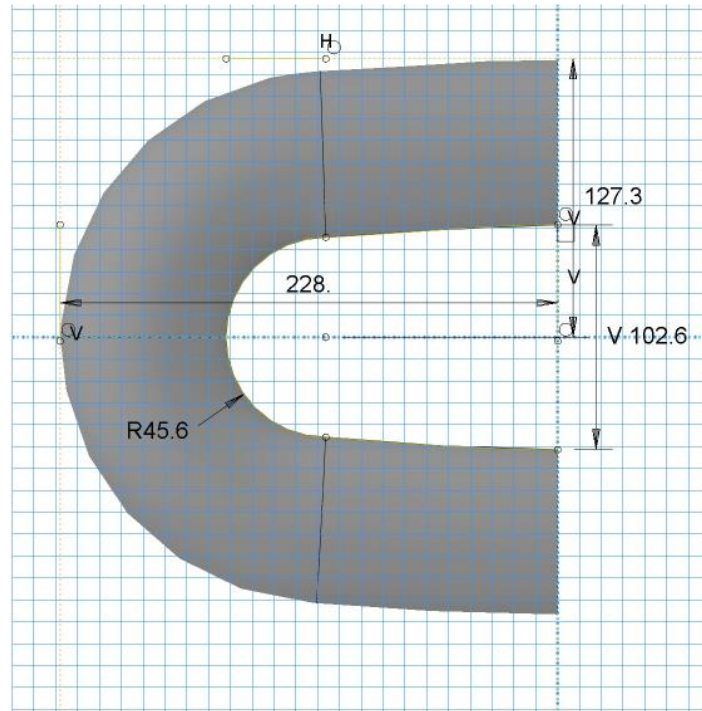


Figure 8-1: Path sketch of 76mm diameter studless link

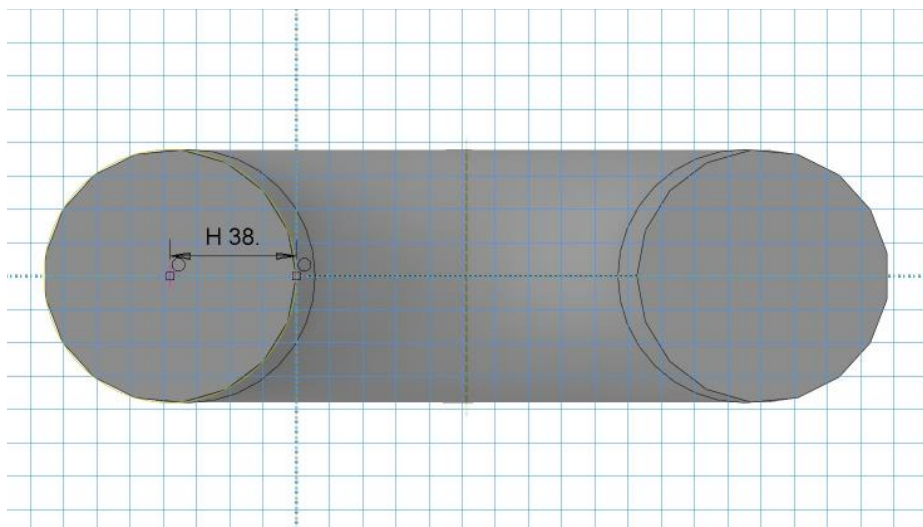


Figure 8-2: Section sketch of 76mm diameter studless link

8.1.2. Material properties

When developing a performance prediction FE model, material properties are crucial. When evaluating a failure mode, it is important to accurately reflect specific material properties. Yield strength, ultimate strength, and uniform elongation (defined as strain in the material at the greatest stress) are the most essential parameters for predicting chain break loads.

An elasto-plastic material model was used to represent the material behaviour for the chain string. The segments of the mooring line chain are studless R3 with elastoplastic behavior. with a catalogue minimum breaking load of 4884kN from product specification manual of a manufacturer called INTERMOOR[39]. In consideration of corrosion, the midlife link diameter is 72mm and full life 68mm. This corresponds to a corrosion rate of 0.4mm each year based on a design life of 10 and 20 years.

Chain (mm)	R3 Studless Proof	R3 Studlink Proof	R3 Break	R3S Studless Proof
76	3417	3417	4884	3811

Figure 8-3: Break load for 76mm diameter chain link from INTERMOOR catalogue

The chain links were modeled as enormous, uniform steel objects. The modulus of elasticity was adjusted to 210,000 MPa, and the Poisson ratio was set at 0.29. As specified by NS-EN 1991-1-1, the density was fixed to 7850 kg/m³. According Table 5-2, R3 chain grade has a yield stress (engineering) of 410 MPa, tensile Stress (engineering): 690 MPa, and tensile Strain (engineering) of 0.17.

8.1.3. Interaction

As may be seen in Figure 8-4, the two parts were linked together. The one-half end was held fixed while the other half was stretched with a uniform distributed force. In Abaqus, the three parts were found to interact via surface-to-surface contact, regardless of node placements or mesh densities. The middle section is represented by the master surface while the two end sections by slave surfaces. A 'Hard' Contact-Pressure over-closure treatment was applied.

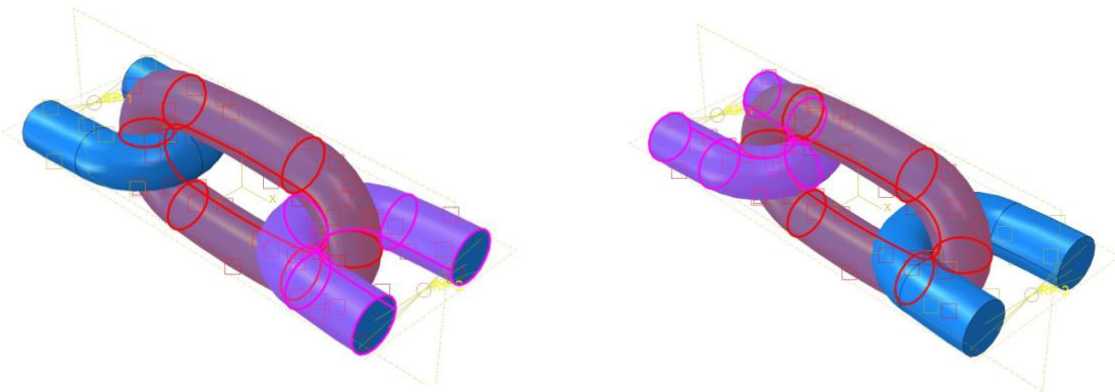


Figure 8-4: *The red zone is the master surface, while the pink zones are the slave ones.*

The zones of possible physical contact are shown by the red and pink colours. The range of these predetermined contact surfaces is where the actual contact takes place.

Interaction properties defines how surfaces responds to contact. Abaqus provides a range of friction models that take into account various elements of interface behavior owing to friction. The tangential frictional force was calculated using the friction coefficient multiplied by the normal contact force, as this is the simplest Coulomb friction model. Based on previous studies and research, penalty friction model with coefficient of 0.35 was included in analyses.[18]

8.1.4. Loading and boundary conditions

For FE models to produce reliable results, it is crucial to include realistic boundary conditions. An FE model cannot accurately represent the system's behavior without appropriate boundary conditions. In this study, the load-bearing capability of the deteriorated chain is of importance, and the projected load-displacement response is retrieved from the FE model outputs. To transfer loads and boundary conditions to the model's ends, couplings are utilized.

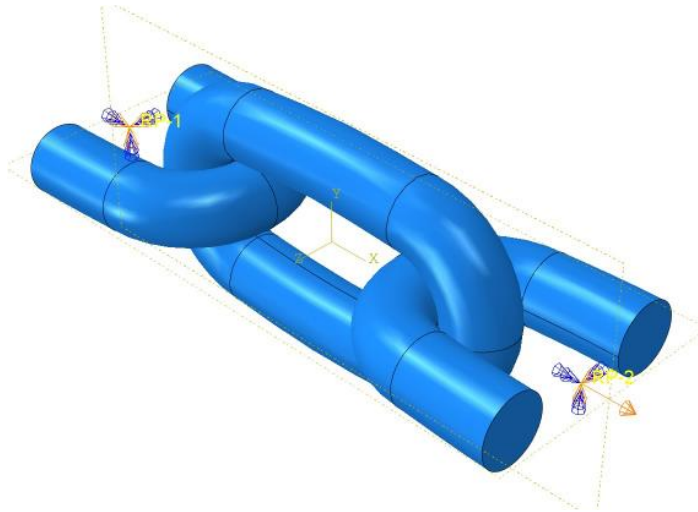


Figure 8-5: 3D FE Model of Chain Links in Abaqus

8.1.5. Element selection and mesh convergence

Selecting an appropriate element for numerical accuracy and convergence can be challenging due to the enormous number of elements available in FE codes. While Abaqus's full integration brick elements (C3D8 in the software) are the gold standard for solid models, other element types can be used as well. The specific chain model under consideration may also influence the element of choice.

Reduced integration hexahedral (brick) elements with 8 nodes (Abaqus type C3D8R) are used to mesh the chain model, as they are the computationally cheapest and are suggested for models whenever possible. The elements' behavior might be mellowed out and the precision of the computed results could be enhanced by using a reduced integration. The approximate global element size is set to 11 mm. The mesh of stud links is shown in Figure 8-6.

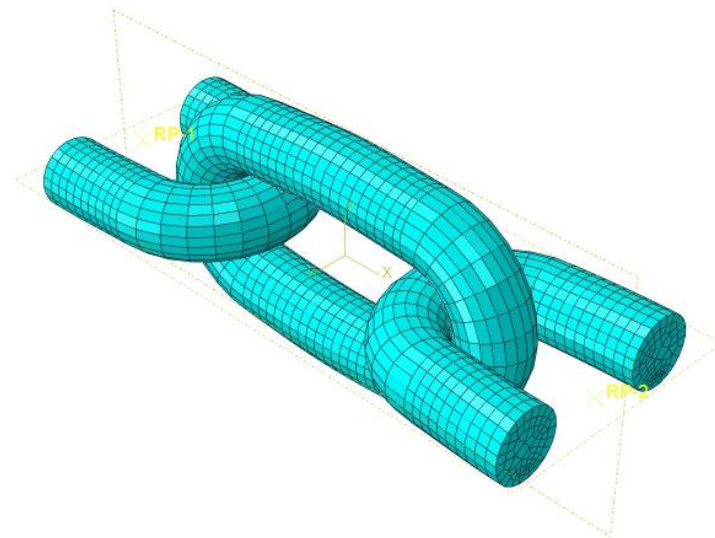


Figure 8-6: Meshed studless link in Abaqus

8.2. Results and discussion

By watching the model's peak maximum principal plastic strain, you can figure out the load at which the chain will break. When this equals the maximum amount of stretch that the R3 material can take, the chain is thought to have reached its limiting load.

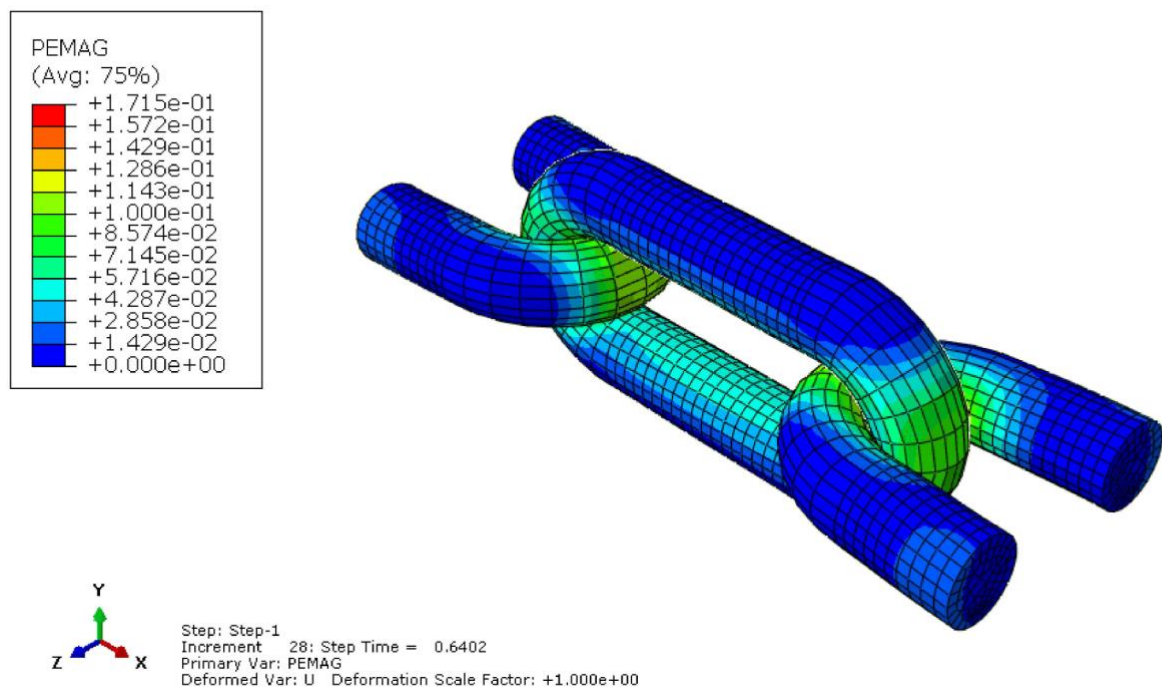


Figure 8-7: Strain Profile of 76mm Chain Links at MBL

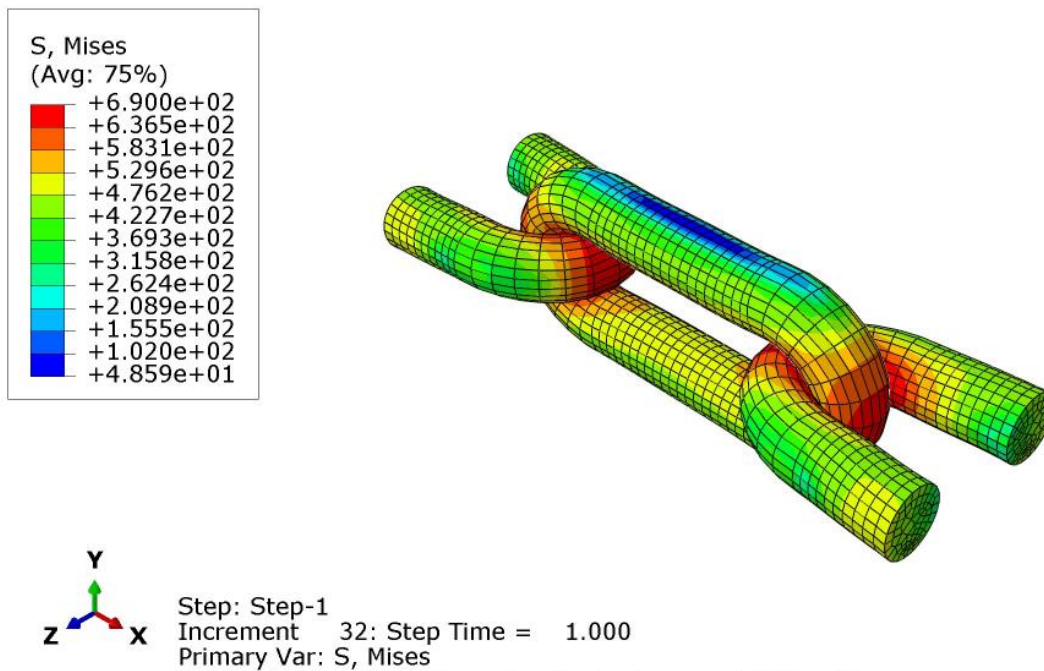


Figure 8-8: Von Mises Stress Profile 76mm Chain Links at MBL

Graph below shows the ultimate load carrying capacity when it is subjected to tensile load. Initial or healthy specimen shows 3164.14kN resistance before reaching its ultimate strength. Strain is observed which is 0.17 and that is against the ultimate stress of 690MPa. Once the 0.17 strain reaches in the analysis then it assumed to reaches a necking level. Experimentally, results are different for healthy material but that can be justified in terms of that, while manufacturing the chain either cold bending or hot bending processes etc that induces residual stresses and that could help the material to resist further load. For midlife the chain has 2847.49kN resistance and for end life 2710.8kN break loads before failure.

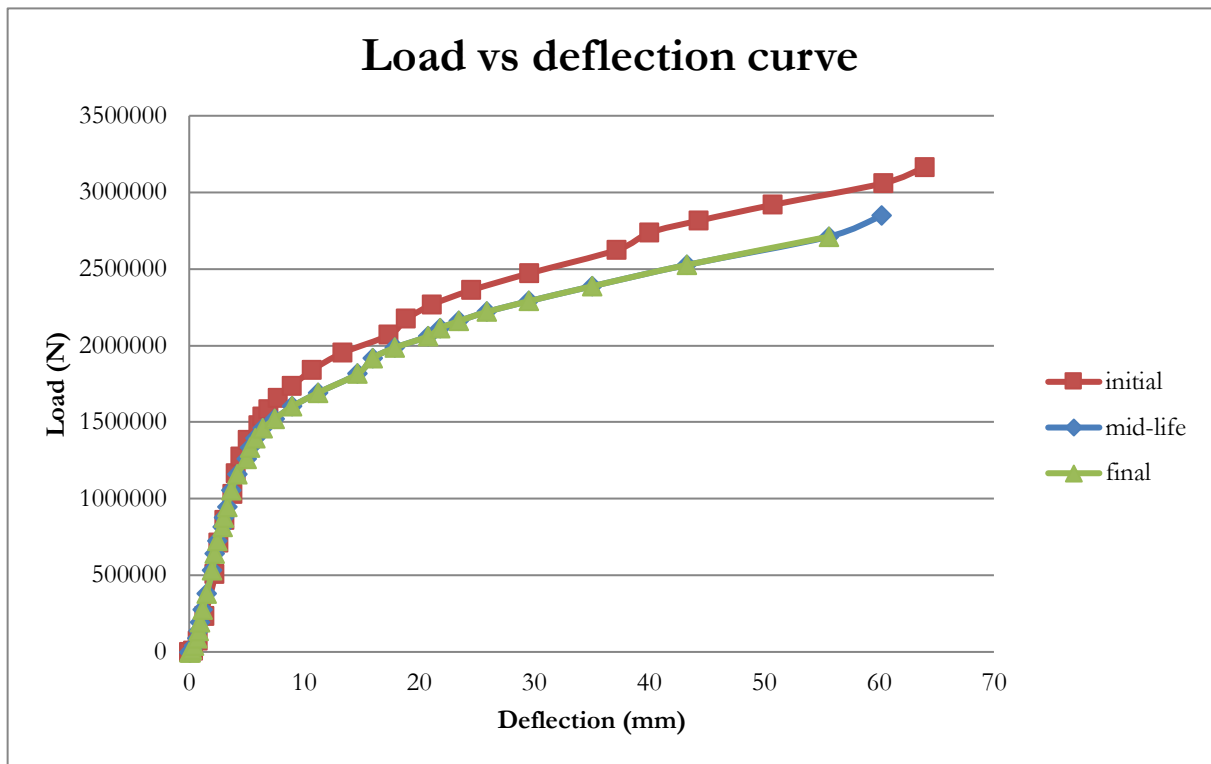


Figure 8-9: load-elongation curves

The percent area loss due to general corrosion for the mid-life and end of life can be calculated using equation 5.2 and they are approximately 10 and 20 percent respectively. Hence, the percent MBL decrease from the above results are 10 and 14.3 percent respectively. The results of the FEA model of uniform corrosion were compared against results on Figure 5-4 and Figure 5-5 there is consistent agreement between the findings for the mid-life and with slight error for end life.

9. Case study 3: Cathodic protection design

The primary goal of this section is to explain the design of cathodic protection for uniformly corroded mooring structures and to perform cathodic protection design calculations for uncoated deeply submerged areas, thereby providing a discussion based on the results. Coatings are usually applied for the splash and atmospheric zones and CP is inefficient in these areas due to deficiency of submergence of seawater, whereas CP is applied for the submerged zone as mentioned in previous sections. According to chapter 6, it is recommended to design sacrificial cathodic protection for the external surface of a hypothetical mooring chain and is assumed that it is submerged from a depth of 200m to 1200m below sea level of the North Sea. In this case study, the 800 m length chain will be assumed it extended on water and the rest 200 m buried on the sea floor. A separate spreadsheet has been prepared for the CP design, so that it will be easier to make a design with the required inputs for any specified chain of different dimensions and different environmental conditions. Similar CP design spreadsheets for ships can cost up to 99.99 US dollars online, but the spreadsheet prepared in this study can be used just for academic purposes. The type of anode selected is new on the market. It has been implemented by some companies in West Africa, far east and the North Sea. The company that has developed and producing these anodes is a Norwegian company and they need to be motivated for their initiation for developing this new technology that can resolve the problems of many offshore structures for better safety and economic improvements of mooring chains in deep water. Their products are approved by NACE(Nomenclature of Economic Activities) and the detail of these products performance will be included at the end as market recommendations.

9.1. Cathodic protection design

According to § 7.13 DNV RP B401 the CP design should be detailed/documented and should contain the following items:

- Design premises: all design procedures in this section are according to DNV RP B401
- Surface area calculations: to find the total surface of chain links extending on a certain length, it is assumed that the two extreme ends of a chain as half torus sections.
- Current demand calculations (initial/final and mean): are made according to § 7.4 DNV RP B401

- Current drain calculations, (initial/final and mean): there will not be current drain calculations as it has not been applied due to the reason that the mooring line was assumed as a continuous chain link without other mooring parts in between.
- Calculations of minimum required net anode mass: Are made according to § 7.7 DNV RP B401
- Anode resistance calculations: according to DNV RP B401 Table 6-6
- Calculations of minimum number of anodes required:
- Calculation of net anode mass based on required number of anodes (if higher than required net anode mass): can be approximated to the nearest high integer number of anodes from the required number of anodes.
- Calculation of total current output based on number and type/size of anodes to be installed: will be made according to § 7.8.2 DNV RP B401.
- Tentative anode design (incl. any special provisions for structural integrity and electrical continuity. Any requirement for utilization factors higher than the default values in Table 10-8 shall be highlighted): a new design shape which is not available on DNV RP B401 called Pacu anodes (not slender stand-off, elongated, flush mounted or bracelet) made by IMENCO AS (a company which is developing a new CP design for mooring chains in deep water) was assumed. According to its shape and design, some assumptions out of the design rules and regulations of the DNV RP B401 were taken and will be discussed in detail in the coming sections.
- Anode distribution drawings: an elaborate of sample distribution will be shown at the end.
- Provisions for electrical continuity, including verification by testing: this section is not included to the design as this is prepared just for academic purposes and doesn't have experimental verifications.

9.1.1. Basic design data

Chain diameter: diameter of chain is assumed to be 76mm, the same as in previous sections. Easier in cases of comparison of results and to have better flow in the study.

Temperature: The temperature of seawater can vary with depth but due to the limited data available the average temperature for North Sea is assumed 8 °c as this study is just for understanding of academic purpose.

Chain length: Assumed as 1000m in length extending from a depth of 200m to 1200m. The 800 meters extending in water and the rest 200 meters buried on the sea floor. The detail of the calculations for the 800 m length chain is elaborated step by step. The steps for the rest of the 200 m chain length will not be shown as it is the same except that a protective potential of -0.90 V is utilized for sediment, but a separate spreadsheet will be prepared for that case to check the results.

Design life(t_d): the design life of mooring systems is usually from 20 to 30 years. According to § 6.2 DNV RP B401, it is usually decided by the owner considering the likelihood of the design life of the protection object being extended. Assuming the mooring line design life is 30 years and has been on site for five years a 25-year design life for the CP is assumed in this case.

Seawater resistivity: according to § 6.7 DNV RP B401, in temperate locations like the North Sea (year average surface water temperature of 7 to 12°C), resistivities of 0.30 and 1.3 ohm.m, irrespective of depth, are recommended as conservative estimates for the computation of anode resistance in saltwater and marine sediments, respectively. In this calculation a 0.30 ohm.m of resistivity is applied in seawater.

Protection potential (E^0_c): according to § 5.4 DNV RP B401, for carbon and low-alloy steels such as mooring chains, a potential of -0.80 V relative to the Ag/AgCl/seawater reference electrode is widely recognized as the design protection potential $E^0(V)$. In the case of anaerobic conditions, including sediments characteristic of saltwater, a protective potential of -0.90 V is utilized.

Closed circuit anode potential (E^0_a): Pacu anodes have aluminum-based material. According DNV RP B401 § 6.5 & Table 6-2, for Al based anode material, the closed-circuit anode potential is -1,05 V.

Anode capacity (ϵ): In reference to DNV RP B401 § 6.5 & Table 6-2, the anode capacity for aluminum based is 20000 A.h/kg.

Anode density: as the anode is aluminum-based material, the density is $\rho_{alm} = 2700 \text{ kg/m}^3$

9.1.2. Structure design data

Surface area calculation of chain links

According DNV RP B401 § 7.2, in the design of CP systems for big and/or complicated things, it is usually advantageous to split the item to be protected into units. In this case study, it is assumed that there are no other components in between the chains. To find the total anode mass that can protect the whole chain length, it is mandatory to find out the total surface area of chain links exposed to corrosion which are extending up on a length of 800m. Primarily, finding the surface area of a single chain link with a given diameter: the dimensions should be annotated according to Figure -5-1. Hence, to calculate the surface area, it is divided in to two sections, one section with a torus shape which represent the two ends of a chain (crown parts) and two cylinders on the side. According to Figure -5-1, for 76mm diameter chain link:

Torus section:

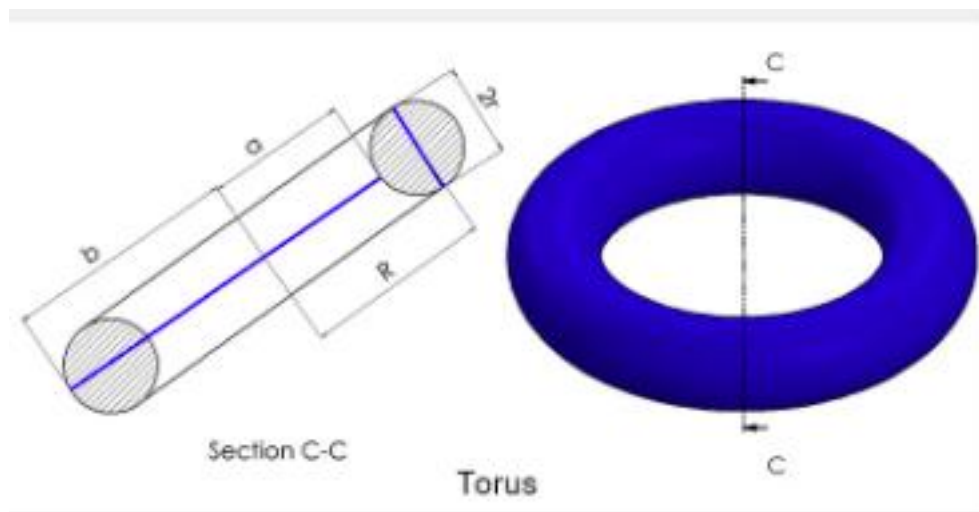


Figure 9-1: An illustration of a torus section

Chain diameter (d) = 76mm = 0.076m

Chain radius(r) = 0.076m/2 = 0.038m

Inner radius (a) = 0.6 x d = 0.6 x 0.076m = 0.0456m

Outer radius(b) = 0.0456m + 0.076m = 0.1216m

Radius of revolution (R) = 0.0836

Area of torus (A_L) = $2 \times \pi \times r \times 2 \times \pi \times R = 4 \times \pi^2 \times r \times R = 0.1254 \text{ m}^2$

Cylinder section:

The remaining length of the chain on sides, taking away both half sections of the torus (crown parts) from both ends will be:

$L = 6d - 2b = 6 \times 0.076\text{m} - 2 \times 0.1216\text{m} = 0.2128\text{m}$

6d is chain length from Figure -5-1: Common link design [31]

Length on both sides = $2L = 2 \times 0.2128 = 0.4256\text{m}$

Surface area of a cylinders on both sides (A_C) = $\pi d \times 0.4256 = 0.1016\text{m}^2$

Total surface area of a chain $A_T = A_L + A_C = 0.227\text{m}^2$

To find the number of links in 800m chain length:

In each of three interlinked chains, there are two full chains lengths and an intersecting chain link with a length L in between. So, a link of three chains is the summation of two full chains and L.

$3 \text{ Links} = 2 \times 6d + L = 2 \times 6 \times 0.076\text{m} + 0.2128\text{m} = 1.1248\text{m}$

And the number of links in 500m length chain will be (N) = $3 \times 800/1.1248 = 2133.71$

Hence the total surface area of chains links in 500m depth = $A_T \times N = 484.35\text{m}^2$

A separate spreadsheet is prepared to calculate the surface area of mooring chains with chain diameter and chain length as inputs in Appendix A3.

Coating breakdown factors for cp design

According to DNV RP B401 § 6.3, the coating breakdown for the mooring chains ($f_c = 0$) as there is no coating so that the anticipated reduction in cathodic current density due to the application of an electrically insulating coating is zero.

9.1.3. Design current density - for seawater exposed bare metal surfaces

Cathodic current densities for achieving and sustaining CP rely on parameters that vary with geographic location and operating depth.

Design initial and final current density (i_{ci} & i_{cf}): in reference to DNV RP B401 § 6.3 & Table 6-3, the design initial and final current densities are 220 and 170 mA/m² respectively. According to DNV RP B401 § 6.3.4, using Ohm's law and assuming that the initial and final current densities are constant, the starting and final current densities are used to calculate the needed number of anodes of a given type (DNV RP B401 § 7.7) to obtain a suitable polarizing capacity.

- The anode potential is in accordance with the design closed circuit potential DNV RP B401 § 6.5.3 and
- The potential of the mooring chains is at the design protective potential for low-alloy steels - 0.80 V.

Design mean-current density (i_{cm}): according to DNV RP B401 § 6.3 & Table 6-4, the design mean current density is 110 mA/m². The mean or maintenance design current density, i_{cm} (A/m²), is the projected cathodic current density once the CP system has reached its steady-state protection potential.

9.1.4. Required current for CP

Shall be calculated according to § 7.4 DNV RP B401, total area and multiplied by the relevant design current density, i_c (A/m²). Where f_c is 1 for uncoated materials. In addition, in reference to DNV RP B401 § 7.4.2, the CP current demands for initial polarization and for polarization at the end of the design life, I_{ci} (A) and I_{cf} (A), shall be calculated along with the mean current demand I_{cm} (A) required to maintain cathodic protection throughout the design period, for items with major surfaces of uncoated metal.

Thus, using equation 6.1:

$$I_{ci} = 220 \text{ mA/m}^2 * 484.35 \text{ m}^2 / 1000 = 106.57 \text{ A}$$

$$I_{cm} = 110 \text{ mA/m}^2 * 484.35 \text{ m}^2 / 1000 = 53.27 \text{ A}$$

$$I_{cf} = 170 \text{ mA/m}^2 * 484.35 \text{ m}^2 / 1000 = 82.35 \text{ A}$$

9.1.5. Anode mass calculations

The total anode mass based on the mean required current according to § 7.7 DNV RP B401 and equation 6.2 is equal to:

Where: 8760 refers to hours per year for $t_f = 25$ years, u (anode utilization factor) and ϵ (anode capacity) are previously selected as 2000 (Ah /kg) and 0.8, respectively. Thus $M_a = 7293.56 \text{ kg}$

9.1.6. Details of anode selected

Anode geometry (mass and radius)

As described above, according to DNV RP B401 § 7.6, assume that the Owner/Purchaser or the contractor selected the Pacu type of anodes considering the net anode mass to be installed and available space for location of anodes. In addition to stresses put on anodes during installation and operation, the selection is principally affected by the size and geometrical configuration of the chain.

Then, according to DNV RP B401 § 7.8.1, from the anode type selected, the number of anodes(N), anode dimensions and anode net mass (m_a)in kg, shall be defined to meet the requirements for:

1. Initial/final current output, I_{ci} / I_{cf} (A)
2. Anode current capacity C_a (A.h)

Let's say 50 kg mass anode is selected and the volume will be 50 kg divided by density of aluminum which is 2700 kg/m³ equals 0.0185 m³. According to IMENCO, the anode has more of a donut(torus) shape attached using as shown in Figure 9-1 attached using a Piraha clump with no need for welding or bolt connection with chains. The inner radius for all anode designs is constant equals to $a=6.6$ cm. As shown on Figure 9-2, the shape of the anode looks like a donut, and we can assume it having a torus shape (the rest dimensions of the anode are kept confidential by the company).

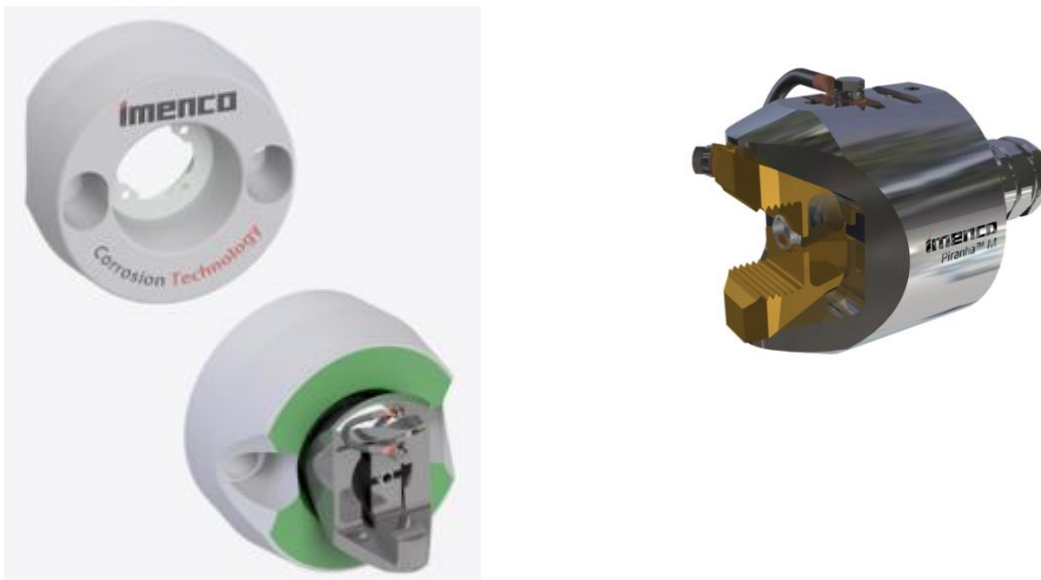


Figure 9-2: An illustration of Pacu® anode (left) and Piranha® anode Clamp (right) [40]

Thus, volume of the torus is equal to the cross-section area of the anode times the perimeter of the anode along it's radius of revolution(R).

$$\text{Perimeter of anode} = 2*\pi*R \text{ and Area of anode cross section} = \pi*r^2$$

$$\text{Volume of a torus} = 2*\pi*R* \pi*r^2 = 2*\pi*(a+r)* \pi*r^2, \text{ but } a = 0.066 \text{ m}$$

$$\text{Volume} = 0.0185 \text{ m}^3 = 2\pi^2r^2 (a+r)$$

$$\text{This will give a cubic equation} \Rightarrow r^3 + 0.066r^2 - 0.0009382 = 0$$

$$\text{Then, the radius of the anode, } r = 0.080 \text{ m}$$

$$\text{Anode outer radius} = a + 2r = 0.066 + 2 * 0.080 = 0.226 \text{ m}$$

Radius of revolution(R) = $a + r = 0.066 + 0.080 = 0.146$ m

Anode surface area (A_i) = $4 * r * R * \pi^2 = 0.463$ m²

Then, we can say that the anode geometric shape (type and size) is compatible with the chain dimension. To prove this, diameter of the anode which is 0.08 m is less than selected chain side length which is 0.2128 m, so that it can easily be placed on position as there is adequate space to put the anode on the chain link.

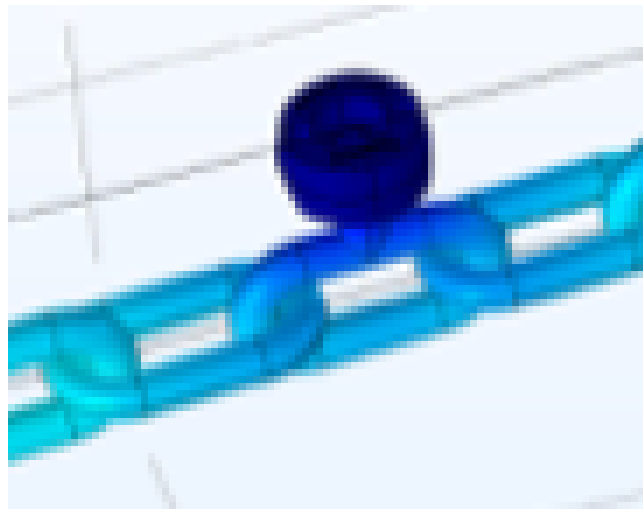


Figure 9-3: Pacu anode attached to the chain using Piranha clump [40]

Anode utilization factor (u): in reference to DNV RP B401 § 6.8 and Table 6-5, the utilization factor (u) equals to 0.8 as the anode type is other type than the once described on DNV RP B401 (not slender stand-off, elongated, flush mounted or bracelet). This means 80% of the net anode mass required to sustain protection throughout the design life of a CP system.

9.1.7. Number of anode requirement

- The number of anodes based on the mean current required (N_2) = $M_a/m_a = 145.88$ kg
- The number of anodes based on the initial current required (N_1) = I_{ci}/I_{ai}
 - But I_{ai} must be calculated first and from previous part, anode radius(r) and area (A_i) were found according to certain steps. Thus, anode resistance can be found from the Lloyd's formula Table 6-6 for short flush-mounted, bracelet and other types which is:

$$R_a = \frac{0.315 \cdot \rho}{\sqrt{A}}$$

- Where ρ is the seawater resistivity and $A = A_i$ is the initial anode surface area. By substituting the values for the indicated coefficients, $R_{ai} = 0.1389$ ohm.

- Then from this, initial individual anode current output can be found using ohm's law (equation 6.3), $I_{ai} = 1.8 \text{ A}$
- Therefore, number of anodes based on initial current required (N_1) = $I_{ci}/I_{ai} = 59.21$
- The number of anodes based on the final current required (N_3) = I_{cf}/I_{af} . but I_{af} must be found first. To find I_{af} , the following terms must be calculated:
 - I. The remaining net anode mass (m_{af}) kg, when the anode has been consumed to its utilization factor (u), at the end of the design life (t_f) years, is given by equation 6.6 which equal 10 kg.
The volume of the anode (V_f) = $m_{af}/\rho_{alm} = 0.004 \text{ m}^3$
 - II. Depleted anode radius (r_f) = 0.042 m, detailed calculations are on spread sheet on Appendix A3.
 - III. Depleted anode area (A_f) = 0.18 m
 - IV. Depleted anode resistance: according to DNV RP B401 § 7.9.2 and Table 6-6:

Using the same formula as previous on initial, $R_{af} = 0.223 \text{ ohm}$

Then, using equation 6.3 $I_{af} = 1.112 \text{ A}$

Number of anodes based on final current required (N_3) = $I_{cf}/I_{af} = 73.4$

Therefore, the number of anodes that is going to be selected will be the maximum of N_1 , N_2 or N_3 , which is $N = 145.88$. This can be rounded up to the nearest integer, so that $N = 146$

Applying this number of anodes, the total initial and final current outputs can be calculated as

The total initial anode current output $I_{a_{tot i}} = N * I_{ai} = 263 \text{ A}$

The total final anode current output $I_{a_{tot f}} = N * I_{af} = 164 \text{ A}$

9.1.8. Anode current capacity (life)

According to § 7.8.3 DNV RP B401, the individual anode Current Capacity is given by equation 6.5, $C_a = 80,000 \text{ A.h}$.

And the total anode current capacity ($C_{a_{tot}}$) = $C_a * N = 11680000 \text{ A}$

And according to § 7.8.4 DNV RP B401, the total required current capacity can be calculated as:

$$I_{c \text{ tot m}} = I_{cm} \cdot t_f \cdot 8760 = 11669689,61 \text{ A}$$

From this, the anode life can be predicted as $(t) = t_f \cdot C_{a \text{ tot}} / I_{c \text{ tot m}} = 25.03$ years

Finally, before deciding and concluding, there are some criteria should be fulfilled which are for the anode dimensions and for the net mass initially selected. If these criteria are not met another anode size shall be selected and the calculations repeated until the criteria are fulfilled. According to § 7.8.4 calculations that has been carried out must demonstrate that the the requirements on equation 6.6 are met:

$$C_{a \text{ tot s}} = 11680000 \text{ A} > I_{c \text{ tot m}} = 11669689,61 \text{ A}$$

$$I_{a \text{ tot i}} = 263 \text{ A} > I_{ci} = 106.573 \text{ A}$$

$$I_{a \text{ tot f}} = 164 \text{ A} > I_{cf} = 82.351 \text{ A}$$

A separate cathodic protection design can be prepared for the part of the chain buried in the seabed. From the previous discussed literature, this should be considered if the bottom layer is soft soil condition rather than hard rock. So, the only variable values from the previous design are just the length of the chain (200 m) and according to § 5.4 DNV RP B401 it has been argued that a design protective potential of - 0.90 V should be applied in anaerobic environments, including typical seawater sediments.

Checking if all the criteria are met:

$$C_{a \text{ tot s}} = 2960000 \text{ A} > I_{c \text{ tot m}} = 2917422 \text{ A}$$

$$I_{a \text{ tot i}} = 40 \text{ A} > I_{ci} = 26.64 \text{ A}$$

$$I_{a \text{ tot f}} = 25 \text{ A} > I_{cf} = 20.59 \text{ A}$$

9.2. Results and discussion

From the results shown above, all requirements are met. Therefore, a total of 146 anodes with a net mass ($M=N \cdot m_{ai}$) of 7300 kg at 5.5 m ($D=L/N$) distance between anodes can be used for the cathodic design of mooring chains extending in 800 m depth of seawater.

From the results, of the two designs we can see the difference between a chain extending in seawater and a chain laid on seabed that the chain part buried on seabed need more protection due to the increase in corrosion capacity due to the existence of microbial activity if present. Therefore, anodes of similar mass but at different distance in between can be used to protect the additional corrosion due the presence of microbial activity. In this case, a 10 cm difference in anode distance is used

between the buried chain (5.4 m) and chain extending in seawater (5.5 m). A summary of the calculation is shown as a spreadsheet on Appendix A1,A2 and A3.

10. Conclusions

- Melchers' linearized corrosion rate estimation can be used for mooring chains under environmental conditions with or without high annual variations in environmental parameters (seawater temperature and DIN concentration). The predictions of the model show a good correlation with data for observed corrosion losses at different sites. Consistent with data and trends for more moderate sea conditions. Melchers showed that increased concentration of DIN and/or seawater temperature causes increased corrosion. Corrosion allowance is given in DNVGL-OS-E301 as guidance. If MIC are suspected, the application of the model is practical and precise to estimate the additional corrosion rate that occurs due to bacterial growth, which can expose the chains to high corrosion rates than expected during their design life. In addition, not considering all degradation modes during design might result in very likely probability of deterioration rates higher than expected.
- From previous research, it has been stated that the ratio of capacity loss to area loss due to uniform corrosion is estimated to be 1.05:1 on average. This thesis provides guidance on what parameters should be used to construct an accurate FEA model of a chain. The results of the model of uniform corrosion were compared against previous studies and there is an agreement between the findings.
- Deepwater mooring chains were difficult to protect in recent times because the task cannot be done with divers but using the IMENCO Pacu anodes and ROV system, they can easily be installed, maintained, or replaced. Cathodic protection design and calculations in this thesis are made according to these sacrificial anode types. These anodes have no statistical data to prove their efficiency as they are new to the market (two years since implementation) and hence further study might be crucial in the future to show their results and effect.

References

- [1] H. Meng, L. Kloul, and A. Rauzy, “Production availability analysis of Floating Production Storage and Offloading (FPSO) systems,” *Appl. Ocean Res.*, 2018.
- [2] J. Crapps, H. He, and D. Baker, “An FEA-Based Methodology for Assessing the Residual Strength of Degraded Mooring Chains,” *Int. J. Offshore Polar Eng.*, Sep. 2018.
- [3] “NOAA Ocean Explorer: Expedition to the Deep Slope.”
https://oceanexplorer.noaa.gov/explorations/06mexico/background/oil/media/types_600.html
- [4] L. Keshavarz, “Analysis of Mooring System for a Floating Production System,” 2011.
- [5] E. Bjørnsen, “Chains in Mooring Systems,” 2014.
- [6] Jon Henrik S. Johnsen, “Loss of Integrity on Mooring Systems – Causes and Consequences,” 2016.
- [7] O. S. SANNI, “Analysis of mooring and anchoring systems for offshore vessels in deep waters,” 2012.
- [8] K.-T. Ma, Y. Luo, T. Kwan, and Y. Wu, “Types of mooring systems,” in *Mooring System Engineering for Offshore Structures*, Elsevier, 2019.
- [9] I. Martinez Perez, A. Constantinescu, P. Bastid, Y.-H. Zhang, and V. Venugopal, “Computational fatigue assessment of mooring chains under tension loading,” *Eng. Fail. Anal.*, 2019.
- [10] T. J. M. Braut, “Numerical Investigation of 3D Scanned Mooring Chains,” 2017.
- [11] M. O. Chrolenko, “Dynamic Analysis and Design of Mooring Lines,” 2013.
- [12] K.-T. Ma, Y. Luo, T. Kwan, and Y. Wu, “Types of mooring systems,” in *Mooring System Engineering for Offshore Structures*, Elsevier, 2019.
- [13] OFFSHORE STANDARDS and DNVGL-OS-E301, “Position mooring.” 2018.
- [14] K.-T. Ma, Y. Luo, T. Kwan, and Y. Wu, “Hardware—off-vessel components,” in *Mooring System Engineering for Offshore Structures*, Elsevier, 2019.
- [15] A. Potts and A. Kilner, “SCORCH JIP - Overview of Project and Summary of Findings,” *Offshore Technol. Conf. Houst. Tex. USA*, 2018.
- [16] T. M. Lee and R. E. Melchers, “Microbiologically influenced corrosion (mic) of mooring systems: diagnostic techniques to improve mooring integrity,” 2015.
- [17] Joint Industry Project Steering Committee, *Microbiologically influenced corrosion of mooring systems for floating offshore installations*. The National Archives, Kew, London, 2017.

- [18] J. Crapps, H. He, D. Baker, S. Bhattacharjee, S. Majhi, and E. Wilutis, "Strength Assessment of Degraded Mooring Chains," presented at the Offshore Technology Conference, Houston, Texas, USA, 2017.
- [19] "cathodic-protection-offshore-gn-dec18.pdf."
- [20] J. Rosen, K. Jayasinghe, A. Potts, R. Melchers, and R. Chaplin, "SCORCH JIP - Findings from Investigations Into Mooring Chain and Wire Rope Corrosion in Warm Waters," presented at the Offshore Technology Conference, Houston, Texas, USA, May 2015.
- [21] "Northsea," <https://www.worldatlas.com/>, 2021.
- [22] Det Norske Veritas, "Position mooring." 2018.
- [23] K. Jayasinghe, A. Potts, and A. Kilner, "Mooring Chain Wear Experiments and Findings," *Offshore Technol. Conf. Houst. Tex. USA*, 2018.
- [24] J. Rosen, A. Potts, E. Fontaine, K.-T. Ma, R. Chaplin, and W. Storesund, "SCORCH JIP - Feedback from Field Recovered Mooring Wire Ropes," May 2014.
- [25] K. De Baere *et al.*, "The influence of concretion on the long-term corrosion rate of steel shipwrecks in the Belgian North Sea," *Corros. Eng. Sci. Technol.*, no. 1, 2021.
- [26] R. E. Melchers, "Modeling of Marine Immersion Corrosion for Mild and Low-Alloy Steels—Part 1: Phenomenological Model," *CORROSION*, Apr. 2003.
- [27] R. E. Melchers, "Long-term immersion corrosion of steels in seawaters with elevated nutrient concentration," *Corros. Sci.*, Apr. 2014.
- [28] R. E. Melchers and R. Jeffrey, "Early corrosion of mild steel in seawater," *Corros. Sci.*, 2005.
- [29] H. Ikhwan, S. M. Atikanta, and W. L. Dhanistha, "The Literature Study on Corrosion Rate in Mooring Chain for Tropical Seawaters – Class Rules Review," *Int. J. Mar. Eng. Innov. Res.*, vol. 6, no. 1, 2021.
- [30] R. Kovalenko, R. E. Melchers, and B. Chernov, "Long-term immersion corrosion of steel subject to large annual variations in seawater temperature and nutrient concentration," *Struct. Infrastruct. Eng.*, Aug. 2017.
- [31] L. Mundy, "Offshore mooring chain," 2016.
- [32] Offshore standard and DNV OS E302, "Offshore mooring chain." 2018.
- [33] G. H. Farrow, A. E. Potts, S. Dimopoulos, and A. A. Kilner, "Effects of Uniform and Mega Pitting Corrosion on Residual Strength of Degraded Offshore Mooring Chain," presented at the Offshore Technology Conference, Houston, Texas, Apr. 2019.

- [34] Joint Industry Project Steering Committee for the Health and Safety Executive, “The effect of wear and corrosion of steel components on the integrity of mooring systems for floating offshore installations. Mooring Integrity Joint Industry Project Phase 2.” 2017.
- [35] American Bureau of Shipping, “Cathodic protection of offshore structures.” 2018.
- [36] “DNV-RP-B401: Cathodic Protection Design,” 2010.
- [37] “UFC 4-150-09 Permanent Anchored Moorings Operations and Maintenance,” 2019.
- [38] C. G. S. T.-A.-C. Ltd, “North Sea Water Temperature (NY) | United States | Sea Temperatures,” *World Sea Temperatures*. <https://www.seatemperature.org/north-america/united-states/north-sea.htm>
- [39] “Intermoor Product specification manual.”
- [40] “Cathodic Protection of Mooring Systems & Mooring Lines,” *Imenco AS*. <https://imenco.no/product/cathodic-protection-of-mooring-lines>

Appendix

Appendix A: Cathodic protection design spreadsheets

Table A1: Summary of calculations for mooring chain immersed in seawater and laid on seabed

Mooring Chain CP Design	Symbol	Units	Immersed in seawater	laid on seabed
Basic Design Data				
Chain diameter	d	m	0,076	0,076
Chain Length	L	m	800	200
Temperature	T	°C	8	8
Design life (t_f)	t_f	yr	25	25
Seawater Resistivity (§ 6.7 DNV RP B401)	ρ_{sw}	ohm.m	0,3	0,3
Protection Potential (§ 5.4 DNV RP B401)	E^0_c	V	-0,8	-0,9
Closed Circuit Anode Potential (DNV RP B401 § 6.5 & Table 10.6)	E^0_a	V	-1,05	-1,05
Anode Capacity (DNV RP B401 § 6.5 & Table 10.6)	ϵ	A.h/kg	2000	2000
Anode Density(Aluminium)	ρ_{alm}	kg/m ³	2700	2700

Structure Design Data				
Total surface area (DNV RP B401 § 7.3)	A_c	m ²	484,42	121,11
Painting/Coating Breakdown Factor (f_c) (DNV RP B401 § 6.4 & Table 10.4)	f_c	No Painting or coating	1	1

Design Current Density - for seawater exposed bare metal surfaces				
Design initial current density (DNV RP B401 § 6.3 & Table 10.1)	i_{ci}	mA/m ²	220	220
Design mean current density (DNV RP B401 § 6.3 & Table 10.2)	i_{cm}	mA/m ²	110	110
Design final current density (DNV RP B401 § 6.3 & Table 10.1)	i_{cf}	mA/m ²	170	170

Required Current for CP				
Initial Current Demand (I_{ci}) (§ 7.4 DNV RP B401)	I_{ci}	A	106,573	26,643
Mean Current Demand (I_{cm}) (§ 7.4 DNV RP B401)	I_{cm}	A	53,286	13,322
Final Current Demand (I_{cf}) (§ 7.4 DNV RP B401)	I_{cf}	A	82,351	20,588

Anode Mass Calculations				
Total Anode Mass Based on the Mean Required Current (§ 7.7 DNV RP B401)	M_a	kg	7293,56	1823,39

Details of Anode Selected (Other types)			Pacu	Pacu
Anode Utilisation Factor (u) (DNV RP B401§ 6.8 Table 10-8)	u	-	0,80	0,80
Selected anode mass	m_{ai}	kg	50,00	50,00
Anode radius	r_i	m	0,080	0,08

Number of Anode Requirement				
Number of Anodes Based on initial current required	N_1	Unit	59,08	24,61
Number of Anodes Based on mean current required	N_2	Unit	145,88	36,47
Number of Anodes Based on final current required	N_3	Unit	73,4	30,6
Final number of anodes needed (Max of N1, N2, N3)	N	Unit	145,88	36,47

Anode Output - Initial				
Anode surface area	A_i	m^2	0,465	0,465
Anode radius	r_i	m	0,081	0,081
Anode Resistance (Lloyd's formula), (DNV RP B401 § 7.9.2 & Table 10.7)	R_{ai}	ohm	0,1386	0,1386
Initial Individual Anode Current Output (§ 7.8.2 DNV RP B401)	I_{ai}	A	1,804	1,083
Total initial Anode Current Output (§ 7.8.2 DNV RP B401)	$I_{a\ tot\ i}$	A	264	40

Anode Output - Final				
Remaining net anode mass (§ 7.9.3 DNV RP B401)	m_{af}	kg	10	10
Depleted anode volume (§ 7.9.5 DNV RP B401)	V_f	m^3	0,004	0,004
Depleted Anode Radius	r_f	m	0,042	0,042
Depleted anode area	A_f	m^2	0,180	0,180
Depleted anode resistance: (DNV RP B401 § 7.9.2 & Table 10.7)	R_{af}	ohm	0,223	0,223
Final anode current output (I_{af}) (§ 7.8.2 DNV RP B401)	I_{af}	A	1,122	0,673
Total final anode current output ($N \times I_{af}$) (§ 7.8.2 DNV RP B401)	$I_{a\ tot\ f}$	A	164	25

Anode Current Capacity (Life)				
Individual Anode Current Capacity (§ 7.8.3 DNV RP B401)	C_a	A.h	80000	80000
Total anode current capacity	$C_{a\ tot}$	A.h	11680000	2960000
Required current capacity (§ 7.8.4 DNV RP B401)	$I_{c\ tot\ m}$	A.h	11669689,61	2917422,402
Anode Life	t	yr	25,03	25,37

NUMBER OF ANODES SELECTED	N	Unit	146,00	37,00
Total Net Mass of Anodes	M	kg	7300,0	1850,0
Total Gross Mass of Anodes	M	kg	7300,0	1850,0
Distance between Anodes	D	m	5,5	5,4

Table A2: Summary of calculations area for mooring chain in seawater and laid on seabed

Surface Area calculator				
Torus Section		Unit	Value	Value
Chain diameter(d)		m	0,076	0,076
Chain radius(r_i)		m	0,038	0,038
Inner radius(a)		m	0,0456	0,0456
Outer radius(b)		m	0,1216	0,1216
Radius of revolution(R)		m	0,0836	0,0836
Area of torus(A_I)		m^2	0,12541504	0,12541504
Cylinder Section				
Length on both sides		m	0,4256	0,4256
Area of cylinders(A_C)		m^2	0,1016167	0,1016167
Total Surface area of a chain		m^2	0,22703174	0,22703174
Number of Links				
Length of chain(L)		m	800	200
Total number of links(N)		number	2133,71266	533,428165
Total surface area of chain		m^2	484,42049	121,105123

Table A3: Depleted anode cross section radius calculator

Anode radius calculator						
Torus Section		Unit	Value	Comments		
Anode mass(m_a)		kg	50	Selected Mass		
Anode volume(V_i)		m^3	0,019	Constant to all anode shapes		
Inner radius(a)		m	0,066			
Outer radius(b)		m	0,227			
Radius of revolution(R)		m	0,147			
		r^3	r^2	r^1	Constant	Y
Coefficients		1	0,066	0	0,0009626	-2,43921E-05
Anode radius(r_i)		0,08012615				
Anode Surface Area(A_i)		0,46499829				
Depleted anode radius calculator						
Torus Section		Unit	Value	Comments		
Anode mass(m_a)		kg	10	Constant to all anode shapes		
Anode volume(V_i)		m^3	0,004			
Inner radius(a)		m	0,066			
Outer radius(b)		m	0,15			
Radius of revolution(R)		m	0,109			
		r^3	r^2	r^1	Constant	Y
Coefficients		1	0,066	0	0,0002026	-1,5011E-05
Depleted anode radius(r_f)		0,0417329				
Depleted anode Surface Area(A_i)		0,17958282				

Appendix B: Market recommendation of CP for mooring chains in deep water

Following extensive research, the Pacu design developed by Imenco corrosion technology (ICT) was found to be practical and effective, and extensively tested and validated through a Technology Qualification Project with a major international operator. There is currently no documented prevention against mooring chain corrosion on permanently moored offshore facilities. Pacu intends to offer a comprehensive solution for mooring system protection. ICT (Imenco Corrosion Technology) has proved that by connecting sacrificial anodes to the mooring chains, it is possible to significantly increase their lifespan through computer simulation and field experiments. Pacu is intended to be connected to mooring chains. The solution, which consists of ICT's well-known Piranha clamp and an integrated bracket-mounted sacrificial anode, will significantly increase the lifespan of mooring chains. They are working on a technique for cathodic protection of permanently placed mooring chains at all water depths using an anode clamp that can be fitted by ROV.

The system was originally designed for use in the chains of Floating Production, Storage, and Offloading units, but it is equally applicable to any mooring system, such as those on floating wind platforms or offshore aquaculture sites. Pacu is intended to be connected to mooring chains.

The product has undergone extensive internal and external testing, and with the transition from qualification to commercialization, operators may now take use of the whole ICT package, which includes computer modeling, testing, installation, and protection certification.

Prior to the launch, ICT collaborated with a major multinational operator on a Technology Qualification Project to de-risk an anode retrofit option for mooring chains. The research proved that cathodic protection and the usage of Pacu™ provided operators with a feasible option.

Pacu™ from ICT will revolutionize corrosion control by drastically decreasing the rate of corrosion and extending the life of mooring systems. Applicable to all geographical regions, but notably in areas where quick corrosion has been highlighted as an issue.

The use of Pacu™ reduces the likelihood of mooring system breakdowns. while offering a low-cost solution that can be readily adapted to existing chains. Cathodic protection of chains allows for lower corrosion allowances, allowing for thinner chains to be employed in new and replacement systems. As a result, there is less weight and hence less equipment required for handling, transit, and installation, lowering the carbon footprint of activities.

"This technology signifies the beginnings of significant transformation in not just what can be done, but how it can be done," said Nils Olav Digre, Vice President of Imenco, "and it will raise the promise for cathodic protection to a larger market." Pacu™ will alter supply chain management by delivering a cost-effective, adaptable solution while supporting the energy industry's push for greener operations. We are thrilled to bring this fully developed product to market after extensive testing."

With the Pacu™ technology, any permanently anchored structure may benefit from its adaptability. Each mooring system's anode size, shape, and spacing were custom designed to meet the specific corrosion protection needs of the system. Because of its huge size and well-documented mechanical grip and electrical conductivity, the Piranha® clamp can effectively clamp on to common FPSO mooring chain dimensions, despite their extensively corroded or painted surfaces.

The clamp used for the connection of the Al anode to the mooring chain is renowned for its mechanical robustness and electrical continuity and can be fitted using a ROV. Testing revealed this to be true. Validation of the model's applicability was achieved by comparing model findings to actual test results. In conclusion, all results are good and inspire confidence in the realization of the aforementioned cathodic protection technique for free-hanging mooring chain.

Pacu™

Cathodic Protection of Mooring lines



Dramatically extend the lifespan of mooring systems with Pacu™

The corrosion of mooring systems for permanently moored offshore structures has long been a recognized challenge and is a leading cause of mooring failures and costly, unplanned replacements.

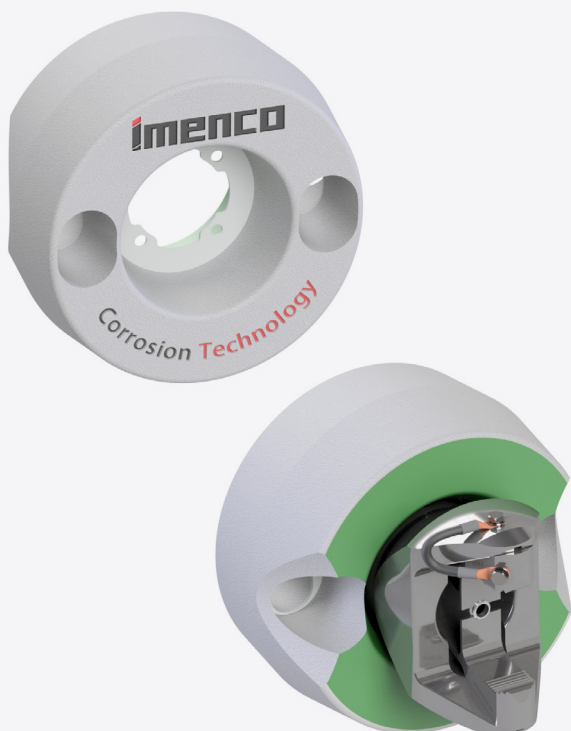
With rates of corrosion varying significantly across the globe, the only solution until today has been to accept this corrosion with an 'allowance' in the form of thicker chains, using more steel. However, with Imenco's revolutionary Pacu™ system, which uses cathodic protection in the form of sacrificial anodes that can be easily retrofitted along the length of the chain, Pacu™ is transforming the available strategies for subsea chain protection.

Setting a new standard in the protection of mooring systems

With extensive experience in cathodic protection, we are setting a new standard in protecting the integrity of your operations. Applicable to any permanently moored structure, the Pacu™ system is adapted to meet the requirements of each installation, ensuring optimal corrosion protection no matter how challenging the environment.

Combining the incredible strength and conductivity of our industry-leading Piranha® clamp with our tailored sacrificial anode solution, Pacu™ is transforming subsea chain protection and halting the progress of corrosion in its tracks to immediately extend the lifespan of mooring systems.

Installed safely and efficiently using an ROV with our custom-built Tool Deployment Unit, Pacu™ avoids the need for costly workovers to replace existing chains and reduces the carbon footprint of mooring chain management. New chains can be thinner and lighter, thereby further supporting the drive for greener, more sustainable operations.



Why Pacu™?

At Imenco, we pride ourselves in ensuring that every aspect of planning, installation and follow-up is thoroughly taken care of, so you can rest easy, knowing that your valuable equipment is fully protected.

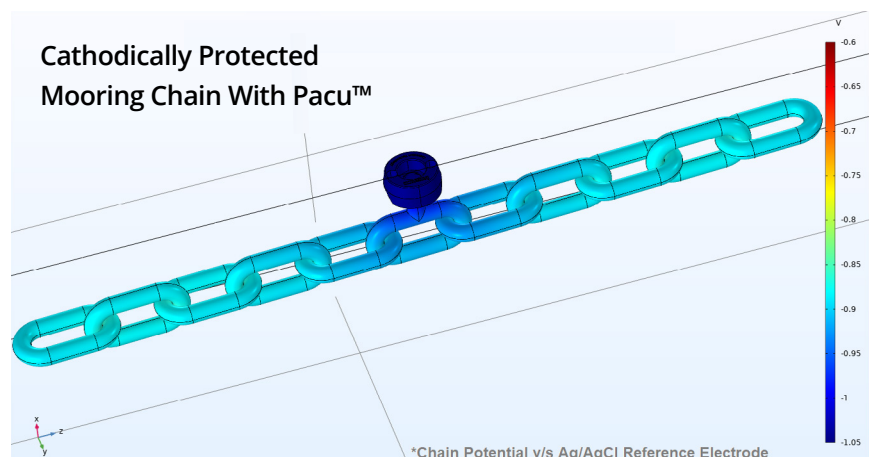
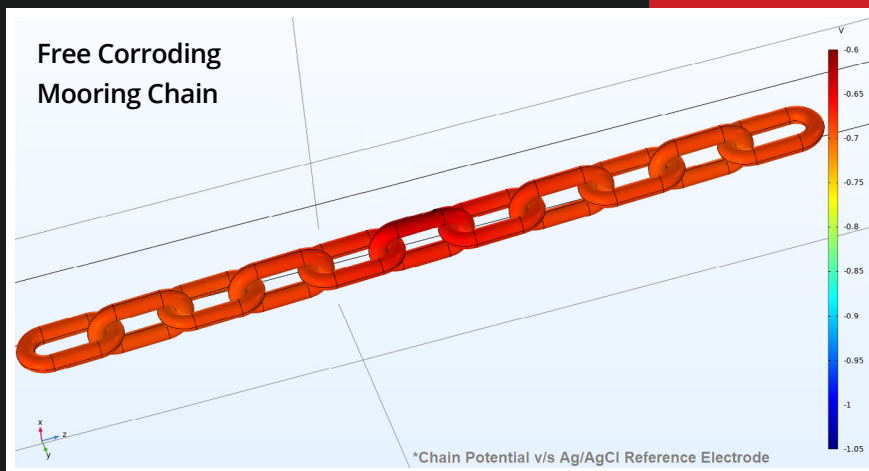
Harnessing the leading expertise of our team within corrosion technology, we have developed a comprehensive combination of service and hardware to offer unrivalled protection from the corrosion of mooring chains.

Pacu™ provides a comprehensive corrosion-management solution and comprises of the following:

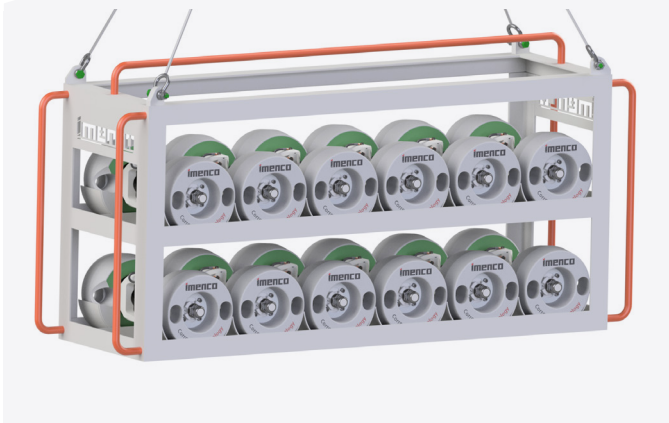
- ✓ Expert modelling and engineering capabilities for optimum solution design
- ✓ High quality, field-proven materials
- ✓ Specially designed discrete sacrificial anodes
- ✓ Easy, safe and efficient installation using ROVs
- ✓ Documented confirmation of protection

Benefits

- ✓ Extend the lifespan of existing and new mooring chains
- ✓ Reduce risk of damage or failure of mooring systems
- ✓ Lower costs related to unbudgeted, pre-emptive replacements
- ✓ Retrofit to existing mooring chains
- ✓ Use thinner, lighter chains in the future
- ✓ Reduce carbon footprint of operations
- ✓ Easy, safe installation process using ROVs
- ✓ Maintenance-free system



Installation Process



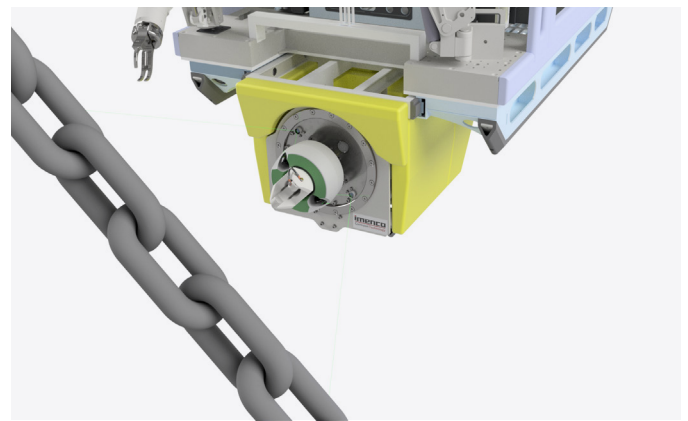
1 Up to 24 anodes and clamps pre-loaded onto Imenco's Subsea Transportation and Storage unit at the deck of the vessel for efficient deployment



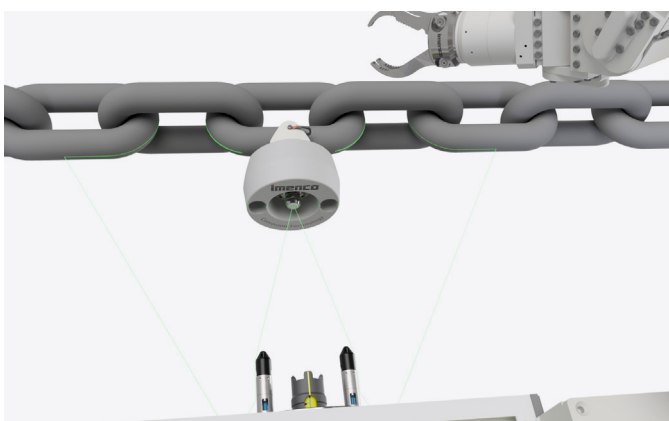
2 At installation depth, the ROV's custom-built Tool Deployment Unit (TDU) collects each unit



3 The anode interface is designed to ensure fast and easy collection



4 Using line lasers and an integrated camera in the TDU are used to ensure precise alignment and installation



5 ROV pilot attaches the clamp to the chain and releases grip

To find out more about how Pacu™ can dramatically extend the lifespan of your mooring systems, contact us at: